# Cosmic Visions Dark Energy: 21-cm Roadmap

Add your name into authorlist.tex,[1] Evan J. Arena,[2] Kevin Bandura,[3,4] Philip Bull,[5,6] Emanuele Castorina,[5] Tzu-Ching Chang,[7,8] Simon Foreman,[9] Josef Frisch,[1] Daniel Green,[10] Dionysios Karagiannis,[11] Adrian Liu,[5,6,12] Kiyoshi W. Masui,[13] P. Daniel Meerburg,[14,15,16,17,18] Laura B. Newburgh,[19] Andrej Obuljen,[20] Paul O'Connor,[2] J. Richard Shaw,[13] Chris Sheehy,[2] Anže Slosar,[2,*] Paul Stankus,[21] Albert Stebbins,[22,†] Peter Timbie,[23] Francisco Villaescusa-Navarro,[24] and Martin White[5]

[1]*SLAC National Accelerator Laboratory, Menlo Park, CA 94205*
[2]*Brookhaven National Laboratory, Upton, NY 11973*
[3]*CSEE, West Virginia University, Morgantown, WV 26505, USA*
[4]*Center for Gravitational Waves and Cosmology, West Virginia University, Morgantown, WV 26505, USA*
[5]*Department of Astronomy, University of California Berkeley, Berkeley, CA 94720, USA*
[6]*Radio Astronomy Laboratory, University of California Berkeley, Berkeley, CA 94720, USA*
[7]*Jet Propulsion Laboratory, California Institute of Technology, Pasadena, CA, USA*
[8]*California Institute of Technology, Pasadena, CA 91125*
[9]*Canadian Institute for Theoretical Astrophysics, University of Toronto, Toronto, ON M5S 3H8, Canada*
[10]*University of California San Diego, La Jolla, CA 92093*
[11]*Dipartimento di Fisica e Astronomia "G. Galilei",Università degli Studi di Padova, via Marzolo 8, I-35131, Padova, Italy*
[12]*McGill University, Montreal, QC H3A 2T8, Canada*
[13]*University of British Columbia, Vancouver, BC V6T 1Z1, Canada*
[14]*Kavli Institute for Cosmology, Madingley Road, Cambridge, UK, CB3 0HA*
[15]*Institute of Astronomy, University of Cambridge, Madingley Road, Cambridge CB3 0HA, UK*
[16]*DAMTP, Centre for Mathematical Sciences, Wilberforce Road, Cambridge, UK, CB3 0WA*
[17]*Kapteyn Astronomical Institute, University of Groningen, P.O. Box 800, 9700 AV Groningen, The Netherlands*
[18]*Van Swinderen Institute for Particle Physics and Gravity, University of Groningen, Nijenborgh 4, 9747 AG Groningen, The Netherlands*
[19]*Department of Physics, Yale University, New Haven, CT 06520*
[20]*SISSA - International School for Advanced Studies, Via Bonomea 265, 34136 Trieste, Italy*
[21]*Oak Ridge National Laboratory, Oak Ridge, TN 37831*
[22]*Fermi National Accelerator Laboratory, Batavia, IL 60510*
[23]*Department of Physics, University of Wisconsin - Madison, Madison, WI 53706*
[24]*Center for Computational Astrophysics, 162 5th Ave, 10010, New York, NY, USA*

(Dated: June 25, 2018)

* anze@bnl.gov
† stebbins@fnal.gov

**CONTENTS**

## PREAMBLE

The Department of Energy (DOE) of the United States government has tasked several Cosmic Visions committees to work with relevant communities to make strategic plans for the future experiments in the Cosmic Frontier of the High Energy Physics effort within the DOE Office of Science. The Cosmic Visions Dark Energy committee was the most open-ended with a broad effort to study periods of accelerated expansion in the Universe, both early and late, using surveys. It has conducted two community workshops and produced two white papers [1, 2].

In [1], the 21-cm cosmology technique was discussed as one possible new observational avenue for the DOE's dark energy program. In the intervening years, an informal 21-cm working group has been working towards charting a science case and the research and development (R&D) path towards a successful experimental program. This white paper summarizes the work of this group to date.

## EXECUTIVE SUMMARY

In the next decade, two flagship DOE dark energy projects will be nearing completion: (i) DESI, a highly multiplexed optical spectrograph capable of measuring spectra of 4000 objects simultaneously on the 4m Mayall telescope; and (ii) LSST, a 3 Gpixel camera on a new 8m-class telescope in Chile, enabling an extreme wide-field imaging survey to 27th magnitude in six filters. DESI will perform a redshift survey of 20-30 million galaxies and quasars to $z \sim 2.5$ to measure the expansion history of the Universe using baryon acoustic oscillations [3] in the matter power spectrum. Prominent among LSST's science goals are the study of dark energy/dark matter through gravitational lensing, galaxy and galaxy cluster correlations, and supernovae.

This white paper proposes a post-DESI, post-LSST dark energy program based on intensity mapping of the redshifted 21-cm emission line from neutral hydrogen out to $z \sim 6$ at radio frequencies. This will quadruple the volume of the Universe surveyed following the optical programs, providing a percent-level measurement of the expansion history to redshift $z \sim 6$ and thereby opening a window for new physics beyond the concordance $\Lambda$CDM model, as well as significantly improving precision on standard cosmological parameters. In addition, dark energy precision parameters and new physics will be powerfully enhanced by multiple cross-correlations with the optical surveys and cosmic microwave background measurements.

The rich dataset produced by a 21-cm intensity mapping instrument will be simultaneously useful in exploring the time-domain physics of fast radio transients and pulsars, potentially in live "multi-messenger" coincidence with other observatories.

The core Dark Energy/Inflation science advances enabled by this program are the following[1]:

- Measure the properties of dark energy in the pre-acceleration era at percent level, providing an unprecedented window for new physics.

- Observe, or constrain, the presence of inflationary relics in the primordial power spectrum, improving existing constraints by an order of magnitude.

- Observe, or constrain primordial non-Gaussianity to unprecedented precision using bi-spectra across wide volumes, improving constraints on several key numbers by an order of magnitude.

Detailed mapping of the enormous, and still largely unexplored, volume of space observable in the mid-redshift $z \sim 2 - 6$ range range will thus provide unique and unprecedented information on fundamental questions of vacuum energy.

The field of 21-cm intensity mapping is currently in its infancy. Intensity mapping experiments now underway or proposed fall into two main classes: those targeting the so-called "Epoch of Reionization" at redshift 7 - 20, and those attempting to observe in the low-redshift range where dark energy begins to dominate the expansion rate around redshift $\sim 1$. In addition, there are currently operating and proposed large-aperture, high angular resolution radio telescopes targeting a range of redshifts with a limited field of view, appropriate for observations of individual astrophysical objects. The program proposed here will fill the redshift gap for intensity mapping experiments, overlap in survey area with precursor experiments, and take advantage of their progress in addressing the challenges of beam calibration, receiver stability, and foreground component separation. Early science results and operation practicalities from all of these programs will inform the design decisions for the next-generation 21-cm survey.

In this document we lay out a long-term program in three overall stages (see Table II). Stage 1 will consist of targeted R&D, finalizing and elaborating the science case and collaboration building, which we foresee as the main activities through the early 2020's. This time frame will also see first-generation dedicated intensity mapping experiments release their first datasets. This work will enable Stage 2, the construction and operation of a new US-led, dedicated radio facility to accomplish the science

---

[1] See Section 2 for quantitative forecasts.

mission centered on HI intensity mapping in the $z = 2 - 6$ range, starting in the mid-2020's and running through the early 2030's. The promises and challenges of this Stage 2 experiment are the main subject of this paper, see Sections 2 and 3. We currently designate Stage 3 to refer to an aspirational but currently speculative program of extending HI intensity to map the pre-stellar "Dark Ages" at $z \gtrsim 30$, which could begin in the 2030s; see Section 4 for discussion and physics promise.

A cost-effective approach to achieving these science goals is now possible thanks to the explosive growth of wireless communications technology enabled by mass-produced digital RF microelectronics and software-defined radio techniques. It is safe to assume that these electronic components will continue to decline in price over the years leading to a construction project. In contrast, detectors for optical telescopes use specialty silicon fabrication technologies which do not benefit from Moore's law scaling: we have seen very little decrease in price per pixel over several decades. Moreover, the current generation of optical experiments is pushing the boundaries of what can be built with current optical technology. A new optical instrument with a considerable increase in etendue to succeed LSST and DESI will require not only tremendous resources but also significant investment in R&D to build optical components. Therefore, we argue that a highly-scaled next-generation survey instrument will be far more practical in the radio than in the optical domain.

MW: There is also the optics problem. Things like LSST and DESI are at the limit of what optics is buildable. Scaling to a larger aperture with a larger focal plane requires lenses nobody knows how to make. **[AS:I've added sentence after "Moreover"]**

Expertise within the DOE OHEP network can be leveraged to address the needs of the 21-cm program. The principal reasons why this program naturally belongs to the DOE program is not only that the science goals addresses topics that are traditionally in the cosmic frontier of the DOE OHEP, but also that the the difficulty in this measurements calls for an approach involving a single large collaborations tightly integrated with experimental design and construction. This way of operating has been a traditional strength of the DOE program. There are also concrete synergies at the level of existing expertise within DOE, namely: RF analog and digital technique for accelerator control and diagnostics, comprehensive detector calibration methodology, high-throughput, high-capacity data acquisition and large-scale computing for simulations and data analysis. These are coupled with management-side capabilities, including facility operations (with partner agencies) and management of large-scale detector construction projects.

From the standpoint of both physics return and engineering feasibility, we believe that a strong case can be made for including a large scale 21-cm intensity mapping experiment in the DOE's Cosmic Frontier program in the late 2020's timeframe.

## 1.  INTRODUCTION

### 1.  Overview and Scientific Promise

The 2014 Particle Physics Project Prioritization Panel (P5) report "Building for Discovery" contained five goals, of which three are amenable to study through cosmological probes. These three are: i) pursue the physics associated with neutrino mass; ii) identify the new physics of dark matter; and iii) understand cosmic acceleration: dark energy and inflation. New knowledge in cosmology that will help us address these topics is acquired by mapping and studying ever increasing volumes of the Universe with improved precision and systematics control. No cosmological theory can predict the location of individual galaxies or cosmic voids, but such theories can predict the statistical properties of the observed fields, such as correlation functions and their evolution with redshift. Studying fluctuations in the gravitational potential and associated density contrast across space and time thus forms the bedrock of cosmological analysis. Since cosmological constraints are inherently statistical, measurements over increased cosmological volume will improve current bounds. Past galaxy surveys at optical wavelengths have explored Large Scale Structure (LSS) over increasingly large cosmological volumes; however, this approach faces practical limits in the number of high redshift galaxies that can be observed per unit time. To extract the full statistical volume available for further constraining dark energy a new, higher-throughput technique is required.

In this report we advocate a novel technique: 3D mapping of cosmic structure using the aggregate emission of many galaxies in the (redshifted) 21-cm line of neutral hydrogen as a tracer of the overall matter field. Although currently less mature than optical techniques, we will argue that the coming decade is an ideal time to make large 21-cm surveys a reality. Such surveys will allow us to probe to higher redshifts with higher effective source number densities for a smaller investment. They scale better in cost by relying on Moore's law in a way that optical surveys cannot. However, these methods need to be developed and validated and this document aims to set the roadmap for this research.

In the field of low-redshift 21-cm cosmology, one attempts to measure the fluctuations in the number density of galaxies across space. Each galaxy typically emits at many wavelengths: optical emission is mostly integrated star light, while at low RF frequencies they shine in synchrotron radiation and also the 21-cm line of neutral hydrogen. For instance, our own Milky Way galaxy observed in 21-cm has the appearance in Figure 1. 21-cm emission comes from the (hyperfine) transition of electrons from the triplet to the singlet spin state. In this process a photon of wavelength 21.11 cm is emitted which, by virtue of its narrow linewidth and isolation from other features, can be readily and unambiguously identified in the galaxy's radio spectrum. Hence, a single line at low RF frequency in a galaxy spectrum can be identified with the 21-cm transition and the galaxy's redshift determined with pinpoint accuracy. In the intensity mapping technique, the intention is not to resolve individual galaxies. Instead, one designs radio interferometers with angular resolution limited to scales relevant for studying the large-scale structure traced by those galaxies. In each 3D resolution element (voxel), given by the coarse angular pixel and considerably finer frequency resolution, emission from many galaxies is averaged to boost the signal-to-noise. The primary obstacle is removing synchrotron radiation foreground from our own galaxy, which is relatively intense but smooth in frequency. This is schematically illustrated in Figure 3.

All neutral hydrogen in the universe below redshift of $z \sim 150$ is in principle amenable to 21-cm observations. This includes the large volume before the first luminous objects were created. This corresponds to tremendous amounts of volume as we illustrate in the Figure 2. In this white paper we mostly focus on the era after reionization, at redshifts lower than $z \sim 6$, where the 21-cm signal is a theoretically well-understood tracer of cosmic structure and any science amenable to study through statistics of cosmic fields can be studied using this technique. We will also discuss the signal from the "Dark Ages" (Section 1 7) whose observations should be an aspirational goal once the technique matures.

### 2.  Primary Science Drivers

This is driven by the following high-priority science objectives, which are deeply connected to some of the biggest problems in fundamental physics:

> **A1**.  **Measure the properties of dark energy in the pre-acceleration era at percent level.**  We will measure the energy density in the *dark energy component* with the precision of X% at redshift $z > 2$. In the pre-acceleration era, it is very difficult to measure the energy density in dark energy, because the total energy density and thus expansion history of the Universe is dominated by the matter density. **[SF: Should say here why the S2 experiment can do the measurements, despite the difficulty just mentioned.]** However, the pre-acceleration era is precisely where deviations caused by a dynamical scalar field are likely to be the largest as the field changes from tracking Daan: ? to behavior to exponential acceleration. LN also echoes Daan's ?: maybe we can make this general like: Dynamical dark energy models based on extentions to particle physics predict unique time dependence of the expansion in this era, and so measurements from 21cm instruments of this epoch can be used to confirm and rule out these classes of models. Or something.
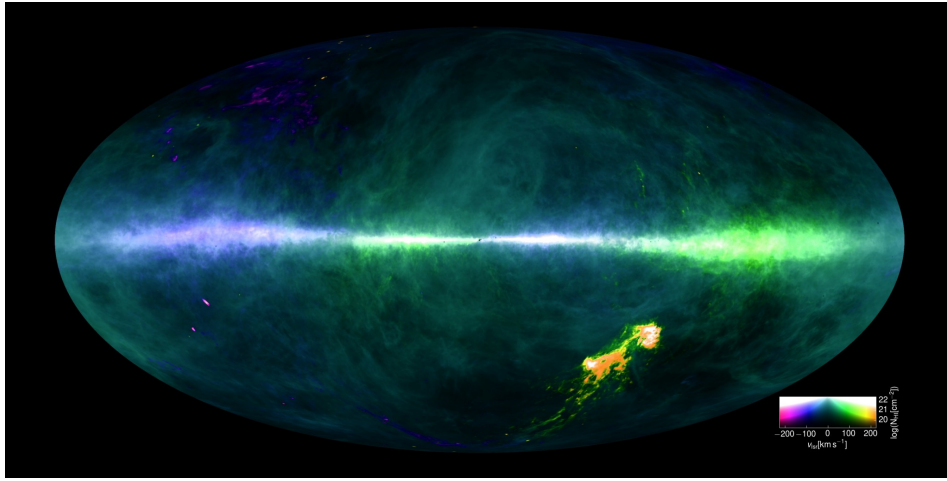
FIG. 1. Galaxies are rich in neutral hydrogen. The Milky Way galaxy in 21-cm is shown here. Data are from the HI4PI survey [4]; colors represent relative velocity of the gas.
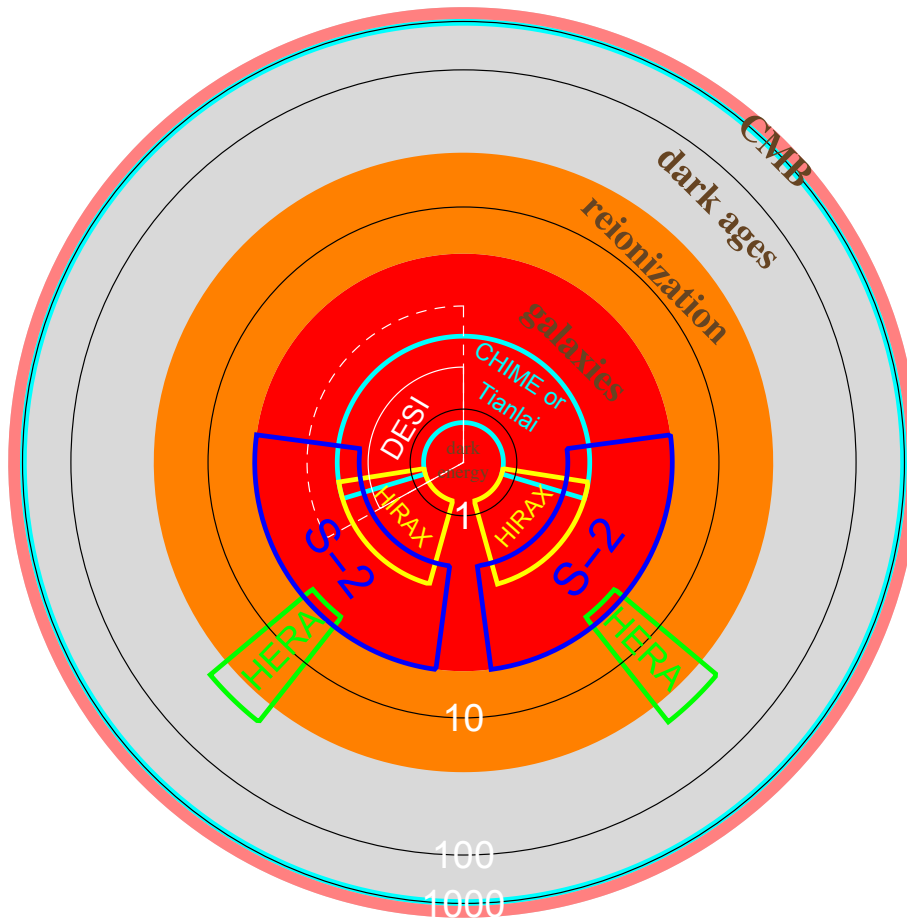


FIG. 2. Plotted is a 2D representation of the observable universe where the area is proportional to the comoving volume and the distance from center monotonically increases with distance from Earth. Different epochs are color coded: the epoch of galaxies ($z < 6$) red; the epoch of reionization ($6 < z < 20$) orange; the dark ages ($20 < z < 700$) gray; the epoch of the last scattering ($700 < z < 1300$) cyan; and the early universe ($z > 1300$) pink. The volume surveyed by various current experiments with dense redshift space sampling are outlined, including the DESI optical spectroscopic survey of galaxies (white) and quasars (white dashed); an HI intensity mapping surveys of the intergalactic medium during the epoch of reionization HERA (green) and HI intensity mapping surveys of galaxies: CHIME or Tianlai (cyan), HIRAX (yellow) and the stage 2 (S-2) project proposed here.

6
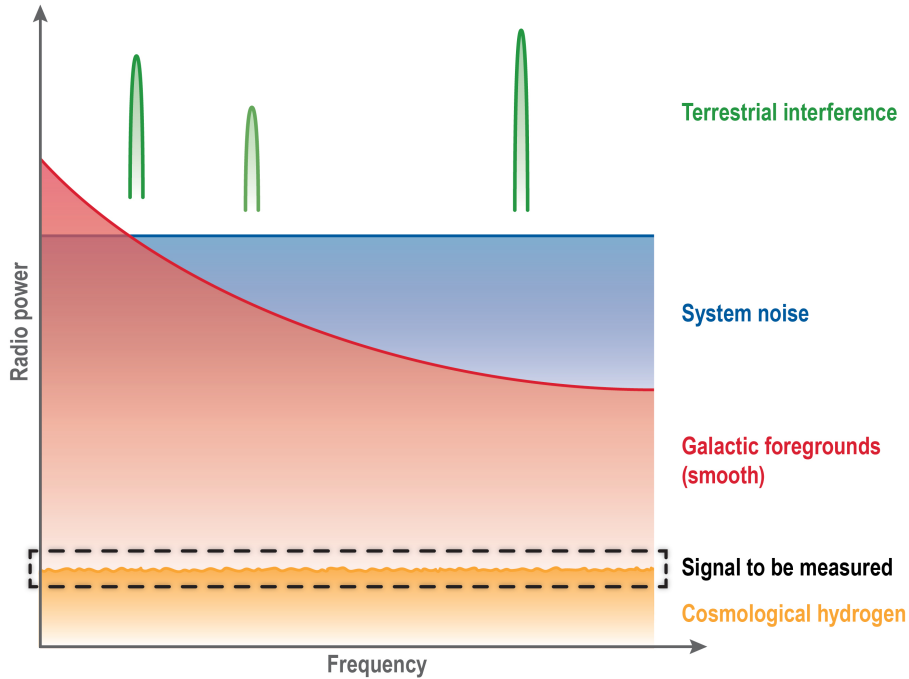
FIG. 3. Schematic illustration of 21-cm emission spectrum in a resolution element.

**A2**. **Constrain inflationary relics in the shape of features present in the primordial power spectrum.** We will measure the precise shape of the primordial matter power spectrum at precision that will exceed DESI **[SF: Equal DESI? It sounds funny to say exceed, and then exceed by order of magnitude]** at $k = 0.02h$/Mpc and exceed it at over order of magnitude at $k = 0.5h$/Mpc. Sharp features in the primordial matter power spectrum survive mild non-linear evolution and biasing and are generically predicted in some inflationary models.

**A3**. **Constrain the equilateral and orthogonal non-Gaussian bispectrum with unprecedented precision** $\sigma(f_{\mathrm{NL}}^{\mathrm{equil.}}) = XX$, $\sigma(f_{\mathrm{NL}}^{\mathrm{ortho.}}) = YY$. Primordial non-Gaussianities are one of the very few ways in which we can learn about the epoch of inflation and are generically predicted for non-minimal inflationary models. The large number of well-measured modes from the volume accessible to this survey will allow us to constrain the non-Gaussianity of the primordial fields. Squeezed, equilateral and folded bi-spectrum triangle configurations are all amenable to being constrained using high redshift surveys of LSS, but equilateral and folded triangles are especially competitive given less pronounced non-linearities at higher redshift.

The main goals outlined above directly follow from the ability of 21-cm emission to directly measure numerous linear modes with essentially no tracer shot-noise. Such an experiment will provide new capabilities that might open completely new, for now unforeseen windows.

## 3. Science capabilities enabled by a large-scale 21cm experiment

In pursuing the primary science drivers listed above, we will need to build an instrument with high spectral resolution, a broad bandwidth, unprecedented sensitivity, and exquisite instrumental stability. These characteristics represent a giant leap in cosmological survey capability in the radio, and will enable a range of new scientific applications – including the potential to open completely new windows that are unforeseen at present. **[SF: Last part is redundant with previous paragraph]**

In the following, we list some of the new capabilities that will be enabled by an experiment of the scale envisioned in this document:

**B1**. **Measure the expansion history to the percent level out to** $z = 6$. This will extend the measurements performed by DESI, LSST and other optical precursor experiments deep into the pre-acceleration era.

7

**B2**.  **Quadruple the observed volume at an increased fidelity.**   The volume between $z = 2$ and $z = 6$ is approximately three times the volume between $z = 0$ and $z = 2$. 21-cm intensity mapping can probe this volume with a very high effective number of sources, leading to a large increase in the number of available linear modes. MW: Does this factor of 3 include redshifting of $k_{\rm nl}$? Have we defined 'modes' to mean 'Fourier modes' already?

**B3**.  **Constrain models of modified gravity.**   When combined with additional observations, the 21-cm data will also provide measurements of the growth of fluctuations in the universe at high redshifts. Such measurements can, in principle, distinguish between dynamical dark energy and modified gravity.

**B4**.  **Measure modes not directly present in survey.**   Couplings between different modes of the cosmic density field will allow us to reconstruct modes that are not directly present in the survey through their effects on the observed small-scale modes. In particular, the tidal effect of large-scale modes on the small-scale power will give access to the large-scale modes (which may otherwise be obscured by foregrounds in certain scenarios). Furthermore, gravitational lensing effects on small scales will provide information about lower-redshift structure. Three-dimensional 21-cm observations will provide several source "screens" for lensing analyses; the signal to noise of a joint analyses of all such screens will exceed that for CMB-S4 lensing reconstruction in cross-correlation.

**B5**.  **Improve measurements of the standard cosmological parameters, including neutrino mass, radiation content of the early universe, and curvature.**   21-cm observations can, in conjunction with other synergistic measurements, aid in constraining the standard cosmological parameters. In particular, we should achieve an independent detection of neutrino mass and constrain the radiation content to within a factor of few of the guaranteed correction due to electron-positron annihilation.

**B6**.  **Directly detect the expansion of the Universe.**   The Universe expands at the Hubble rate and in principle this expansion can be detected over a length scale of a decade. The advantage of radio observations is that the clocks stable enough to drive the digitization circuits at the required time stability are nearly off-the-shelf equipment.

**B7**.  **Explore modified gravity using pulsars.**   The same instrument that can be used for cosmology will also be able to observe numerous pulsars and study general relativity through precision changes in pulsar timings. MW: Explore MG or 'study' GR?

**B8**.  **Explore physics of fast radio bursts (FRBs).**   This instrument will also detect numerous FRBs. The physics of FRBs is currently poorly understood, but in some models they could act as standard candles, opening another possible window into the expansion history of the universe.

These scientific possibilities are elaborated further in Section 2.


## 4.  Advantages over optical surveys

Optical galaxy surveys are now a mature observational tool, having gone from pioneering surveys of a few thousand galaxies, through definitive detections of cosmological clustering signals like baryon acoustic oscillations, to now routinely producing precision cosmological constraints. This successive, multi-generational development path continues, as next-generation experiments like DESI are poised to improve over current experiments by an order of magnitude in depth, and by pushing to significantly higher redshifts.

The 21cm intensity mapping technique is much earlier along its development track, and must yet pass through a series of milestones before it can be considered truly competitive with optical surveys. The technique holds several inherent advantages over traditional optical surveys however, which will become especially important as physical constraints slow and eventually stall the further development of optical surveys in the future:

**Full 3D information:**   In optical experiments, one is forced to observe individual galaxies, because if one took spectra in coarse pixels such as those used in 21-cm, the signal would be dominated by starlight and sky-glow. Intensity mapping in optical might be possible from space and probably only in cross-correlation to avoid mixing from interloper lines. This means that a typical optical experiment must first detect target objects in a photometric optical survey, select objects of interest based on their broadband fluxes and then measure redshifts of individual objects before making the full resolution map of galaxy positions. In other words, a survey must choose between being a photometric survey like LSST that gets all galaxies (up to certain magnitude limit), but loses the majority of the radial information, or being a spectroscopic survey like DESI that gets full spectra for a subset of galaxies, but loses the precision that comes with sheer number of galaxies. On the other hand, 21-cm intensity maps directly measure the full 3D structure, without the limitations in redshift accuracy or number density that affect photometric

or spectroscopic samples. LN suggests: Optical galaxy surveys are inefficient and have to choose between surveying a huge sample of galaxies at low redshift resolution (photometric) or surveying a subset of selected galaxies at high redshift resolution (spectroscopic). The result are surveys that either lose radial information because they have poor redshift resolution, or statistics because they have fewer galaxies they can measure. 21-cm provides an avenue to do both simultaneously, allowing an efficient mapping of 3D structure and a path towards an cost-effective survey at high redshift that is untenable with optical telescopes.

**Negligible shot noise:** Any point tracer of large-scale structure suffers from the fact that we are sampling a continuous field using a finite number of objects. This Poisson component, also known as shot-noise, acts as a source of noise in any statistics derived from the field. To reduce it, one needs to take spectra of more objects, but most often there simply are not any more objects up to a given flux limit. In 21-cm observations we are measuring integrated intensity from all objects down the very small and faint objects and are only limited by continuous sources of noise (sky noise and thermal amplifier noise). Consequently, the noise on 21-cm measurements can be improved by longer observations (or bigger array) with a strict $t^{-1/2}$ scaling. MW: Is this true even at $z \geq 4$?

**Better scaling towards higher redshift:** Optical measurements become increasingly difficult as the redshift range of surveys is pushed toward the more distant universe. First, observations must be performed in the infrared, where they suffer from brighter sky that has many more sky-lines, which are also more variable than in the optical. Second, the infra-red detectors are more expensive and less efficient than optical CCDs (charge coupled devices). Third, the objects themselves are fewer in number and fainter, since we are observing a younger universe. In radio, the primary limitation is from foreground emission, however the same foreground removal techniques vetted by previous generations of 21-cm experiments can be applied because the foregrounds do not fundamentally change across the redshift ranges of interest. In addition, at higher redshift, the same bandwidth covers more cosmic volume and requirements on reflector surface accuracy, etc. become less demanding. In short, unlike optical surveys, extending 21-cm observations towards higher redshift are not intrinsically more difficult than measurements at lower redshift.

**It's cheaper for the same survey size:** One of the main advantages of the 21-cm technology is that it benefits from Moore's law in a way that other observing techniques do not. For example, the technology that goes into optical telescopes, such as lenses, is not getting cheaper with time. While CCDs are becoming sensitive over an increasing frequency range and with ever increasing die size and pixel count, the actual cost per pixel has not decreased significantly over the past few decades and the quantum efficiency of these devices has been close to unity for some time now. However, the cost of the main tools of radio frequency interferometry, such as network bandwidth and correlators keeps decreasing with time. In fact, it is conceivable that within the next 30 years, these costs would become negligible and the cost of 21-cm experiments would be dominated by cost of mechanical parts (reflector dishes, etc.) and infrastructure (land, wiring, etc.). However, we are currently still in the limit at which building costs for an equivalent experiment decrease on year time-scales. MW: There is also a 'buildability' problem for large optical systems (unless they move to reflective surfaces) which is not present for us.

It is therefore natural to consider large 21-cm experiments as the next stage in our exploration of the post-recombination universe. It offers several important advantages over optical surveys and is perhaps the most cost-effective way of mapping truly large swaths of the universe.

## 5. Current State of the Art

21-cm cosmology has only been made possible recently through developments in infrastructure to achieve correlations at full bandwidth (e.g. high-throughput computing and commodification of low noise radio-frequency technology) at the necessary scale. Tools and techniques have been developing rapidly and the first steps towards extracting cosmological information from 21-cm observations have already been demonstrated.

The first detection of the redshifted 21-cm emission in the intensity mapping regime was achieved by Chang et al. in 2010 [5]. The redshifted 21cm intensity mapping 3D field, obtained from the Green Bank Telescope (GBT) 800 MHz receiver, spans the redshift range of $z = 0.53$ to 1.12 and overlaps with 10,000 galaxies in the DEEP2 survey [6] in spatial and redshift distributions. This enabled a cross-correlation measurement on $9h^{-1}$ Mpc scales at a 4-$\sigma$ significance level. On large scales, the amplitude of the cross-correlation constrains the value of $\Omega_{\mathrm{HI}} b_{\mathrm{HI}} r$, the combination of the cosmic HI abundance $\Omega_{\mathrm{HI}}$, the effective bias of 21-cm emission $b_{\mathrm{HI}}$, and the stochasticity parameter $r$ between the optical and 21cm as tracers of the underlying density field, where $0 < r \leq 1$, and the DEEP2 galaxy bias is assumed known [7].

This cross-correlation detection is significant as it verifies that the 21cm intensity field at $z \sim 1$ correlates with and thus traces the distribution of optical galaxies, which are known tracers of the underlying matter distribution. It is also a proof of concept for the intensity mapping technique to establish it as a viable tool for studies of large-scale structure.

A continuing observing campaign to expand the GBT 21cm IM survey in both sensitivity and spatial coverage has yielded two

| Name | Optimized | Steerable | Type | Elements | Redshift | First light |
|------|-----------|-----------|------|----------|----------|-------------|
| Existing w data: | | | | | | |
| GBT | N | Y | Single Dish | 1 | $\sim 0.8$ | 2009 |
| | | | | | | |
| Dedicated experiments: | | | | | | |
| CHIME | Y | N | Cylinder Interferometer | 4 cyl x 256 dual-pol feeds | $0.75 - 2.5$ | 2017 |
| HIRAX | Y | limited | Dish Interferometer | 1024 6m dishes, dual-pol | $0.75 - 2$ | 2020 |
| TianLai Dish | Y | Y | Dish Interferometer | 16 6m dishes, dual-pol | $0 - 1.5$ | 2016 |
| TianLai Cylinder | Y | N | Cylinder Interferometer | 3 cyl x 32 dual-pol feeds | $0 - 1.5$ | 2016 |
| OWFA | N | Y | Cylinder Interferometer | 1056 single-pol | $\sim 3.35$ | 2019(??)**[AS:check]** |
| BINGO | Y | N | Single Dish | $\sim 60$ | $0.12 - 0.45$ | 2020 |
| | | | | | | |
| Dedicated R&D: | | | | | | |
| BMX | Y | N | S. Dish + Interferometer | $4 \times 4$m off-axis, dual-pol | $0 - 0.3$ | 2017 |
| | | | | | | |
| Non-dedicated: | | | | | | |
| MeerKAT | N | Y | Single-Dish | 64 13.5m dishes, dual-pol | $0 - 1.4$ | 2016 |
| SKA-MID | N | Y | Single-Dish | $\sim 200$ 15m dishes, dual-pol | $0 - 3$ | 2023 |
| | | | | | | |
| Proposed Here: | | | | | | |
| Stage 2 | Y | limited | Interferometer | 65,536 6m dishes, dual-pol | $2 - 6$ | 2030 |

TABLE I. List of current and planned experiments. In the "First light" column we mean first light for 21cm observations for non-dedicated experiments. In the "Optimized" column we note whether the telescope has been design with intensity mapping as primary scientific goal. HIRAX is steerable, but only using human intervention. For SKA-MID dishes will likely be used in a single-dish mode with intereferometeric capability used only for gain calibration. Daan: Should we mention the NCLE (NETHERLANDS-CHINA LOW-FREQUENCY EXPLORER ? This is a pathfinder that will be sent to the moon this month. From their website: "The NCLE baseline design concept involves 3 co-located, orthogonal, monopole antenna elements, each of 5 meters in length". Operation frequencies are 1-80MHz. So everything $z \geq 18$.

subsequent publications: An updated cross-power spectrum at $z \sim 0.8$ [8] between 21cm and optical galaxies in the WiggleZ survey [9], and an upper limit on the 21cm auto-power spectrum [10], have been reported. Combining the cross- and auto-power spectrum measurements yields a $\sim 3$-$\sigma$ measurement on the combination of the cosmic HI abundance $\Omega_{HI}$ and bias $b_{HI}$ parameters, $\Omega_{HI} b_{HI} = 0.62^{+0.23}_{-0.15} \times 10^{-3}$ [10]. Further analysis of 800 hours of GBT observations taken during 2010-2015 is currently on-going.

There are currently five major experiments that are attempting to measure LSS with the 21-cm intensity mapping technique with dedicated instrumentation: CHIME in Canada, HIRAX in South Africa, Tianlai in China, OWFA in India, and BINGO, a UK experiment situated in Uruguay. In addition, there are several smaller efforts dedicated to R&D, such as BMX at Brookhaven National Laboratory and PAON at Nançay in France. We list the main properties of these instruments in Table I. The success of these small-scale experiments will teach us about the viability of the technique. CHIME is the most advanced and has recently upgraded from a prototype to the full instrument. It consists of 4 cylindrical radio antennas with no moving parts, observing the entire accessible sky which passes above it as the Earth rotates. It operates from 400-800 MHz, equivalent to mapping LSS between redshift $z =$0.75 to 2.5. We expect first results from CHIME in the next 3 years, which should include foreground removal or mitigation techniques for intensity mapping measurements of LSS in 21-cm emission.

Another experiment often mentioned in this context is the SKA (Square Kilometer Array). As we discuss later in the text, the SKA is not optimized for intensity mapping examined in this document and does not represent a direct competitor for this field. Therefore it does not present an obstacle to DOE for entry into this field.

In figure 4, we plot the same information as Table I, but compressed into in a figure of merit analogous to optical etendue measure:

$$\text{FoM} = \text{collecting area} \times \text{number of receiving elements} \times \text{bandwidth} . \tag{1}$$

Such a quantity cannot convey the full complexity of the experiments' abilities: for example, a compact interferometric array with the same figure of merit will in general perform better and the survey speed at the same figure of merit will be lower at higher redshifts due to increased sky noise. Nevertheless, it is a rough proxy of instrument capability Daan: and visualizes the impressive improvement for a Stage 2 intensity mapping experiment envisioned in this paper –for this particular usage pattern.
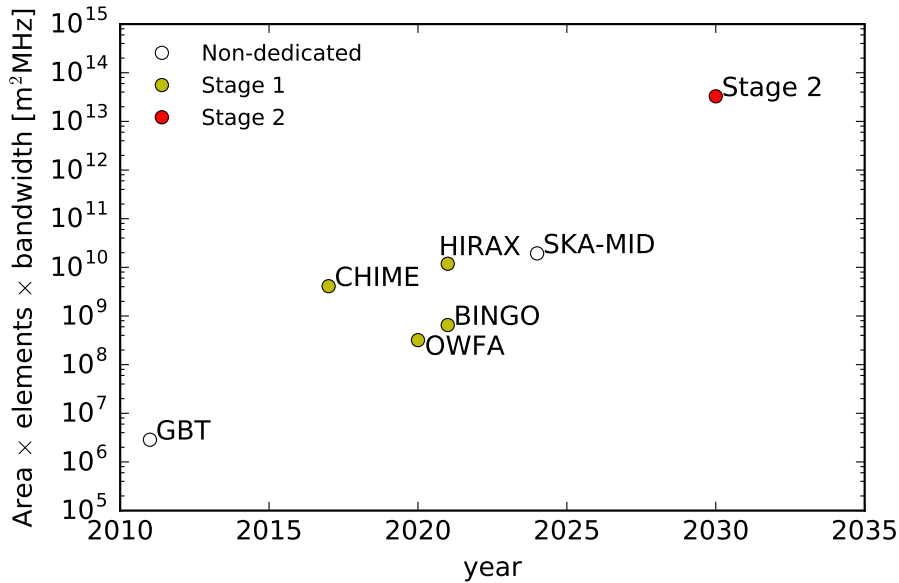
FIG. 4. Representation of improvements from current-generation to future proposed experiments in a figure of merit analogous to optical etendue measure: collecting area × number of receiving elements × bandwidth. See text for discussion.

## 6.  Cosmic Dawn and Epoch of Reionization measurements

21 cm techniques have been used for studying the Cosmic Dawn and the Epoch of Reionization (EoR) at redshifts around $z \sim 6$ to 30. During these periods, first-generation stars and galaxies were formed, and a number of experiments such as HERA [11], PAPER [12], LOFAR [13], MWA [14], and GMRT [15] are seeking to make the first measurements of how these first luminous objects affected the large-scale distribution and ionization state of hydrogen. While these efforts target a currently unexplored phase of galaxy formation, they do not have P5 goals as primary science and thus we are not proposing these for consideration by the DOE. However, they do have an indirect relevance to the goals outlined in this roadmap, for two reasons. First, these experiments may detect signatures of exotic physics that are relevant to P5 goals, provided these signatures cannot be easily be explained by $\Lambda$CDM, even when allowing for extreme astrophysical scenarios. Second, these experiments face many of the same technical challenges as the experiments proposed in this roadmap, and thus any breakthroughs on either side in instrumentation, observation, or data analysis will be mutually beneficial.

A prime example of possible exotic physics would be the recent results from the EDGES experiment [16]. EDGES has recently claimed a first detection of a large dip in spectral energy distribution of the cosmic radio monopole at around 78MHz, corresponding to $z \sim 17$ if this is due to the 21 cm line. While such an absorption feature is predicted by most theories of Cosmic Dawn, the dip measured by EDGES is anomalously large, implying hydrogen gas that is considerably cooler than is allowed by $\Lambda$CDM or an additional source of background besides the CMB [17]. This discovery has yet to be confirmed, and there are some serious concerns related to the foreground modeling [18]. However, if true, it would present a remarkable measurement which has already generated considerable interest within the high-energy physics community. The EDGES result, if validated, could potentially point to the first hints of interactions between baryons and the dark sector [19–25], or place constraints on the primordial power spectrum [26], relic neutrino decays [27], dark energy [28, 29], axions [30–32], interactions between dark matter and dark energy [33], dark matter annihilations [34–36], decaying dark matter [37], primordial black holes [37, 38], fuzzy dark matter [39], and warm dark matter [22, 40, 41].

Fundamentally, a 21 cm experiment aims to make large, three-dimensional maps of the distribution hydrogen, regardless of the epoch it is probing. Thus, breakthroughs with Cosmic Dawn and EoR experiments also represent breakthroughs for any experiment described within this roadmap. In this respect, discoveries like the EDGES result (again, provided it is confirmed) are significant steps forward. A confirmed EDGES detection would be analogous to the first measurements of the CMB blackbody spectrum, while follow-up measurements of the spatial fluctuations of the 21 cm line would be analogous to the first measurements of CMB anisotropies. Just as with the CMB, such measurements would herald the beginning of a new workhorse probe of cosmology.
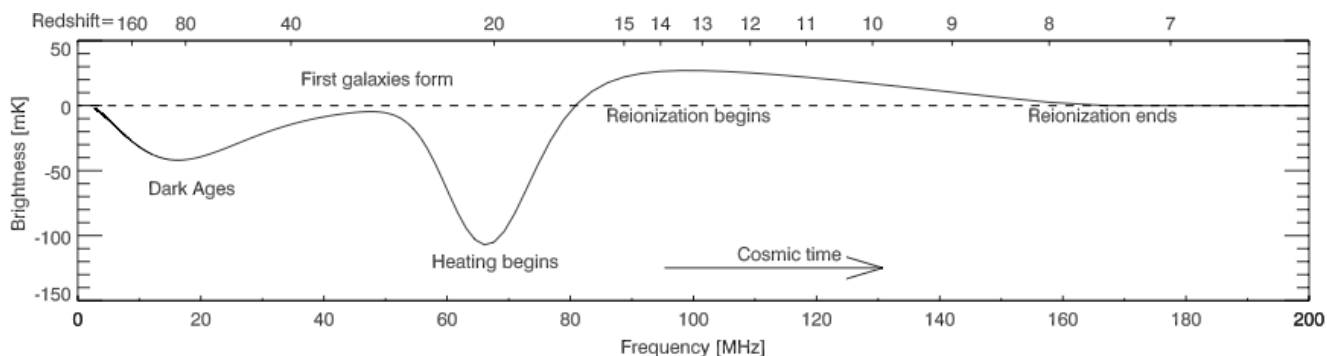
11

FIG. 5. The 21-cm monopole intensity through cosmic times (plot adatped from [42]).

## 7. Dark Ages: the ultimate goal

In this document we have so far talked about the 21-cm intensity mapping as mapping of the aggregate emission from many unresolved galaxies. However, this is a correct picture only in the universe at redshifts lower than $z \lesssim 6$, where the universe is mostly ionized with a few pockets of neutral hydrogen residing in galaxies.

After recombination[2] of hydrogen, when the Cosmic Microwave Background (CMB) was created at redshifts around $z \sim 1150$, the universe was completely neutral. In particular, neutral hydrogen was formed. As matter continued to cluster in the post-recombination universe, peaks in the matter density were enhanced and eventually led to the formation of the first generation of stars and galaxies, which emitted radiation capable of reionizing the ambient neutral hydrogen. Between recombination and reionization, there is thus a high-redshift epoch that is ideal for the cosmological mapping of density fluctuations through 21 cm intensity mapping, during which hydrogen is neutral and and traces the overall matter distribution.

Several astrophysical details prevent the mapping of density fluctuations over the entire redshift range from recombination and reionization. For instance, when $z \gtrsim 150$, residual free electrons from recombination provide a coupling between the CMB and the temperature of the hydrogen gas through Compton scattering. In turn, collisions drive the spin temperature (which quantifies the relative number of hydrogen atoms in the ground versus the excited hyperfine state) Daan: Should we not have a recap of the physics of the spin temperature before everything else? Just 2-3 equations? to the gas temperature. With the CMB temperature in equilibrium with the spin temperature, there is no net absorption or emission from the 21 cm line, and therefore no signal to observe. At $z \sim 150$, Compton scattering becomes inefficient. The spin temperature and the gas temperature remain coupled to one another, but together decouple from the CMB temperature. The gas then cools as $(1 + z)^{-2}$, in contrast with the CMB's cooling as a $(1 + z)^{-1}$, which results in a net absorption signal. This continues until $z \sim 30$, at which point the neutral hydrogen is sufficiently dilute that the collisional coupling between the gas temperature and the spin temperature become ineffective. Direct absorption of emission of 21 cm photons then couples the CMB temperature to the spin temperature once again, and the signal disappears.

This provides a redshift window in the range $30 \lesssim z \lesssim 150$ where 21 cm intensity mapping could be used to provide large-scale maps of density fluctuations. There are several advantages to doing so. First, the regime is too high in redshift for the first luminous objects to have formed yet, and therefore the signal is driven by cosmology rather than astrophysics. Second, the signal is not Silk damped, and thus density perturbations can in principle be mapped to extremely fine scales Daan: with perhaps the Jeans scale being the only limitation. Third, these small-scale structures are still in the linear regime at such redshifts, making theoretical modeling efforts considerably simpler than analogous efforts for $z \sim 0$ galaxy surveys. Finally, the volume of our observable Universe that falls in the range $30 \lesssim z \lesssim 150$ is substantial, leading to exquisite statistical errors on parameters. We will revisit all these opportunities in more detail in Section 4

**[AS: TODO for ACLIU. Done! But probably needs references]**.

## 8. Practical Challenges

There are several known issues for achieving 21-cm cosmology goals compared to traditional galaxy surveys. These call for a coherent development plan that will allow this technique to reach its full potential. We stress that the challenges are in the

---

[2] Recombination is really a misnomer for this epoch since protons and electrons were never combined before. Primordial combination might be a more appropriate phrase.

| | Stage 1: Post-Reionization Pathfinders $(0 < z < 2)$ **Early R & D** | Stage 2: Post-Reionization Experiment $(2 < z < 6)$ | Stage 3: Dark Ages Exp't $(30 < z < 150)$ | Context |
|---|---|---|---|---|
| 2018-2020 | Decadal Survey submission & community building | | | LSST/DESI ongoing, Stage 1 (CHIME) first results |
| 2020-2025 | Vibrant R&D based on test beds, numerical work, participation in Stage 1 Pathfinders | | | LSST/DESI ongoing, Stage 1 (HIRAX, Tianlai) first results, P5 submission, Decadal Survey results, P5 results, SKA online |
| 2025-2030 | Firm science case and optimum experiment configuration | Collaboration forming and CD0/1 | | LSST/DESI ending, SKA results expected |
| 2030-2035 | | Construction, start of data taking | Feasibility study, preliminary design | ? |
| 2035 - 2040 | | Data taking & analysis | Construction | ? |
| 2040 - | | | Data taking | ? |

TABLE II. Roadmap of proposed 21-cm cosmology program. [PT: Should we choose a different name for 'Post-Reionization Expt's'? Clarify connection to existing Stage 1 experiments? Enumerate phases after CD0/1?]

instrument and not fundamental to the signal – with sufficient care, we can build a calibrated system that will be dominated by statistical rather than systematic errors. These complications and our suggested mitigation for a successful survey are:

- **Loss of small-$k_\parallel$ modes**. The foreground radiation is orders of magnitude brighter than the signal, but spectrally smooth. Thus, the signal can be isolated but only for modes whose frequency along the line of sight ($k_\parallel$) is sufficiently large. As a consequence, the low-$k_\parallel$ modes are lost and this precludes direct cross-correlation with tomographic tracers such as weak lensing. However, as we discuss, these modes can be reconstructed from their coupling to the measurable small-scale modes, with non-trivial precision for a sufficiently aggressive system.

- **The foreground wedge**. A frequency varying source at the phase-center of a radio interferometer cannot be distinguished from a monochromatic source off the phase-center for a single interferometric baseline. This effect is known as a foreground wedge, since it imposes a wedge-like cut on the Fourier plane of modes that are naturally "clean" (cannot be contaminated by foregrounds even for a source at the horizon). This problem becomes more important at higher redshift and is acute for epoch of reionization experiments. We note that there is nothing fundamental about this problem: a well calibrated system with sufficient baseline coverage can in principle perfectly separate the foregrounds from the signal even inside the wedge. The problem is therefore primarily a technical challenge rather than a fundamental limitation. Daan: Should we cite this paper [43].

- **The mean signal is not measured.** Because the mean signal is not measured, the redshift-space distortions are related to the growth parameter $f\sigma_8$ via an unknown constant. Therefore, in absence of additional information, the 21-cm observations cannot use the redshift-space distortions as a direct probe of growth. However, there are several ways to go around this problem as we discuss later in the text. Most promising is to use cross-correlations or directly quantify the mean signal from a statistical sample of hydrogen systems (damped Lyman-$\alpha$ (DLA) and high column-density (HCD) systems) in the Lyman-$\alpha$ forest.

These issues need to be studied in detail, both in theoretical terms and through a vigorous experimental program. We argue that major US agencies should support this program in order to allow truly competitive experiments to become reality in the coming decades.

## 9. Roadmap

This white paper argues for a long-term development of the 21-cm cosmology program in the USA, led by Department of Energy but working in conjunction with other agencies where shared science warrants cooperation. In particular, a similar model to that of LSST is envisioned, in which DOE takes up particular aspects of the development which are well matched to its expertise and a collaborating agency takes over some of the other aspects that might not be an optimal fit for the DOE. To this end, we argue for a staged approach that includes three nominal steps leading to a Dark Ages experiment, as outlined in Table II.

- Our first step in the roadmap is an era of vigorous research and development, probably in conjunction with a small-scale test-bed experiment. During this stage, the following should be accomplished:

13

- **Refine the scientific reach of Stage 2 experiment.** In Chapter 2 we start this process by describing some of the most exciting science that is achievable using a strawman design. The design of the instrument should be driven by science and not the other way round, but in practice one needs to start with a given design to see the ballpark science achivable and then iterate until a convincing science-driven experiment design emerges. Our Chapter 2 is the first step in this direction.

- **Advocate for support from major scientific commissions.** In particular, the 2020s *Astronomy and Astrophysics Decadal Survey* and the next P5 report will need to strongly endorse this technique to keep it a viable option.

- **Resolve technical challenges.** There are numerous technical challenges in particular in terms of calibration and data analysis. We suggest a two-pronged approach: first to benefit from the experience of current-generation experiments in mitigating these challenges, and second to support instrumentation development and theoretical progress using a combination of computer simulations, lab experiments, and small, dedicated path-finder instruments. We describe this program in greater detail in Section 3.

- **Optimize a Stage 2 instrument configuration.** Parameters like redshift range, number of elements and their optical designs, calibration schemes, etc. can crucially affect scientific outcome. We will refine and optimize the array parameters to both minimize the systematic effects and maximize possible science.

- **Maintain flexibility in approach** If LSST or DESI find hints of new physics, our work will reflect that. Daan: I guess it does not have to be new physics as you mention below. Suggestion: New exciting scientific developments obtained with optical surveys will be considered when designing the 21-cm array proposed here. A sign of early dark energy might push us towards higher redshift, while evidence for non-zero equation of state parameter $w$ might favor lower redshift. Moreover, if fast radio bursts, for example, turn out to have useful cosmological applications, they might also change the course of events. The most important point is that sufficient resources must be available at this stage to develop the technique and maximize its promise.

- The next step is a post DESI/LSST experiment, which we call a Stage 2 experiment in this document, happening in the later part of the next decade. To reach interesting cosmological constraints, the experiment will have to be an order of magnitude larger than current experiments. In this document we consider a particular straw-man Stage 2 experiment operating at redshifts $z = 2 - 6$, whose parameters we discuss in Section 2.1. This is motivated by the intuition that this volume of the universe is least explored and might offer new low-hanging fruit. However, this particular aspect of the design, as any other, remains on the table to be changed and optimized as we learn more about the most compelling scientific targets.

- If successful, we expect this could be followed by the Dark Ages experiment. This is the least well defined and forecasted instrument that will require significant improvements and R&D and will happen two or three decades from now. To motivate an experiment probing the high redshift 21-cm signal, we discuss some of the unique science opportunities in Chapter 4.

## 2. SCIENCE CASE FOR A POST-REIONIZATON 21-CM EXPERIMENT

This section focuses on preliminary science forecasts for a Stage 2 21-cm experiment to demonstrate the potential science reach of such an instrument. A *Stage 2 experiment* refers to an experiment that will build upon the current set of non-US Stage 1 pathfinder telescopes such as CHIME and HIRAX. We focus on redshifts after reionization has completed, but that will be mostly unexplored by optical surveys. We design an array to probe these redshifts, based on what would be possible with current technology at a price-point that is consistent with a medium-size high-energy physics experiment. The complementary and exciting science that could be addressed by a more futuristic array probing the pre-reionization era will be discussed in Chapter 4. In this Chapter, however, we remain thoroughly grounded with a realistic experiment that is "shovel-ready", assuming the technical challenges discussed in the next chapter are feasible and Stage 1 experiments do not uncover any unexpected significant issues.

We will describe the science potential that our proposed design could achieve, as a brief summary in Chapter 2 1 and then in more detail in the following subsections. We conclude with a discussion of other relevant science. We emphasize that this design is intended as a first exploration of the capabilities of a large project of this type, so we have not attempted any detailed optimization. In later stages of the planning process, the science goals and instrument parameters will be refined further, likely motivating various modifications or improvements to the design choices we present here.

### 1. Science drivers and the straw-man experiment

The main motivation is to achieve the new science that can be opened up by measuring a large number of linear modes in density field at redshift beyond those accessible by current probes. In particular, we want to

- **Measure the properties of dark energy in the pre-acceleration era at percent level.** In the pre-acceleration era, it is very difficult to measure the dark energy density because the total energy density and thus expansion history of the Universe is dominated by the matter density. However, there are strong theoretical motivation to look carefully at this particular era. In particular, one of the mysteries of dark energy is the so-called *Why now?* question. If the dark energy is realized as energy density of the vacuum, which is currently the simplest theory consistent with the data, then the magnitude of the vacuum energy density seems to be strangely fine-tuned to be come dominant just when the universe enters non-liner stage. It if it was an order of magnitude stronger, it will dominate before structure formation and if it was an order of magnitude weaker, we would never have measured it. However, a dynamically triggered dark energy could naturally explain this coincidence. The pre-acceleration era is precisely where such component could be caught in action. This science goal is discussed in Section 2 3

- **Constrain inflationary relics by the shape of features present in the primordial power spectrum.** Sharp features in the primordial matter power spectrum survive mild non-linear evolution and biasing and are generically predicted in certain classes of inflationary models. A large volume giving a fine wave-number precision and numerous modes can open up parameter space for detection. This science goal is discussed in Section 2 7.

- **Constrain the primordial non-Gaussianity through its signatures in the bispectrum.** The large number of well-measured modes will allow us to constrain the non-Gaussianity of the primordial fields. Squeezed, equilateral and folded bi-spectrum triangle configurations are all amenable to being constrained using this technique, but equilateral and folded triangles are especially competitive given less pronounced non-linearities at higher redshift. Primordial non-Gaussianities are one of the very few ways in which we can learn about the epoch of inflation and are generically predicted for non-minimal inflationary models. This science goal is discussed in Section 2 8.

The second and third bullet point here are best served by an experiment that has access to a large number of linear or quasi-linear modes. The total number of modes scales as $V k_{\mathrm{max}}^3$, where $V$ is the survey volume and $k_{\mathrm{max}}$ is the maximum usable wave-number. Going to higher redshift helps both cases. First, there is more volume per unit redshift at higher redshifts as indicated in the Figure 6. Moreover, the effect is even more pronounced if one considers the amount of cosmic volume per unit bandwidth. Second, going to higher redshift naturally improves linearity of the field and allow one to increase $k_{\mathrm{max}}$ at the same time. This is illustrated in the Figure 7 where we show the perturbation theory can accurately describe the results of hydrodynamical simulations out to a very high wave-number.

These science drivers naturally lead to a $z = 2 - 6$ experiment. The upper limit is set by the requirement that the universe has reionized and thus astrophysics does not limit our modeling. The lower limit is set by the fact that much more than one octave of bandwidth is difficult to achieve in realistic radio receivers. We have identified a $256 \times 256$ array of 6-m dishes operating at 200-500 MHz as a straw man configuration that would achieve the three main scientific goals specified above. Such experiment is 64 time larger than the partly funded HIRAX experiment currently under construction in South Africa, but the total bandwidth is only ∼40 times larger and the expectation is that with falling cost and large-scale efficiencies the experiment would be only
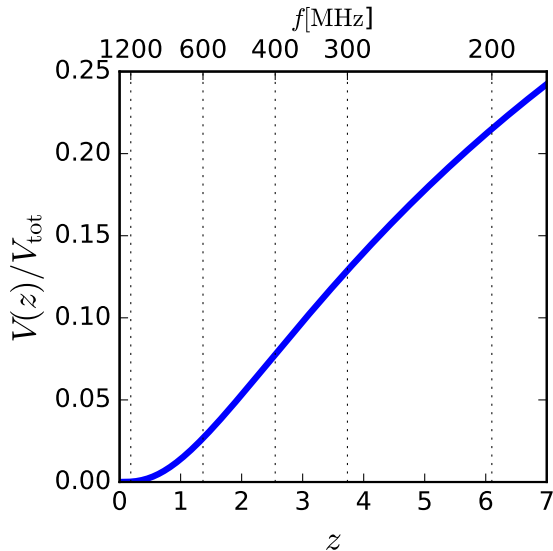
FIG. 6. The left plot illustrates the fraction of total cosmic volume in our past light-cone available as a function redshift (bottom $x$-axis) or observed frequency (top $x$-axis).

$\sim 10 - 20$ times more expensive thus falling very comfortably in the cost profile similar to that of LSST or DESI. The total collecting area of such experiment would be around 1.8 square kilometers. While this is more than SKA, we stress that the low frequencies and in particular the non-actuating nature of the transit arrays makes such a design orders of magnitude cheaper. We assumed a 5 year on-sky integration, which would lead to somewhat longer total duration of experiment, but note that compared to optical experiments that achieved observing efficiency can be considerably large since radio telescopes can observe during the day,

In addition to the main science goals, such experiment would achieve numerous other science goals, both in the field of cosmology and fundamental physics as well as in related astrophysical science that could be of interest to a broad community. In the rest of this chapter we study a subset of the most interesting goals.

In our forecasting we assume the existence of the DESI and LSST experiments. When relevant we also discuss and compare with the CMB-S4 survey, but we note that its final design is less certain that that of DESI and LSST. In some sections, we impose additional 2% or 5% priors on cosmic neutral hydrogen abundance as motivated by [44] or achievable using cross-correlation with other tracers. The results presented in this chapter were derived using several forecast codes. The common assumptions used to forecast main results can be found in Appendix A, but even when slightly different assumptions are used, the results are typically consistent to around 20% in accuracy over the relevant scales.

## 2. Foreground filtering and foreground wedge considerations

Foregrounds present a major calibration issue for 21-cm cosmology. At the minimum, one looses low $k_\parallel$ modes due to filtering of smooth foregrounds. Since foregrounds on the sky are truly perfect power-laws, the minimum requirement, for a perfectly calibrated instrument is that the minimum value of $k_\parallel$ is the fundamental mode that fits in the radial range under consideration. In practice, however, the amplifier gain stability and beam response changes due to change in environmental factors (e.g. temperature affecting the shape of the reflector) means that the lowest $k_\parallel$ min will be somewhat higher. It is useful to parameterize this in terms of fractional bandwidth over which we consider the instrument perfectly calibratable, since both mechanical beam considerations and analog electronic considerations scale with $\Delta f / f$. In Figure 8 we plot the minimum value of $k_\parallel$ (and thus total $k = \sqrt{k_\parallel^2 + k_\perp^2}$) accessible as a function of fractional bandwidth. We find that it is only a weak function of redshift. For 20% fractional bandwidth we find that $k_{\parallel,\min} \sim 10^{-2} h/\text{Mpc}$ is appropriate over a wide range of redshifts.

A different issue, first discovered in the context of the epoch of reionization experiments is the the foreground wedge [45] (see also Section 1 8). It has mainly been studied for interferometric 21-cm experiments, although a related issue also exist for single-dish experiments. In short, for a single base-line, a non-monochromatic source at zero delay cannot be distinguished from a mono-chromatic source at an appropriate non-zero delay. A full array can tell them apart, provided the relative phase calibration is sufficiently accurate, but reaching sufficient calibration in practice has so far proven elusive. The wedge is particularly acute
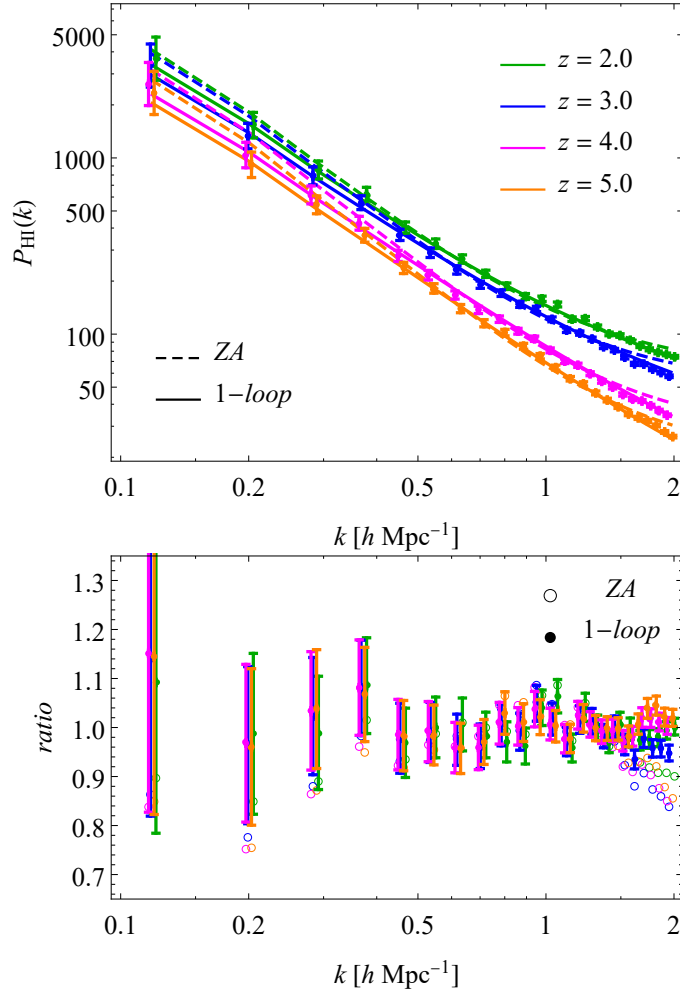
16

FIG. 7. Comparison of the first order Eulerian perturbation theory and Zeldovich approximation (Lagrangian perturbation theory) against Illustris simulation (cite). This plot demonstrates that a very high $k_m$ is possible, both due to more linear universe at higher redshift and greater linearity with which the neutral hydrogen gas traces these structures. [What is the ratio (bottom panel) with respect to, i.e. what is 1?]

at higher redshifts. It acts as a cut on $\mu$, the cosine of the angle along the line of sight, where all modes $\mu < \mu_w$ are lost. The value of $\mu_w$ increases with redshift and is determined by the fringe rate of a source at a particular angle with respect to the line of sight. See also equation A5. The most pessimistic case known as horizon wedge assumes all sources above the horizon can contaminate the signal. In this work, we take a less pessimistic assumption, and only consider contamination from sources that are no further than $N_w$ times the primary beam size away from the beam center. In Figure 9 we plot the effect of the effective volume loss for these cases for an experiment with 6m dishes. We see that the effect is dramatic for horizon-wedge.

When calculating various forecasts we noticed that constraints typically worsen by almost 2 orders of magnitude in the most pessimistic case when a full horizon wedge is excised. We therefore take the position that this systematic will have to be overcome to fully exploit the possibilities offer by the 21-cm technique. We reiterate that it is a technical rather than fundamental problem. Instrumental design choices are vital to support this – for example, dishes result in a characteristic 'pitchfork'-shaped region of foreground contamination within the wedge, which leaves modes between the pure radial ($k_\parallel \sim 0$) and horizon boundary of the wedge relatively uncontaminated, while dipoles have strong contamination throughout the entire wedge region. Other design choices, such as reducing sidelobes and generally improving the stability of the primary beam response with frequency will also be valuable for allowing modes inside the wedge to be recovered. There have also been promising methodological advances that render full wedge calibration realistic in the future [43].

Therefore, when forecasting, we use two possibilities: we either assume that the wedge has been completely calibrated out (optimistic) or that calibration allows use to cut at $N_w = 3$ times the position of the primary beam (pessimistic). This motivated by the notion that for a typical antenna design, the beam response is suppressed at the signal/foreground level at those distances.
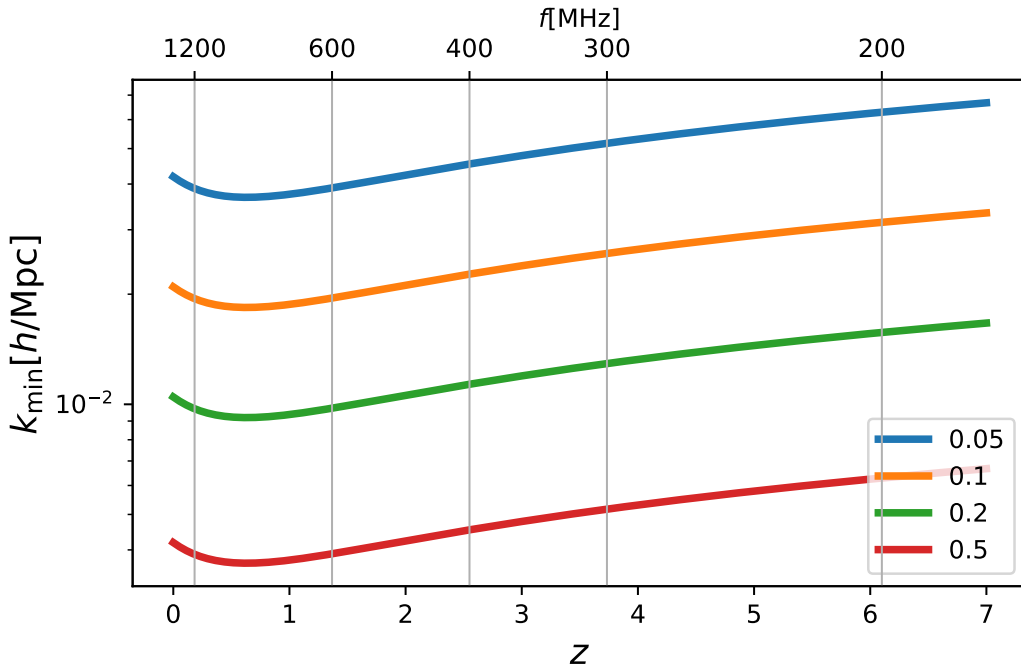
17

FIG. 8. The minimum $k_\parallel$ accessible as a function of fractional bandwidth.
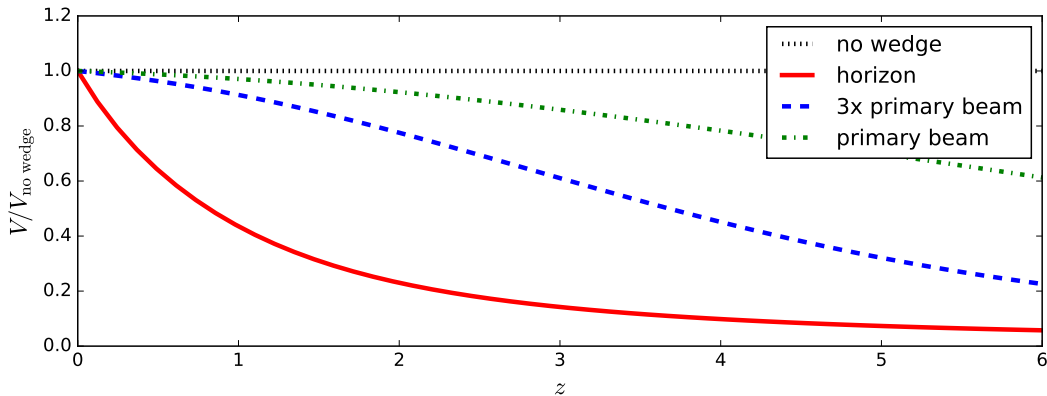


FIG. 9. The effect of foreground wedge on the volume loss for 6m dishes as a function of redshift.

### 3. Early Dark Energy and Modified Gravity

A concerted, community-wide effort to explain the origin of cosmic acceleration over the past couple of decades has uncovered a vast zoo of dark energy and modified gravity models. These can be broadly classified according to how they modify or replace the cosmological constant, $\Lambda$, and/or GR – for example, by adding new scalar, vector, or tensor fields; by adding extra spatial dimensions; by introducing higher-derivative operators in the action; or by introducing non-local operators or other exotic mechanisms for mediating gravitational interactions. Daan: no Refs?

A systematic study of these models suggests a number of new gravitational phenomena that generically arise if there are any deviations from the standard cosmological model. These include the possibility of a time-varying equation of state for the component that sources the cosmic acceleration; time- and scale-dependent variations in the gravitational constant (leading to modifications to the growth rate of large-scale structure and gravitational lensing); and 'screening' effects, where the strength of gravity becomes dependent on the local environment. It is also the case that current constraints on possible deviations from GR are quite weak on cosmological scales, compared to the extremely precise measurements that have been obtained on Solar

18

System and binary pulsar scales. The application of GR to cosmology therefore represents an extrapolation of the theory over many orders of magnitude in distance from where is has been well tested. Precision constraints on GR on cosmological scales are therefore a natural programmatic goal for cosmology.

Observational constraints on possible deviations from GR+$\Lambda$ are only now becoming sufficiently accurate to constrain a wide variety of these scenarios. Recent theoretical work has significantly simplified the task of testing dark energy and modified gravity theories, by collecting the various possibilities into a handful of broad classes, such as the Horndeski class of scalar field theories, which can then be studied in a general sense, instead of on an individual 'model-by-model' basis [46–48]. Although measurement of the speed of propagation of gravitational waves based on gravitational wave event GW170817 and its electromagnetic counter-part GRB170817A [49] has killed a large number of possible modified gravity theories[50–55], large parts of parameter space remains unconstrained.

One can make predictions for observables within the context of these general classes, to see where the possibility of detecting a (potentially quite small) deviation from the standard cosmological model might be maximized. This exercise has so far been performed for a handful of theory classes and observables. In [56], for example, generic predictions were obtained for the behavior of the equation of state of dark energy $w(z)$, within the full Horndeski class. Interestingly, many of these theories predict a 'tracking' type behavior, where $w(z)$ scales along with the energy density of the dominant fluid component at any given time. This leads to the expectation that $w \simeq -1$ at low redshift, $z \lesssim 2$, where dark energy begins to dominate, but $w \to 0$ at higher redshift, deep within the matter dominated regime. This behavior is caused by couplings between the scalar field and the matter sector that generically arise in many branches of the Horndeski theories (although tracking can also be realized in models without such couplings, e.g. freezing quintessence models). The fact that this behavior is a reasonably generic prediction of a large and important class of models (most scalar field dark energy theories are included within the Horndeski class) highlights the need for precision observations in the intermediate redshift regime, $z \gtrsim 2$. If the equation of state can be reconstructed at these redshifts, possible tracking behaviors can be either definitively detected or thoroughly ruled out. Without such direct observations however, it will be difficult to tell whether a transition is occurring, or whether a possible disconnect between observations at low and high redshifts is due to some other factor (e.g. systematic effects). In the next Section 2 4 we discuss how the Stage 2 experiment will measure the expansion history.

It is similarly important to test the growth rate of large scale structure over a range of redshifts, to ensure that possible deviations from GR on large scales have not been missed or absorbed into constraints on other parameters at late times. As with the equation of state, the $z \gtrsim 2$ range is currently lacking in direct observational probes of the growth rate. In Section 2 6 we will discuss ability of Stage 2 experiment to measure the growth rate at high redshift.

## 4. Measurements of the expansion history

Baryonic Acoustic Oscillations are the staple of survey science for the past ten years. They allow measurements of the expansion history of the universe, whose relative calibration is naturally below percent level and whose absolute calibration depends only on the well understood plasma physics in the early universe.

In the early Universe, before hydrogen recombination, electrons, baryons and photons were tightly coupled in a plasma state. Perturbations in this plasma, seeded at much earlier time by inflation, propagated as acoustic waves. After recombination, photons can freely travel through the Universe at the speed of light, and matter behaves as a non-relativistic fluid. Nonetheless, the characteristic distance traveled by the acoustic waves before decoupling, $r_d \simeq 150\,\text{Mpc}$, leaves an imprint in the distribution of matter at late times, generating a peak in the correlation function at $r_d$, or equivalently, a series of oscillations in the power spectrum, known as baryonic acoustic oscillations (BAOs).

These correlations have been successfully detected using galaxies, quasars and the Lyman-$\alpha$ forest [57–61]. In fact, due to differential nature of this measurement (a series of peaks on top of a smooth background signal), BAOs are among the most successful observable in cosmology. Because the physics of early universe is well known, BAO allow us to estimate the standard ruler $r_d$ whose weak dependence on certain cosmological parameters (notably physical baryon density $\omega_b$, physical matter density $\omega_m$ and the radiation content of early universe $N_{\text{eff}}$) is well known and understood. More precisely, the transverse BAOs measures the comoving angular diameter distance $D_M(z)/r_d$ to the redshift of interest, while the radial BAOs measure the expansion rate at the redshift of interest $1/H(z)r_d$.

The beauty of BAOs is that it even in the presence of contaminating signals precise measurements can be derived, because these contaminants typically do not produce oscillations in the power spectrum at he relevant frequencies – in fact these are almost invariably slowly varying function of $k$ on large scales. The current cand future crop of experiments using spectroscopy [57, 62, 63] or 21 cm radiation, see Table I, is focused on delivering BAO as the main scientific product.

Complementary BAO measurements to the next generation experiments, which aim to measure BAO to high precision to $z \sim 1.5$ and with some precision to $z \sim 2.5$ all the way to $z = 6$ is one of the scientific opportunities in our proposed Stage 2 experiment.

In Figure 10 we estimate performance for a Stage 2 experiment. The forecasting was done using Seo & Eisenstein approach **[AS:cite]** adapted for 21-cm measurements. The Figure illustrates that the current generation and planned generation of experi-
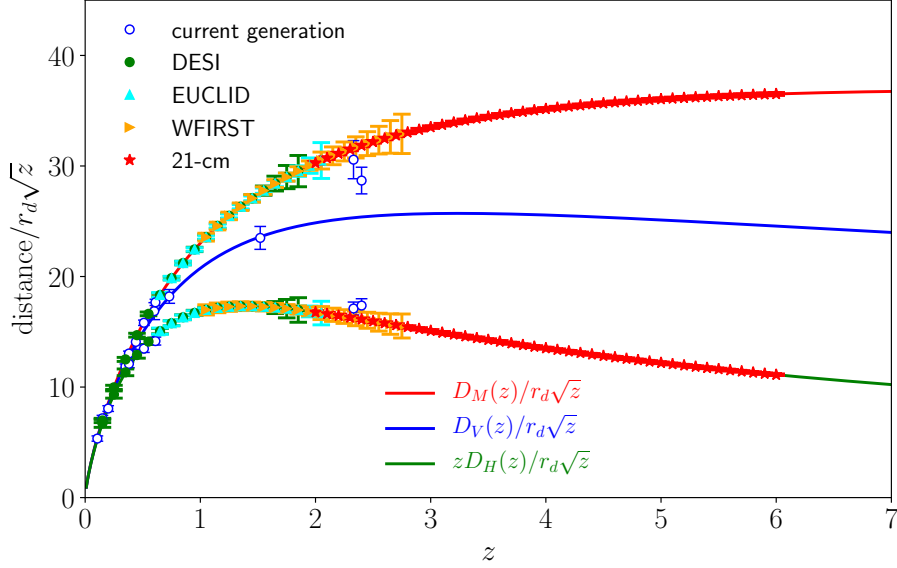
FIG. 10. BAO quantities for a selection of current experiments (empty symbols), a selection of forecasts for the up-cmoming future experiment (based on [64] et al) and a forecast for a Stage 2 experiment (based on [65]). This Figure is an adaptation of Figure 1 from [66]. Lines from top to bottom correspond to transverse, spherically averaged and radial BAO for best-fit Planck $\Lambda$CDM model.
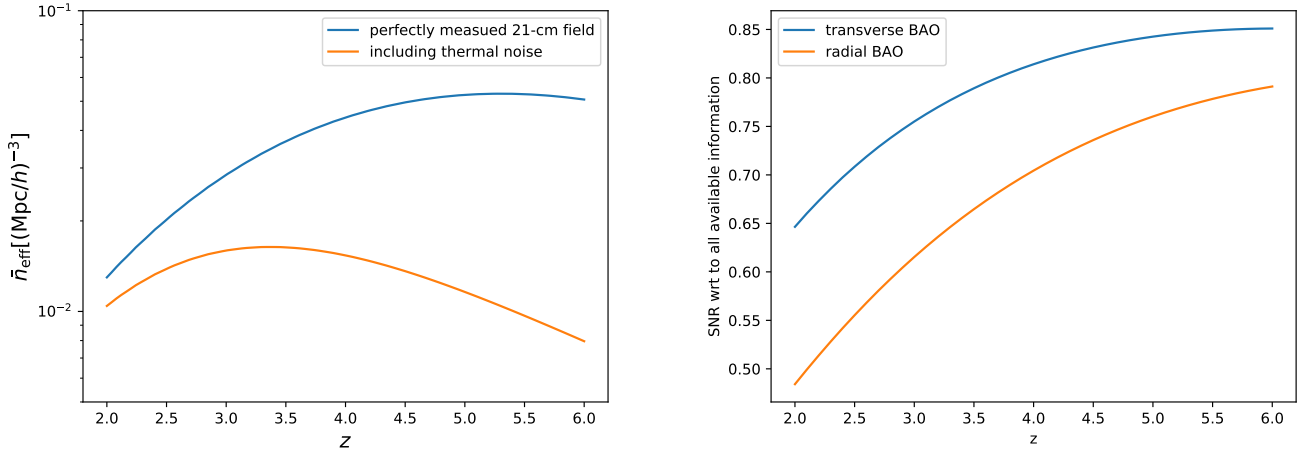


FIG. 11. Left: The effective number density for perfectly measured 21-cm field (blue) and effective number density for Stage 2 experiment after the effect of thermal noise has been accounted for (orange). Right: The fraction of total signal-to-noise obtained by Stage 2 experiment assuming no reconstruction compared to performing BAO measurement on perfectly measured and reconstructed field.

ments loose constraining power at redshifts around $z \sim 2$, while we forecast a Stage 2 21-cm experiment can map the expansion history at high precision all the way to up to the end of epoch of reionization at $z \sim 6$.

This almost incredibly impressive results are result of effectively perfect sampling of the underlying density field by the 21-cm techniques which does not suffer from shot noise in typical galaxy surveys. Since the signal contributing to integrated 21-cm is dominated by numerous small galaxies, the signal-weighted number density of these objects is very high, reaching number densities larger than $10^{-2}(\text{Mpc}/h)^{-3}$ compared to typical values for galaxy surveys which are around $10^{-4} - 5 \times 10^{-3}(\text{Mpc}/h)^{-3}$. The effect of the thermal noise of the system (which is not present in optical galaxy surveys) can be converted into an effective decrease in number density. We see that for our Stage 2 survey this is a modest change. In other words, we are saturating the information content in BAO that can be achieved over half the sky. No BAO experiment could be designed to do considerably better.
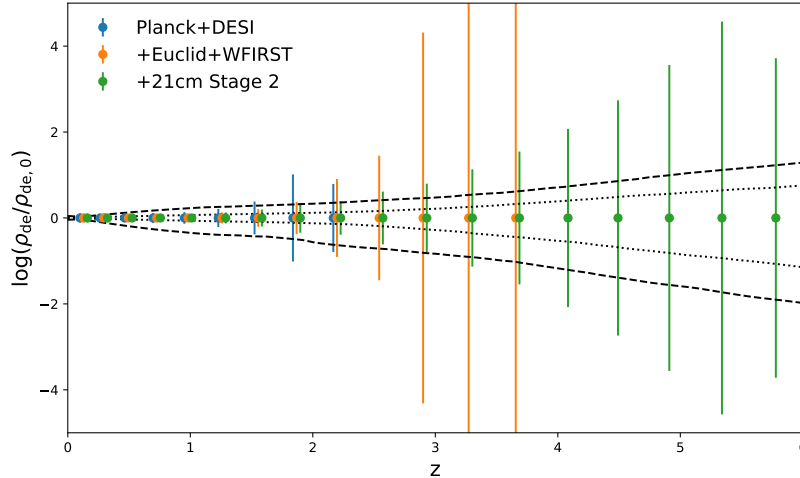
FIG. 12. Constraints on deviations in energy density of dark energy as a function of redshift. The constraints get poorer with increasing redshift, because the energy density of dark energy quickly becomes a very small fraction of the total energy density. Dashed and dotted lines are allowed models for mocker cosmology predicated on current data and data after DESI.

## 5. Cosmic inventory in the pre-acceleration era

**[AS:To be fixed once Phil Bull ads his plots.]** Expansion history measurements can be directly converted into measurements of cosmic evolution. In particular, the expansion history $H(z)$ (directly probed by radial BAO) and the angular diameter distance, given by

$$D_M(z) = \frac{c}{1+z} \int \frac{1}{H(z)} dz, \tag{2}$$

are connected to the evolution of the sum of the energy densities of components in the universe

$$H^2(z) = \frac{8\pi G}{3} \sum_i \rho_i(z). \tag{3}$$

Any non-standard component present in the pre-acceleration era, such as for example an early dark energy, could be uniquely probed by a Stage 2 21-cm experiment as discussed in Section **??** Daan: link not working. In Figure 12 we show forecasted constraints on the energy density in the dark energy component. The fiducial model is the default $\Lambda$CDM paradigm, where the energy density quickly becomes irrelevant at redshifts larger than 2. Consequently, measuring the equation of state of dark energy where it barely contributes to the total energy density content of the universe is hard – hence the errorbars becomes considerably larger towards larger redshift. However, this is also exactly the epoch we expect any deviations to occur.

## 6. Growth-rate measurement in pre-acceleration era

Redshift-space distortions is the name for the anisotropy of the power spectrum along the line of sight caused by the peculiar velocities of sources that add to the cosmic redshift. Since these velocities are sourced by the same fluctuations in the universe, the result is a particular distortion of the power spectrum known as Kaiser distortion. These distortions add a $f\mu^2 P(k)$ to standard power spectrum, where $\mu$ is the cosine of the angle to the line of sight, $f = d\log g/d\log a$ is the logarithmic derivative of the growth factor and $P(k)$ is the linear power spectrum. Given that the shape of $P$ is known to a good degree, the redshift-space distortion in traditional radio surveys measure $f\sigma_8$, where $\sigma_8$ is the linear-theory value of the rms fractional fluctuations in density averaged spheres of 8 $h^{-1}$ Mpc radius at $z = 0$. standard

In 21-cm, the mean signal is unknown, so in effect the redshift-space distortion instead measure the product $\Omega_{\mathrm{HI}} f \sigma_8$ with $\Omega_{\mathrm{HI}}$ being a nuisance parameter. However, there are two main ways to go around this limitation. The first is to use the method of Ref. [65], namely measure the bias from complementary data such as Lyman-$\alpha$ forest, where the source relevant for 21-cm emission appear as individually detected hydrogen systems. In figure 13 we show constraints assuming different levels of
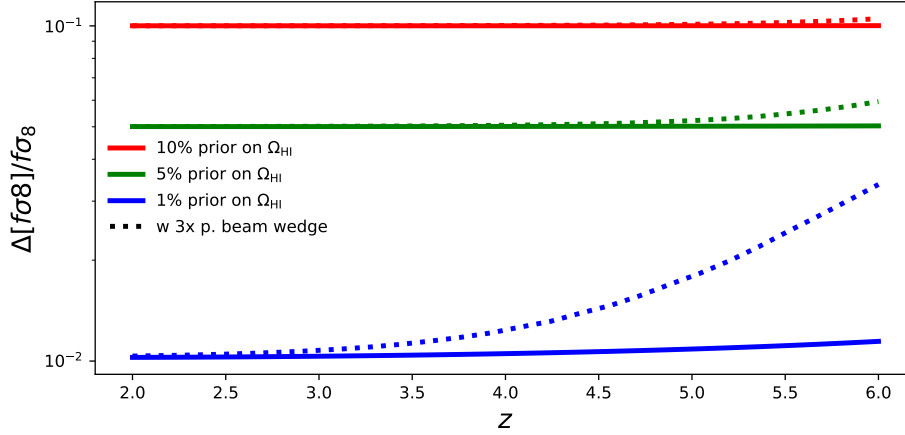
21

FIG. 13. Constraints on the growth rate of structure, $f\sigma_8$, for the Stage 2 experiment assuming priors on $\Omega_{\mathrm{HI}}$ from external data at different levels of accuracy. Dotted lines show the effect of cutting the modes outside the $3\times$ primary beam wedge.

knowledge of the neutral hydrogen abundance. We see that assuming the wedge can be brought under control, the resulting constraints are dominated by this prior if it is weaker than $\sim 1\%$. Alternatively, it is possible to cross-correlate with other tracers at the same redshift as we discuss in Section 2 11 and Figure 16.

Both methods allow redshift-space distortions to be measured with the precision of a few percent. This is also happens at the level where theory modeling of redshift-space distortions becomes more complicated.

We replot the same data in Figure 14 assuming the medium aggressive 5% prior on $\Omega_{\mathrm{HI}}$ together with a selection of current constraints for comparison [67–72]. Theoretical models are the fiducial $\Lambda$CDM model plotted as a solid black line and a moderately tuned modified gravity model plotted as a dashed black line, chosen so that expansion is unaffected at $z > 6$ and that effects are small at low redshift. In particular, we use Horndeski formalism of [48], with $\alpha_{\mathrm{T}} = 0$ and other parameters $\alpha_i(a) \propto (a/a_t)^r/[(a/a_t)^r + 1]^2$. The theoretical models are generated using the `hi_class` package [73, 74]. It is clear from the plot that the Stage 2 will be extremely powerful in telling departures from $\Lambda$CDM growth of fluctuations over significant portions of the evolution of the universe.

### 7. Features in the primordial power spectrum

In addition to BAO, the broad-band power spectrum can be used to search for other features in the power spectrum. The matter power spectrum at a wavenumber $k$ and redshift $z$ in the linear theory is given by

$$P^{\mathrm{matter}}(k, z) = T^2(k, z)P^{\mathrm{primordial}}(k), \tag{4}$$

where $T(k, z)$ is the matter transfer function and $P^{\mathrm{primordial}}(k)$ is the primordial power spectrum. Assuming a standard slow-roll inflation, it is given by $P^{\mathrm{primordial}}(k) = A_s k^{n_s}$ with $n_s \sim 0.96$. There are numerous inflationary mechanisms that would imprint sharp features in the primordial power spectrum (see e.g. [75] for a recent review). Similarly, more exotic physics in the dark sector can add addition acoustic features to the transfer function (see e.g. [76]).

The only such feature in $\Lambda$CDM is the BAO features in the transfer function, whose frequency and phase are fixed by the CMB. Otherwise, the matter power spectrum is smooth function that depends on cosmological parameters. Any sharp feature in observed power spectrum could be cleanly isolated from a change to the BAO or the smooth transfer function. For this reason, these features would also survive non-linear evolution and biasing which also introduce smooth changes to the power spectrum. Mode coupling can only add broadband signals to the power spectrum.

Detecting a deviation from a featureless primordial power spectrum of fluctuations would provide unique insight into the physics of the primordial Universe. These features can provide evidence particular inflation scenarios and the existence of new particles and forces during inflation or in the thermal plasma. The cosmic microwave background (CMB) puts stringent constraints on the amplitude of features, but no significant evidence has been found for such signals [77–81]. In most cases, the amplitude of the feature is a free parameter and could be unobservably small. Furthermore, the precise characteristics of the feature can have a great impact on detectability. For example, although one can distinct two major classes of features, broadly defined as log-spaced and a linear-spaced models, the details can vary significantly, with possible runnings of the frequency [82], locality of the feature [83] and multiple features [84, 85] all possible within the vast landscape of models.
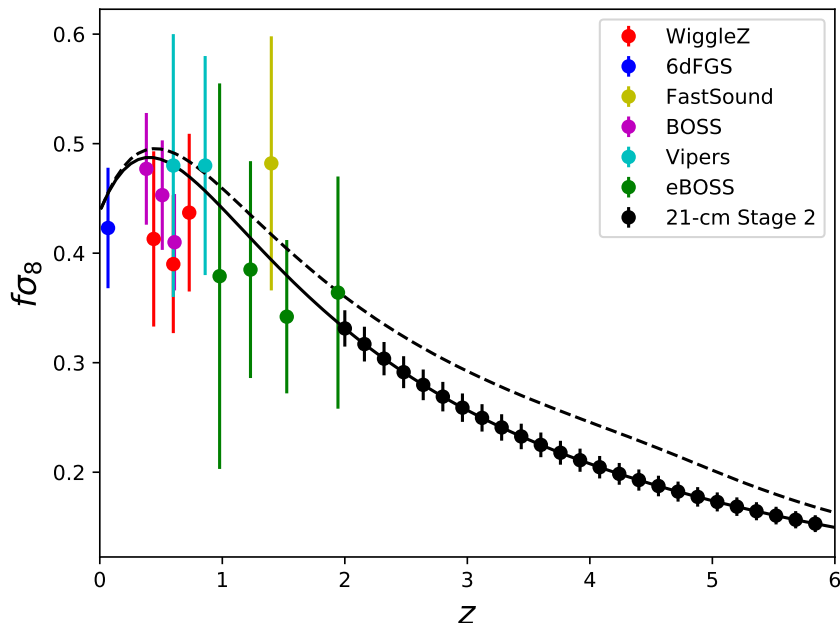
FIG. 14. Compendium of current constraints on $f\sigma_8$ (points) taken from X together with forecasted errors for Stage 2 experiment assuming 5% priors on $\Omega_{\mathrm{HI}}$. Lines are theoretical models: $\Lambda$CDM is plotted with solid line while a modified gravity model described in text is plotted as dashed line.

The 21-cm signal could provide both improved constraints on scales already constrained by the CMB, but also significantly extend the search for features on much smaller scales, beyond those accessible in the CMB. Primordial features are easier to find in the matter power spectrum, relative to the CMB, because of the smooth shape of the transfer function. Furthermore, as can be seen from Fig. 15, 21-cm produces a higher signal to noise measurement than galaxy surveys and can recover more of the small scale modes. These properties make primordial feature a particularly well suited to a 21-cm survey and provides a unique opportunity to explore these models and provide possible evidence for new physics.

Daan: so here we could put a new forecast particularly aimed at Stage 2 redshifts. Mover the old discussions to the DA section.

In Figure 15 we show the total signal to noise in the power spectrum measurement as a function of wave-number. This signal-to-noise can be thought of as most model-independent proxy for comparing different surveys in their ability to constrain these models, because as discussed above the parameter space of models is very large and there no clear priors or measures on this space. We see that the 21-cm covers a very large $k$-range with an exquisite signal to noise.

## 8. Primordial non-Gaussianity

One of the exciting targets of future large scale structure experiments is to obtain evidence for primordial non-Gaussianity (see e.g. [86] for review). In the minimal model of slow-rolling single-field inflation, the primordial density field is perfectly Gaussian. Detection of non-Gaussianity in the primordial field would therefore be immediately informative about the details of inflationary process.

Measurable deviations from Gaussian statistics in the density field are a direct measurement of the particle spectrum and interactions relevant to the inflationary sector. As such, either a detection or upper limit is testing particle physics at inflationary energy scales, which could be as high as $10^{14}$ GeV. These energies are unlikely to be probed in collider experiments and thus are the unique domain of the cosmological surveys. Furthermore, self-interactions of the inflaton that lead to non-Gaussian signatures are often tied to the fundamental mechanism for inflation itself.

These interactions often lead to a non-zero 3-point correlation function (bispectrum) of fluctuations in the primordial curvature $\zeta_{\mathbf{k}}$

$$\langle \zeta_{\mathbf{k}} \zeta_{\mathbf{k}'} \zeta_{\mathbf{k}''} \rangle = \delta(\mathbf{k} + \mathbf{k}' + \mathbf{k}'') B(\mathbf{k}, \mathbf{k}', \mathbf{k}''), \tag{5}$$
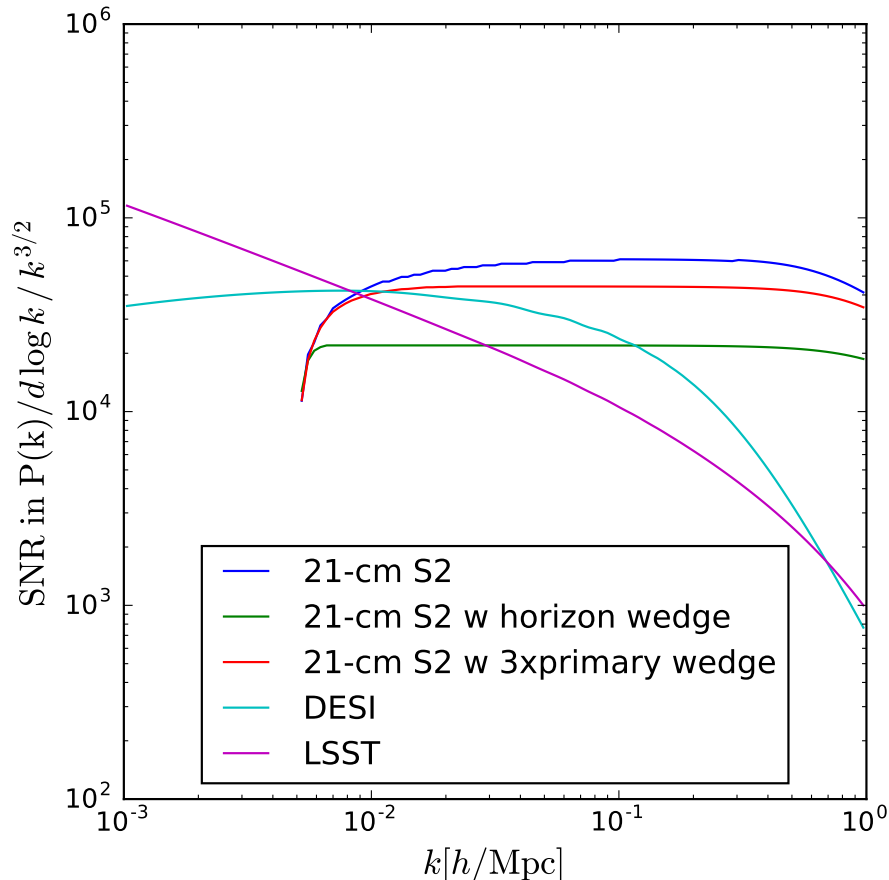
23

FIG. 15. Total signal to noise in the power spectrum measurements as a function of wavenumber. DESI is ultimately limited by the number density of sources, while LSST by the precision of photometric redshifts. 21-cm S2 has the most volume and the most accurate sampling, but it looses sensitivity at low-$k$ due to foreground contamination.

| | $f_{\rm NL}^{\rm loc} \lesssim 1$ | $f_{\rm NL}^{\rm loc} \gtrsim 1$ |
|---|---|---|
| $f_{\rm NL}^{\rm eq,orth} \lesssim 1$ | Single-field slow-roll | Multi-field |
| $f_{\rm NL}^{\rm eq,orth} \gtrsim 1$ | Single-field non-slow-roll | Multi-field |

TABLE III. Table summarizing physical implications for qualitatively different measurements of the shapes of primordial non-Gaussianity, adapted from [86].

where the Dirac delta function is imposed by the translational invariance and $B$ is the bispectrum, whose shape is a function of triangular configuration of wave-vector arguments. A Gaussian field has $B = 0$. Deviations from Gaussian lead to non-zero bispectra, which are described by the shape of the $\mathbf{k}$-$\mathbf{k}'$-$\mathbf{k}''$ triangle that dominates the signal and associate non-Gaussianity parameters $f_{\rm NL}$. There parameters are normalized so that $f_{\rm NL} \sim 10^5$ would correspond to the $O(1)$ non-Gaussianity[3]. References [86] and [87] contain useful pedgaogical reviews.

While the amplitude of $f_{\rm NL}$ reflects the strength of an interaction, the shape, $B$, carries a weather of additional information about the nature of inflation. The local bispectrum, parameterized by $f_{\rm NL}^{\rm loc}$, is one where the shape signal to noise is dominated in the limit of one of the $k$ modes is soft (i.e. $k \ll k', k''$). This shape is of particular interest as it cannot arise in single field inflation and would point directly to multiple light fields [88, 89]. In contrast, equilateral and orthogonal shapes and their respective amplitudes $f_{\rm NL}^{\rm eq}$ and $f_{\rm NL}^{\rm ortho}$ are peak in configurations where $k \sim k' \sim k''$ and are typical of non-minimal interactions of the inflaton itself [90]. The target thresholds are summarized in Table III. With sufficient signal to noise, further information

---

[3] The numerical value of $10^5$ comes from the fact that primordial curvature fluctuations have rms of $\sim 10^{-5}$

| $f_{\rm NL}$ | no cuts | $k_\parallel$ cut | $3\times$ primary beam wedge |
|---|---|---|---|
| squeezed (local) | | | |
| equilateral | | | |
| orthogonal | | | |

TABLE IV. $1\sigma$ constraints on various types of $f_{\rm NL}$ parameters. We consider $k_\parallel$ cut **[AS:to complete]**

718 can be extracted either by considering correlation functions beyond the bispectrum or by carefully exploring the scale dependence
719 of the bispectrum [86]. In principle, from such a measurement once can extract the spectrum particles including masses [91–93]
720 and spins [94, 95], inspiring the name *cosmological collider* physics [94].

721 Current best constraints are coming from the Cosmic Microwave Background [96, 97] indicate no statistically significant
722 deviations from Gaussianity. However, the error bars are too large to draw any meaningful conclusions about the primordial
723 dynamics, which motivates us to explore non-Gaussianity in the large scale structure. Future constraints on non-Gaussianities
724 from the CMB are limited by the number of available modes [98] (although large improvements can still be achieved when
725 considering bispectra involving tensors [99]). With the LSS we have access to a 3D volume of modes and it is expected that
726 constraints from the LSS will eventually become better then those derived from the CMB [86].

727 What makes 21-cm signal unique in this respect is that it present throughout the Universe and in principle could provide us
728 with a volume across the entire sky between redshift 0 and roughly 200 Daan: make this upper limit consistent with the rest of
729 text. The three-dimensional 21-cm field as a probe of non-Gaussianity has been studied in various publications across various
730 redshift ranges [100–110]. Daan: I think we can leave this here. I put a cross reference to this section in DA section. Let me
731 know if it is ok now.

732 In this section we focus on constraints coming from the our proposed Stage 2 experiment (Daan: in the redshift range $2 \leq$
733 $z \leq 6$). We follow the forecasting methodology based on [111]. In particular, the methodology includes a comprehensive
734 list of effects, including the bias expansion for non-Gaussian initial conditions up to second order, redshift space distortions,
735 theoretical errors and trispectrum contributions to the bispectrum. We have expanded the codes used for galaxy forecasting to
736 take into account the instrumental noise by propagating the beam size effects and $u - v$ plane distribution to effective noise in
737 the power spectrum measurements. We have further implemented various cuts to simulate the effect of low $k_\parallel$ cut and wedge
738 effects. Results as summarized in Table IV.

### 9. Weak lensing and tidal reconstruction

740 Gravitational lensing affects any map we make of the universe, by re-mapping the angular coordinates we associate with a
741 given location on the sky. This re-mapping is directly related to the projected distribution of mass between the observer and the
742 source redshift of the photons being measured, without the tracer bias that complicates many other probes of the mass distribu-
743 tion. Therefore, a reconstruction of this re-mapping, either in terms of a deflection field or a decomposition into magnification
744 and shearing effects, can help to address many of the science goals stated earlier, such as constraining the behavior of dark
745 energy, deviations from general relativity, and the masses of neutrinos. A lensing map can further be cross-correlated with other
746 maps of structure, contributing additional constraining power by breaking degeneracies present in individual maps to help us
747 determine the form of tracer bias or isolate systematics.

748 Lensing of the CMB has been detected at high significance (e.g. [112]), and will be one of the main targets upcoming CMB
749 projects such as CMB-S4 [98] and the Simons Observatory. The joint effect of lensing on both CMB temperature and polarization
750 allows for a robust detection in several channels, but since the CMB is effectively a single two-dimensional screen, it only offers
751 access to a single 2d projection of all matter between the observer and the surface of last scattering. Lensing can also be measured
752 from the correlations between observed galaxy shapes in a large optical survey (see Ref. [113] for the current state of the art),
753 and by binning the galaxies by redshift, one can access multiple projections of more nearby structures, with different limiting
754 redshifts and weightings. However, there are multiple pernicious systematics that must be dealt with, ranging from the impact
755 of the telescope's point-spread function on inferred galaxy ellipticities, to control over the uncertainties in photometric redshifts,
756 to the "intrinsic alignments" of galaxies with their nearby environments (e.g. [114]).

757 In some sense, lensing of 21-cm fluctuations represents the "best of both worlds." 21-cm intensity maps have angular resolution
758 and other properties that place them in roughly the same regime as CMB maps, so there is promise that the well-developed
759 estimators and pipelines for reconstruction of CMB lensing can be adapted to 21-cm observations. However, since 21-cm maps
760 will be intrinsically 3-dimensional, they will also enable the same "tomographic" lensing studies as in galaxy lensing, but with
761 finer redshift resolution and free of many of the galaxy-specific systematics mentioned above. The promise of 21-cm lensing has
762 long been recognized in the literature (e.g. [115–119]), and more detailed work has recently been occurring in this area, from
763 both the simulation [120] and analytical [121] sides.

764 Of course, that is not to say that 21-cm lensing analyses will not have their own systematics to account for, but these are
765 steadily being investigated in ongoing work. For example, the quadratic lensing estimators that are standard in CMB analyses

| quantity / experiment | CMB S4 | 21-cm-S2, no wedge | 21-cm-S2, with wedge |
|---|---|---|---|
| Lensing × LSST galaxies | 367 | 676 | 358 |
| Lensing × LSST shear | 178 | 367 | 173 |
| Lensing auto | 353 | 216 | 8 |
| Tidal reconstruction auto | X | 2240 | 266 |

TABLE V. Total signal to noise on measurements of auto or cross power spectra related to gravitational lensing of 21-cm maps. We expect cross-correlations of 21-cm lensing with LSST galaxy clustering or cosmic shear (galaxy lensing) to be measured at a precision competitive with that of cross-correlations with CMB-S4 lensing, with the advantage that the former will contain much more (tomographic) information about the growth of low-redshift structure. The lensing auto spectrum will be more challenging, due to confounding effects from nonlinear clustering in the 21-cm maps [121]. However, these same effects are sensitive to the power spectrum of long density modes at the source redshift, which can be "tidally reconstructed" using similar estimators [121, 124–127]. These measurements can be made very precisely with our fiducial 21-cm instrument, even in the presence of foregrounds.

rely on the Gaussianity and translation-invariance of the intrinsic statistics of the CMB, whereas 21-cm maps will have more complicated statistics that will affect a reconstruction of the lensing map. Refs. [121–123] have shown that these effects will be significant at the redshifts relevant here. Ref. [121] has also presented a technique to mitigate a portion of this impact, which will reduce the additive bias on the power spectrum of a reconstructed lensing map, but will generally increase the noise on an estimate of the underlying lensing power spectrum. In cross-correlations between lensing and other tracers, the additional bias will not be present, but the noise will remain, and this must be taken into account when performing forecasts.

However, the bias on the lensing estimator caused by nonlinear clustering is an interesting signal in its own right, being sensitive to the power spectrum of the long density modes that gravity couples to shorter modes within the 21-cm map. (Note that the long modes referred to here are in the *same* redshift range as the map; lensing also couples long density modes to short modes within the map, but those long modes are at strictly *lower* redshifts than those being directly observed.) These modes can be reconstructed in the same way as for lensing, a process often referred to as "tidal reconstruction" because it chiefly relies on tidal effects [124–127]. This method can be used to reconstruct modes with low line-of-sight wavenumbers, which would be obscured by foregrounds if attempts were made to measure them directly. These modes can then be cross-correlated with the CMB to constrain possible integrated Sachs-Wolfe signatures of early dark energy or modified gravity, or cross-correlated with other measurements of lensing to probe structure growth or neutrino mass.

In Table V, we present forecasts for the total signal to noise on the various auto or cross power spectra related to lensing and tidal reconstruction, applying the forecasting strategy of Ref. [121] to the fiducial 21-cm instrument described in Sec. 2 1. The displayed signal to noise is combined over lensing reconstruction from 10 redshift bins spanning $2 < z < 6$, while, for simplicity, we treat LSST galaxies and shear (i.e. galaxy shape correlations) non-tomographically. We also show equivalent values for CMB-S4 lensing, assuming a $1'$ beam, noise of $2\mu$K-arcmin, and $f_{\rm sky} = 0.4$. Even in the presence of the uncleaned foreground wedge, we expect that cross-correlations of 21-cm lensing with LSST can be measured at a precision competitive with CMB-S4; recall that these cross-correlations will include much more tomographic information than CMB lensing. For the 21-cm lensing auto spectrum, the "bias-hardening" method mentioned above will result in sufficient noise to make this measurement noncompetitive with CMB-S4, even if the foreground wedge can be completely cleaned. Meanwhile, the power spectra of long density modes in each redshift bin can likely be accessed with very high precision, with a total signal to noise of several hundred regardless of the foreground wedge, opening the door the a multitude of cross-correlation science.

The signal-to-noise in these measurements is impressive. Following through with these predictions all the way to their implications for cosmological parameters goes beyond the scope of this white paper, because its main strength will come in particular through interaction of cross-correlations which require assumptions about the existence of other experiments. However, this is a very promising direction to pursue, and warrants further investigations.

### 10. Basic cosmological parameters: neutrino mass, radiation density, curvature

As a natural by-product of measuring the expansion history and precise shape of the power spectrum, we can perform global fits to the observed data in order to improve constraints on some standard and interesting cosmological parameters. While expansion history is directly sensitive to any of the parameters discussed below, it breaks degeneracies with other parameters, that can, in combination with standard datasets such as Planck, often improve results considerably. The shape of the power spectrum depends coarsely on the matter density $\Omega_m$ and the epoch of the matter-radiation equality through their dependence on $T(k)$. Additionally, distances in the universe affect the conversion between observed power spectrum (measured in angles and redshifst) and comoving power spectrum (measured in inverse comoving distance units), effect known as Alcock-Paczyinski test [128]. In practice, redshift-space distortion obscure some of these effects.

In particular, we believe we can provide interesting additional information on:

| parameter / combination | LSST + DESI + Planck | CMB S4 | 21-cm-S2 + Planck? | LSST + DESI + 21-cm-S2 + Planck | CMB-S4 + 21-cm-S2 | everything bagel |
|---|---|---|---|---|---|---|
| $\sum m_\nu$ [meV] | 16 | 59 | 35/29 | 15/14 | 25/23 | 11/10 |
| $\sum m_\nu$ + 3% $\tau$ prior [meV] | - | 15 | - | - | 14/13 | 8.3/8.0 |
| $\sum m_\nu$ [meV] (free $w$) | 32 | - | 38/33 | 17/15 | - | - |
| $w$ (free $\sum m_\nu$) | 0.012 | - | 0.0076/0.0063 | 0.005/0.004 | - | - |
| $N_{\rm eff}$ | 0.051 | 0.026 | 0.046/0.038 | 0.035/0.031 | 0.015/0.013 | 0.0096/0.0091 |
| $\Omega_k$ | | | | | | |
| $w$ for OLCDM | | | | | | |
| EDE params | | | | | | |

TABLE VI. Combination of parameter forecasts for a compendium of future DOE experiments. All combinations assume Planck 15 CMB prior and are for $\Lambda$CDM cosmology unless stated otherwise. In any data combination we assume Planck prior for stability of Fisher matrix result. **[AS:Obuljen, Bull to fill in.] [AO:Used $k_{\max} = 0.4 \, h \, \mathrm{Mpc}^{-1}$ for 21cm and $k_{\max} = 0.2 \, h \, \mathrm{Mpc}^{-1}$ for DESI (LRGs+ELGs only), no BAO damping in both cases; LSST & CMB S4 Fisher matrices from Anže. Two numbers for any combination with 21-cm-S2 correspond to $3\times$primary beam wedge and no wedge, respectively. Used 5% priors on both $b_{\rm HI}$ and $\Omega_{\rm HI}$.]**

**Neutrino mass.** Cosmology is sensitive to the sum of neutrino mass eigen-states $m_\nu = \sum m_i$. We know, from the neutrino oscillation experiments that the minimum value of $m_\nu \sim 0.06$eV in the normal hierarchy and $m_\nu \sim 0.12$eV in the inverted hierarchy. Massive neutrinos affect the expansion history of the universe, but the effect is small. Moreover, they free-stream out of small scales density perturbations, making the field slightly smoother on small scales. Their effect can be detected through a particular scale-dependence of the power spectrum between large and small scales, although this usual takes the form of comparing fluctuation power measured by CMB with fluctuation power measured at low redshift. For extensive review site citecite. The general expectation is that neutrino mass will be detected in the coming years using a number of related methods. In conjuction with standard CMB, DESI should detect it using redshift-space distortions, LSST using weak gravitational lensing of galaxies and CMB-S4 using weak gravitational lensing of background radiation. We expect 21-cm Stage 2 to improve in *all* of the above methods.

**Energy density of radiation.** The amount of radiation in the early universe is usually parameterised by the effective number of massless neutrinos $N_{\rm eff}$. This nomenclature can be misleading, because any component with equation of state $w = 1/3$ like radiation and coupled only gravitationally will contribute to this quantity. This is one of the most important quantity for discovery of new physics. It can be shown that any light particle that was in thermal equilibrium with the Standard Model will contribute an additional $\Delta N_{\rm eff} \geq 0.027$. At the high temperatures thought to be present in the early universe, even very weak interactions are sufficient for thermalization. As a result, percent level measurements of $N_{\rm eff}$ can be an extremely sensitive and broad probe of new physics (see e.g. [129, 130]). Currently the best measurements arise from the CMB+BAO, but future 21-cm measurements of the matter power spectrum could help push the CMB measurement to $\Delta N_{\rm eff} = 0.027$ at more than $1\sigma$ [131].

**Curvature of the Universe.** Global curvature of the universe is a free parameter in Friedman equations, but a modern way to look at it is that it is our way to probe the fluctuations outside the horizon: what is the average density in our observable patch compared to the global critical mean density. In the standard inflationary theories, we expect $|\Omega_k| \sim O(10^{-5})$ and number considerably bigger than this would signal new physics [132, 133]. While it is very difficult to improve significantly upon CMB measurements, improvement of a factor of few are possible. In particular, we can break degeneracies with dark energy parameters [134].

These effects are studied though general Fisher matrix formalism, following the methodology of [65]. We consider the Stage 2 experiment with no wedge and $3\times$primary beam wedge.

In Table VI we summarize these forecasts alone and in combination with some standard cosmological probes that will be available towards the end of the next decade.

Table VI contains forecasts for a number of parameters that will be also focus of the most important DOE-sponsored upcoming surveys.

## 11. Cross-correlation studies

In the next decade, we will see many different probes measure the same volume of space using different tracers and different techniques and the cosmology should enter a golden era of cross-correlations. In general, cross-correlations are extremely useful for two reasons: first, they are considerably safer in terms of systematic effects, because any contaminating signal that is not present in both probes will affect noise, but not the expectation signal and second, because the value of cross-correlations grows as the number of pairs, i.e. with the square of the number of probes, while the total signal-to-noise in auto-correlations grows only linearly.
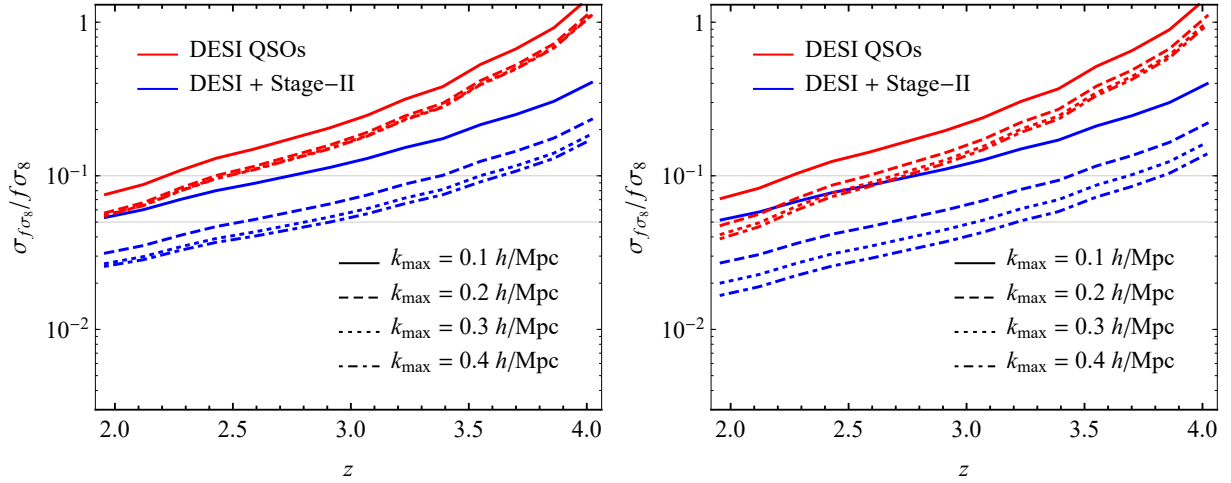
FIG. 16. Predictions for measurements of the redshift-space distortion parameter $f\sigma_8$ using Stage 2 experiment in combination with DESI quasars to calibrate neutral hydrogen bias. **[AS:plot to be iterated]**

Our fiducial experiment has been designed to probe volumes not well sampled by other tracers of large scale structure. Nevertheless, there will be numerous possible avenues for cross-correlation. In the direct cross-correlation, we should be able to obtain signals by cross-correlating with:

- **High-redshift quasars**. These have been measured in larger numbers by eBOSS, but the dataset will gain another considerable boost with DESI. This information will give extra BAO signal and help calibrate both 21-cm and quasar bias parameters (in conjuction with auto-correlation measurements).

- **Lyman-$\alpha$ forest**. The Lyman-$\alpha$ forest has been probed by BOSS, eBOSS and DESI. This cross-correlation will go down to very small scales in the radial direction. Since both probes measure the neutral hydrogen, this cross-correlation will help both probes achieve their full potential [135]. In particular, it will help with measuring the contamination of the Lyman-$\alpha$ forest by damped Lyman-$\alpha$ (DLA) and high column density (HCD) systems and thus bring out full potential of the Lyman-$\alpha$ forest as a probe of a small-scale physics.

- High-redshift forests of other metals. In addition to Lyman-$\alpha$, the high redshift universe also contains other metal forests, like Si III (mixed with Lyman-$\alpha$, Si IV and C IV forest, whose physics and bias parameters can again be constrained in cross-correlations with the 21-cm.

- Lyman-$\alpha$ emitters will be detected in large numbers in surveys like HETDEX [136]. Cross-correlations with 21-cm will allow determination of their physical parameters as well as constrain the interloper fraction coming from low-redshift (whatever they are) lines.

These cross-correlations with other tracers are particularly useful for the 21-cm experiment for a number of particular reasons:

- **Measure bias and enable redshift-space distortions**. Cross-correlation with even low number density tracers can, in conjuction with auto-correlations, constrain bias parameters and thus allow redshift-space distortions as measured by the intensity mapping to be used for determination of growth parameters. This will enable this crucial probe of modified gravity theories.

- **Aid BAO reconstruction.** As discussed in [137], cross-correlation with external tracers is particularly useful to help fill in the missing modes and thus aid reconstruction, which can increase the BAO signal-to-noise.

In addition to direction cross-correlations, there will also be cross-correlations using the large-scale field recovered through tidal-mapping and the weak-lensing of the 21-cm field as discussed in Section 2 9.

## 12. Direction Measurement of Expansion of the Universe

The measurement of the universe's expansion in real time would be the ultimate confirmation of the standard cosmological model. Cosmological sources drift in redshift with the characterizing time-scale of Hubble time. Over a 10 year time-span,
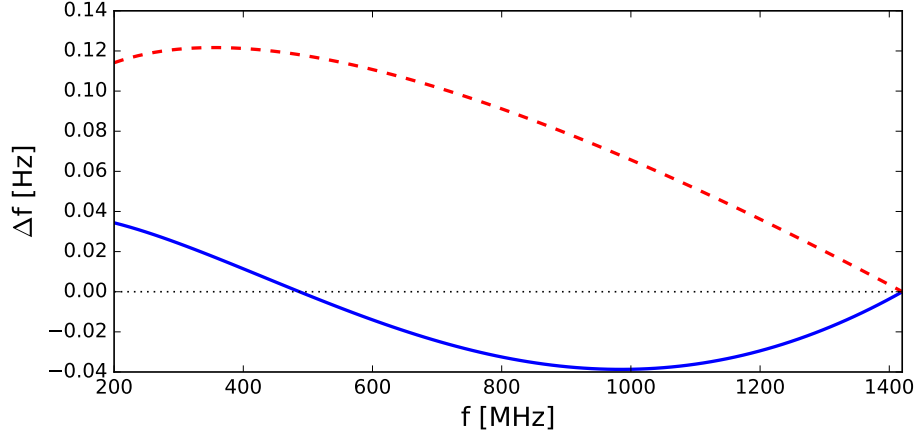
28

FIG. 17. Predicted drift in frequency as a function of frequency for a standard cosmological $\Lambda$CDM model (blue, solid) and flat matter dominated model ($\Lambda = 0$, red, dashed) over 5 years.

this results in the redshift change of around $\delta z = 10^{-9}$. This is challenging both statistically and systematically. However, if measured, it would be one of the very few dimensional quantities that one can measure directly in cosmology[4]. Controlling absolute redshift calibration at the required level over a decade is extremely difficult, but possible in optical [138]. In radio, however, it should be considerably easier, since clock generators with sufficient accuracy are available off-the-shelf. Since in radio system the clock-generator sets the absolute time-scale and thus frequency calibration this dominant part of systematic error is solved. There are additional subtleties to do with subtle changes in the beam due to changes in the physical state of the reflecting material over 10 years, but while these can produce anomalous changes in measured signal, they are unlikely to produce systematic shits and hence we ignore in this section

The basic formula for the redshift drift is given by

$$\frac{dz}{dt} = (1+z)H(0) - H(z), \tag{6}$$

where $H(z)$ is the Hubble parameter at redshift $z$.

In Figure 17 we show a typical prediction for a total drift as a function of frequency for a 5 yr experiment. We see that, in principle, the required accuracy is of the order of $10^{-2}$Hz. If there existed lines whose natural width would be this small, this would have been a trivial measurement. In practice, however, the 21-cm line is velocity smeared to a few 100km/s giving the natural smoothness of the cosmic signal of around $10^5$Hz so one really needs to rely on very precise measurements of the overall structure. On the upside, we see that there is a very definite structure to the shape of this function, so tracing the shift as a function of redshift gives another leverage on systematic control.

There are two basic approaches to this measurement. The first is to rely on a few individually detected sources in the field, while the other is to focus on the entire field, where fluctuations are smaller, but all integration contributes to the signal. In both cases, the scaling is a favorable $t^{3/2}$. This very favourable scaling comes from the fact that signal increases linearly with time while noise falls as $1/\sqrt{t}$.

The first part has been discussed in a recent paper by Yu and collaborators [139]. Although the experiments discussed here would not typically detect and resolve many individual sources, we still expect a few to be detected with high significance. For CHIME, the authors predict 5 sigma detection over 10years.

Alternatively, we can forecast using the entirety of the field. The sensitivity can be estimated using Fisher matrix approach and is given by

$$\sigma(\dot{z}) = \frac{1}{H(z)} \left( \frac{Vt^3}{48\pi^3} \int k_r^2 \frac{P_S(\mathbf{k})}{dP_N/d(t^{-1})(\mathbf{k})} d^3k \right)^{-1/2}, \tag{7}$$

where $V$ is the volume of the survey and $P_S$ and $P_N$ are the signal power and noise power (per inverse year of integration) in comoving space respectively and $k_r$ is the radial wave-vector. This expression is correct even when field is non-Gaussian. We find ...

―――――――

[4] The other prominent examples include time-delays in gravitational lenses that allow us to measure Hubble rate and the temperature of the CMB.

We note that both methods would require saving data at a radial resolution that is beyond what is necessary for the standard cosmological analysis and might increase the overall data-storage requirements by a factor of a few.

## 13. Ancillary Science: Time-Domain Radio Astronomy

### 1. Fast Radio Bursts: A new cosmological probe

The extremely high mapping speed that makes transit interferometers sensitive to large-scale structure also allows them to detect transients at very high rates [140–142]. Of particular interest are fast radio bursts (FRBs), a recently discovered and poorly understood class of radio transient [143, 144]. FRBs are bright, broadband, millisecond flashes, which have now been established to be of extragalactic and cosmological origin [145–147].

A defining feature of FRBs is that they are highly dispersed: their arrival times depend on spectral frequency due to the frequency-dependent refractive index of free electrons in astrophysical plasmas. This dispersion gives a precise measure of the column density of electrons to the burst source, presenting opportunities to study the distribution of plasma on cosmological scales. The large-scale distribution of plasma is poorly understood since it mostly resides at densities and temperatures where it does not significantly emit or absorb radiation. These so-called "missing baryons" have only recently been detected for the first time through stacking analyses of the thermal Sunyaev-Zel'dovich effect [148, 149]. Beyond providing a better understanding of structure formation, a precise measurement of the electron distribution would aid in the interpretation of the kinetic Sunyaev-Zel'dovich (kSZ) effect. The kSZ effect measures a degenerate combination of the electron power spectrum and of large-scale velocity flows. Independent information about the electron distribution would permit the velocity flows to be disentangled, providing a check on the theory of dark-matter structure formation, a probe of the nature of gravity on large scales, and constraints on modified gravity models.

McQuinn [150] proposed measuring the plasma distribution from a sample of FRBs by stacking their dispersion measures on foreground optically-detected galaxies. The contribution to the dispersion measure from the FRB hosts, as well as the redshift-dependent contributions from interloping plasma, can be separated from the signal using its dependence on impact parameter. Such an analysis requires relatively precise sky localizations to significantly better than an arcminute for the FRBs. This could be achieved by adding a number of low-cost outriggers to the array providing $\sim 10\,\mathrm{km}$ baselines.

A second, related method is to measure the 3D clustering of FRBs directly using dispersion, and thus electron column density, as a proxy for radial distance and redshift [151]. FRBs themselves are likely to be biased tracers of the large-scale structure, however, their measured clustering will be distorted by systematic errors in their radial distance measurements from structure in the line-of-sight plasma. These dispersion-space distortions can then be exploited to precisely measure the plasma distribution.

The proposed experiment operates at a factor of two lower frequency than any FRB discovery to date, despite some moderately sensitive searches in this band [152]. At these frequencies, the effects of scattering of the burst signals by inhomogeneous plasma is expected to make them more difficult to detect (although the presence of this scattering helps in interpreting discovered bursts [145]). Nonetheless the instrument should discover between hundreds and thousands of FRBs each day, orders of magnitude more than competing efforts.

### 2. Pulsars: alternative probe of modified gravity

Pulsars are highly magnetized neutron stars that, due to their anisotropic emission and rapid spinning, are observed as lighthouse-like periodic sources that can be used as astrophysical clocks. The extraordinary precision of these clocks permits their use in pulsar timing arrays to search for gravitational waves with light-year wavelengths, as would be emitted by the mergers of super-massive black holes [153–155]. In addition, the extreme compactness of neutron stars permits precision tests of general relativity in the strong gravity regime by tracking the dynamics of multi-body pulsar systems using pulsar timing [156, 157]. These opportunities to test fundamental physics depend on the discovery of new highly stable millisecond pulsars or pulsars in exotic dynamical systems.

Like FRB searches, pulsar searches can benefit from the high mapping speed of transit interferometers. The proposed experiment covers the 200 to 470 MHz band, which includes part of the spectrum that has been identified as promising for discovering the millisecond pulsars [158] that permit searches for gravitational waves and the most precise tests of general relativity. Current state-of-the-art surveys have searched large fractions of the sky, with a few minutes of integration time, using telescopes with order $(100\,m)^2$ of collecting area. Current algorithms for searching for pulsars in collected data require that data to be contiguous in time. As such, a transit interferometer can only integrate down in sensitivity for the duration of a transit which, for the proposed 6 m dishes and 70 cm wavelength, is roughly 27 minutes for a source at the equator and longer at higher declinations. It would take roughly 15 days to survey most of the sky to this depth, at which point the square-kilometer of collecting area and 27 minutes of dwell time would permit the discovery of pulsars 1000 times fainter than current surveys.

In addition, recently proposed algorithms permit the coherent co-adding of observations taken on consecutive days [159], meaning the integration time on a given patch of the sky could be dramatically increased. Depending on the efficacy of these algorithms, which has not yet been demonstrated, this would permit the detection of sources fainter by yet another order of magnitude.

Compared to future surveys, the proposed experiment will be 300 times more sensitive than CHIME, 64 times more sensitive than HIRAX, and 6 times deeper than the maximum depth of FAST (even in a 10-year survey, FAST could only reach its maximum depth over a small fraction of the sky, whereas we are proposing to reach this depth over the full sky). The SKA, having a similar timeline and comparable collecting area, will have a comparable maximum depth. However, due to the non-compact configuration of the SKA antennas, it will only be able to survey a small fraction of the sky to this depth.

## 3. TECHNICAL CHALLENGES AND OPPORTUNITIES

21-cm intensity mapping provides an efficient way to extract cosmological information by building a large radio survey of galaxies capable of mapping the Universe to high redshift [5, 160]. Unlike either optical galaxy surveys or traditional radio imaging, 21 cm intensity mapping accomplishes this by making low resolution, large-area maps of structure at a resolution matched to the cosmological signal of interest. Also unlike traditional surveys, it can uniquely probe the entire history of the Universe through the 21-cm line of neutral hydrogen. While the result is a highly effective (in principle) cosmological survey, the trade-off is that we cannot resolve and image individual galaxies and so cannot use standard radio imaging, processing, and technology, which have all been designed for high-resolution measurements of astronomical objects. As a result, we require new techniques in both analysis and instrumentation and a directed R&D path.

In addition to extending the cosmological science reach of current surveys as noted above, in principle there are no 'show-stoppers' in the measurement itself. First, the anticipated signal level is $\sim 100\mu K$, accessible to array instruments with many detectors. Second, the primary terrestrial signal contaminants come from either the ionosphere, which have been shown to be predictable with GPS data, or from human generated radio frequency interference (RFI), which can be mitigated by a suitable choice of radio-quiet observation site. The most promising of these sites are located within protected radio quiet zones, reducing the risk of degrading the RFI environment in the future. Thus, a ground-based survey is feasible and this allows us to have not simply an instrument, but also a development path for future arrays. **[AS:What do you mean? At z=5, noise is completely dominated by the atmosphere. It is not source of systematic error, but dominated statistical error. LN attempted to address this with updated sentence. ]** Third, the 21-cm transition is extremely low energy and neutral hydrogen is exceedingly abundant, thus there are no other emission lines to act as a source of confusion. We do, however, have to contend with astrophysical foregrounds, primarily synchrotron emission from our own Galaxy, which can be up to five orders of magnitude brighter than the cosmological signal of interest. However, with adequate control on the instrument calibration, we can use the spectral smoothness to separate the foregrounds from the signal. It should be emphasized here that this cleaning removes all sources which have a spectrally smooth shape, including extended sources (our galaxy) as well as radio point sources.

Because the signal is in principle measurable, the remaining challenges for this measurement are *entirely technical*. In this Section, we describe the technical hurdles that 21-cm cosmology faces along three main categories and envision an R&D path that will address them:

- *Technological:* to design and deploy an instrument with optimized sensitivity and stability that has met specifications for instrument characterization and includes sufficient computation power. This will be assessed in all phases (design, testing, integration, deployment, and during operations) to guarantee that we will sufficiently remove the foreground signals and meet sensitivity targets. In Section 3 1 we review the outstanding technological challenges for 21-cm cosmological mapping, heavily informed by the experience of the current generation of experiments. In Section 3 2 we summarize the main R&D areas to address these, and then describe specific technology advances in more detail.

- *Analysis:* foreground mitigation strategies built on knowledge from current generations of instruments. This is discussed in more detail in Section 3 3.

- *Simulations:* To explore additional cosmological parameter forecasts with full instrument characteristics. Simulation needs are described in in Section 3 4.

In addition, in Section 3 5 we relate the technical needs of a 21-cm experiment to historical DOE strengths and capabilities, as well as pointing out opportunities for growth.

### 1. Technical Considerations

While the 21-cm line of neutral hydrogen has been used by astronomers for decades to look at hydrogen in nearby galaxies, its promise as a cosmological tool is far more recent. Early generations of 21-cm instruments have taken a variety of forms. Initial arrays focused on making measurements of the entire sky, at the cost of poor instrument redundancy and characterization, for the purpose of measuring the epoch of reionization around redshift $\sim 8$ [161–165]. This led to a new design which is currently being deployed for the experiment HERA, using dishes which see only a portion of the sky but can be characterized more easily [11, 166, 167]. It was realized in 2006 [160] that interferometers sensitive to redshifted neutral hydrogen could also be used to build a survey of galaxies at unprecedented redshifts to transform constraints on Dark Energy and other cosmological parameters. The first measurements were made on large, steerable dishes [5, 8, 10], choosing a survey region which overlaps with high-redshift galaxy surveys, allowing a detection via cross-correlation. As will be discussed, this instrument choice is limiting at higher redshifts, and so new radio interferometers have been built, dedicated to measuring this signal. The primary instrument is CHIME [168–171], which has chosen a cylindrical dish design to give the instrument a wide field of view in one direction, compromising calibration in one dimension but not in the other, in the hopes that the result can be calibrated. Simulations for

CHIME produced the first specifications on this calibration: the instrument response on the sky ('beam') must be understood to 0.1%, and the time-dependent response of the instrument ('gain') must be calibrated to 1% [172, 173]. Experience from CHIME has shown that these specifications are difficult to meet, and place stringent requirements on redundancy, stability, and early characterization.

• **Required Sensitivity.** In the absence of systematic effects, detecting the 21-cm signal requires fielding instruments including thousands of receivers. The mean brightness temperature of the cosmological 21-cm signal in the redshift range $0.1 < z < 6$ is about 0.1 - 1 mK. State-of-the-art radio telescopes operating in the relevant frequency bands have system noise temperatures that range from 25 K (cryogenic) to 100 K (uncooled) including thermal emission from the ground (beam spillover). As an example of the sensitivity required, consider a survey near redshift $z \sim 1$ that covers half the sky with a spatial resolution of $\sim 10h^{-1}$ Mpc, approximately the nonlinear scale for cosmic structure formation. This scale corresponds to an angular size (in the transverse direction) at that redshift of about $0.3°$ and in the radial direction to a frequency resolution of about 2 MHz. Such a survey would have about $2 \times 10^5$ pixels. At these frequencies, the sky brightness will dominate the instantaneous receiver noise temperature as long as the receiver noise temperature $\leq 100$ K. Assuming 100 K receiver temperatures and a spectral resolution of 2 MHz we would require an integration time of about $4 \times 10^5$ seconds on each pixel to reach 0.1 mK. The survey could be performed with, for example, an array of 4000 receivers operating for 1 year to achieve maps with signal to noise $\sim 1$ on 10Mpc scales at which point information on larger-scale modes will already saturate. In addition, the focus instrumentation, telescopes, and radio correlator must be designed carefully to address cross-talk between channels to minimize correlated noise. **[AS:The last sentence seems out of place here.]**

• **Environmental considerations.** In addition to receiver noise and sky brighness, there are a few other sources of contamination which must be minimized and accounted for in the design process.

• Radio Frequency Interference (RFI) – Radio bands equivalent to the 21-cm redshift range $0.1 < z < 6$ are popular as communications frequencies. This forms a bright RFI signal at discrete frequencies within our measurement band. Because these signals can easily overwhelm the analog amplification, and hence reduce overall instrument sensitivity, radio telescope site locations are chosen to be remote areas with limited communications in countries with suitable infrastructure, such as the middle of South Africa or western Australia [174]. In addition, the digital processing and electronics built for instrument can be the largest source of RFI, and so careful design of RFI enclosures is absolutely critical to the success of the instrument.

• Ionosphere – The ionosphere is a plasma and acts in concert with the Earth's magnetic field to rotate the polarization vector of incoming light. This is proportional to $\lambda^2$, and while it is not expected to impact the shorter wavelengths (frequencies above 500 MHz, $\sim z < 2$), it has been measured at longer wavelengths ($\sim$150 MHz, z$\sim$8). This rotation is proportional to the number of free electrons in the ionosphere and is important for telecommunications, and can be modeled with GPS data and accurate maps of the magnetic field [175].

• The telescope location should also be chosen to maximize 'up time': time the instrument is taking good data. This needs to include reliable power and data infrastructure, a dry location and/or suitable weatherproofing to keep moisture at a minimum in the circuitry at the focus, and ideally a fairly low thermal cycle throughout the day and the year to aid in achieving the instrument stability goals.

• **Astrophysical Foregrounds** Astrophysical foregrounds, primarily synchrotron emission from the Galaxy and unresolved point sources, have much higher intensity than the cosmological signal of interest. These foregrounds have a smooth spectral shape and hence can in principle be distinguished from the 21-cm emission from Large Scale Structure [176–179]. However, any frequency dependence in the instrument response, for example from the instrument beam or gain fluctuations, can complicate our ability to differentiate between the smooth foreground and the essentially Gaussian cosmological signal [172, 173]. Adequately removing this foreground places requirements on our beam and gain that must be carefully integrated into the instrument design, verified during testing and deployment, and include dedicated techniques for instrument calibration.

• **Computing Scale.** Radio astronomy has always been at the forefront of 'big data' in astronomy. Current generation 21-cm instruments produce $\sim$135TB of data per day without any compression, doing an $N^2$ operation on the data where N is the number of elements (currently N$\sim 10^3$), representing a data processing, transfer, and storage challenge. The best compression algorithm would achieve $\sim N \log N$ compression rates [180] but relies on a high degree of redundancy within the interferometer. For order $N \sim 10^4$ elements for future arrays, this compression would reduce the data rate from 13.5 PB per day to 1PB per day. Even compressed, we will record as much data in one month as the LHC does in a year. Like particle physics triggering to reduce data volume, we will also have to explore additional ways to downsample our data, perhaps compressing into maps on a daily or weekly cadence, increasing the pressure on accurate real-time instrument calibration.

## 2. Technologies Enabling Science

Understanding the technical challenges illustrated above allows us to identify dedicated, targeted research and development areas that, when successful, will enable a 21-cm Stage 2 experiment as described in the science case. Here we present first a summary of an R&D agenda, and then go into detail on specific advances and the needs they will address.

### 1. R&D Agenda Summary

Technical areas that we foresee making progress on in the immediate future include:

- 
- 
- 

### 2. Electronics and signal processing

[PWS – This sub-section collects all text on electronic signal processing, ie everything between the pickup and first digital fiber transfers; and is also the current home for details on calibration strategies, parts of which may point to other sub-sections. This will be the longest sub-section by far.]

[PWS – As of 6/21/18 this has all the formerly separate text pieces just gathered together, need now to solidify and trim redundancies all under one roof.]

[PWS – this paragraph seems redundant now and could be taken out.] The primary technical challenges delineated above involve improving the sensitivity and developing technology that can allow for more flexible calibration strategies to meet the foreground removal requirements. We propose a three-pronged development effort: early digitization for improved stability, improvements in beam and gain calibration, and improvements in the noise and uniformity of the radio receiver elements. Together with advances in analysis and computation they can be used to achieve the benchmarks necessary for cosmological measurements.

- **Calibration Drivers and Techniques.** Work in 21-cm calibration focuses on instrument gain and beam measurement for the goal of removing astrophysical foreground power. Current instruments rely primarily on sky signals for calibration, however this has not been adequate to improve foreground removal.

  - Gain Variation – Each antenna has a characteristic response to a signal, which varies with both time and frequency, known as the instrument gain. The frequency-dependent gain for each input must be known to $\sim 1\%$ on time scales between the integration period ($< 5$s scales) and a few hours (depending on the frequency of on-sky radio calibrator sources) [173]. The two primary techniques for achieving this are to design an instrument which is inherently stable enough to meet this specification (as discussed in 'Early digitization' below) or to design a calibration plan which can ensure we meet this specification, or (ideally) both. CHIME [168, 171] is updating a classic radio noise-injection scheme which can be used to calibrate many signal chains at once. To implement such an active calibration technique for dishes will require development of stablized transmission algorithms and may be made easier with early digitization and development of calibration sources which may be independently fielded at the focus or flown on a quadcopter drone. We will also require passive models of gain and beam variation with temperature and dish pointing. This modeling is essentially standard for radio telescopes although precision modelling has been demonstrated with at least one instrument (CHIME).

  - Redundancy calibration – 21-cm interferometric arrays have a history of attempting to use the redundancy of the dishes and spacing to form a real-time on-sky calibration [181–186], however so far these solutions have not proved sufficient to be used in cosmological analysis. This work remains in an early stage of development and so far solutions from the data are not adequate for calibration requirements, however updates using data from current-generation instruments are anticipated to improve these solutions, as will improved uniformity of the array elements.

- **Early Digitization for improved stability.** Analog components (amplifiers and cables) are subject to gain variation, typically due to temperature changes, as the signal travels from the focus of the dish to the later digitization and correlation stages. As noted above, gain variation is one of the limiting factors in removal of astrophysical foreground power. One avenue of development is to digitize directly at the focus of the dish because signal information is "vulnerable" at all points along the analog

34

stages, so the imperative is to digitize as early as possible, after which the signal is (nearly) "invulnerable". The resulting digital signal has more resiliency against time-variable changes in the signal chain, offers the possibility of more flexibility in calibration injection signal algorithms to make gain solutions more robust, and allows us to use commodity or other well-established protocols developed for timing and data transfer. However, this comes at the expense of overcoming the RFI from the digitization in the field, potentially increased cost, and will require all amplification to occur at the focus and thus we may find we need thermal regulation at the focus as well.

Several technology developments make receiver electronics with integrated digitizers (early digitization) a promising technology for 21-cm projects. Critical components that are now available commercially include:

- Room temperature amplifiers with noise temperatures below sky brightness requirements from 100MHz to 1.2GHz.

- Low cost digitizers operating at 5Gs/s with 6 effective bits, with higher cost units providing up to 14-bit resolution. This allows direct digitization of the RF without requiring mixers, high performance band selection filters or high order frequency equalizers, while providing sufficient dynamic range to protect against interfering signals. **[AS:Need to be less precise here, mention trade-offs between digitizer speed and filters, etc.]**

- Low cost programmable logic devices capable of interfacing with a high-speed ADC, providing digital filtering to the frequency range of interest, and interfacing to high speed networks.

- In the near future the availability of integrated RF / ADC / FPGA devices that may provide a path to very compact high-performance receivers

By digitizing at the focus we broaden the possibilities for instrument calibration, bandwidth, and signal processing, however there are a few additional considerations:

- As noted, one of the technical challenges for 21-cm telescopes is the need for high gain stability over at least 24 hours. The primary culprits of gain variation with temperature come from the amplifiers and any analog transmission (either coaxial cable loss or Radio-frequency-over-fiber). By digitizing at the focus, the analog transmission is unnecessary and then any variation will be dominated purely by the amplifiers. The resulting temperature variation can be either mitigated by use of thermal regulation of the circuitry at each dish focus or removed by injecting a calibration signal, or both. Because noise diodes have a gain stability of $2 \times 10^{-3}/°C$, achieving the required gain stability still requires thermal regulation of $\sim°C$. Amplifiers have roughly similar thermal regulation requirements, however they are more difficult to decouple from the environment because they are either connected or embedded in the antenna. Thus, development should be placed towards building calibration sources, digital or otherwise, to enable gain stabilization.

- We must isolate the sensitive RF input with signals in the -100dBm range from the high power digital outputs from the ADC which typically operate near $0\,dBm$. In addition RF radiation from the digital processing system must be shielded from the input and from any other antennas.

- The raw data rate from the digitizer is large, a few $\times 10$Gbit/second. This can be substantially reduced with digital filtering in the FPGA that receives the digitizer data, followed by transmitting only the bandwidth containing useful physics data. For some correlator architectures it may also be useful to transmit data separated by frequency band to an array of correlation processors. The system essentially samples everything up to 6GHz **[AS:Where is this 6GHz suddenly coming from. Even at 5Gs/s we're only getting up to 2.5GHz]** and then digitally filters down to the band of interest. This in theory can do significantly better than an analog filter and should become more cost effective on the time scale of this instrument.

- **Front-end sensitivity, stabilization, and uniformity**

The receiver noise temperature is dominated by loss in the analog feed as well as the noise in the first stage amplification. HIRAX has chosen to reduce the system noise by fabricating the first stage amplifier directly in the antenna itself, reducing the transmission loss and taking full advantage of low-noise transistors available in these bands. We will learn more about the feasibility of this technique for mass production as additional prototypes are fabricated for HIRAX, however it is important to note that current generations of 21-cm experiments [11] have found that their bandpass shape is a limitation of their foreground removal, and are actively working on new feed designs that have a more carefully shaped bandpass. One development path for the active circuitry in the HIRAX feed would be to add additional RF circuitry to flatten bandpass to remove ripple and other features, allowing an easier path for foreground removal.

We expect that we will learn much from the current generation of instruments towards forming a calibration plan for foreground removal, however we anticipate that we will employ a technique known as 'redundant baseline' calibration: similar interferometric baselines should see the same sky signal, and so differences between them can be used to assess relative instrument gains over time. Most 21-cm instruments have chosen their baseline spacing to use this technique, however have been limited by the fact that their interferometric elements are not identical enough to achieve precision calibration. To overcome this,
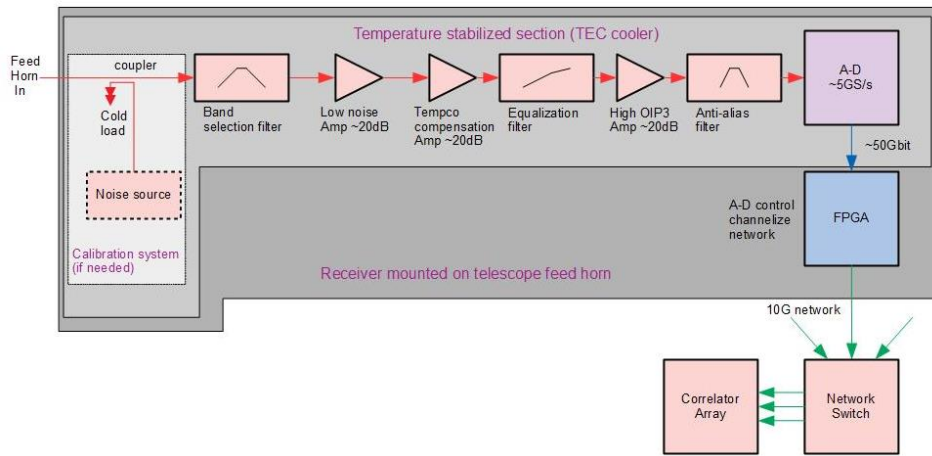
35

FIG. 18. Block diagram for a proposed early digitization front-end.

we would investigate dish fabrication tolerances required for this calibration as well as how we might use new dish fabrication techniques (for example, fiberglass dishes with embedded mesh conductors, currently being prototyped for SKA and HIRAX) to meet these needs. In addition, uniformity between baselines will also allow us to more efficiently decimate our data (either by co-adding similar baselines, or allowing us to form the most efficient FFT-version of this [ref]).

### 3. Analog design optimization *[PWS - Can we just say "optics" here? I defer to LN]*

*[PWS – This sub-section collects all text on dish design and prototyping, including any secondary optics (e.g. horns, sub-reflectors) and receivers. Also includes points on making dishes uniform and minimizing cross-talk, etc., thought that could logically also be moved to Beam Characterization sub-section.]*

- **Optimization of analog design.** Most existing and near-future 21-cm experiments, e.g. CHIME [168], Tianlai [187], HIRAX [140], and HERA [11], all have chosen parabolic reflectors with the receivers supported at the focus with metal legs, leading to some diffraction and reflections. To illuminate the dish, they have also designed open dipole receivers with wide beams that have non-negligible cross-talk and frequency-dependence. These choices are typically made as a cost- and complexity savings, but make calibration more difficult. Further study for optimization, including options such as off-axis geometries (like SKA-mid and ngvLA) and possibly horn/Gregorian receivers, will be important particularly since many of those experiments will have greater experience with the parabolic reflector geometries in the near-term. HIRAX in particular is also experimenting with active amplification in the feed, which can reduce the noise temperature of the receiver by up to 30%, although introduces more stringent oscillation conditions on all amplification stages to reduce the possibility of amplifier oscillation. The optimization would include keeping marginal costs low while also meeting uniformity and bandwidth flatness specifications.

- **Uniform interferometric elements for calibration and data compression.** The two benefits to enforcing sufficient uniformity between receiver elements (dish and receiver chain), and spacing the dishes such that many of the dishes are the same distance apart (so-called baseline redundancy) are: *(i)* redundant measurements can be used as an additional method for gain calibration and stabilization; *(ii)* fewer independent but identical baselines can be used to form an 'FFT telescope' [188–191], allowing us to reduce the data correlation, processing, storage, transfer, and offline analysis from an order $N^2$ scaling to order $NlogN$ for the same overall statistical significance. Many 21-cm interferometers are designed with numerous redundant spacings, however have not yet placed strict requirements on uniformity of each receiver element, and so have found it difficult to take full advantage of the array redundancy. Fully realizing these advantages will place stringent requirements on the uniformity of response, beam shape, mechanical construction and alignment, gain control, etc. across what will ultimately be on the order of thousands of detector copies.

### 4. Beam Characterization

*[PWS – This sub-section collects all text for work on measuring beam response, including drones, satellites, etc.]*

36

- Beam Characterization – Each antenna also has a characteristic response on the sky, known as the instrument beam. Because this response (main beam and sidelobes, as well as polarization) is capable of mixing frequency dependence and sky location, it is expected to be the primary source of contamination from foreground emission into the signal band, and so must be known even more accurately than the gain ($\sim$0.1%) [173]. This level of calibration is difficult for 21-cm telescopes because they are stationary and designed to have large beams for improved survey speed [192]. In addition, some instruments (such as CHIME) have large dish sizes which can be difficult to model and simulate, requiring exceedingly detailed knowledge of support structures and surface mesh (to $\sim$5 centimeter accuracy across each 20 m x 100 m reflector). Many 21-cm instruments are beginning to use quadcopter drones to map the beam shape (HERA[193], SKA[194, 195], LOFAR[196]) and while this technique is likely to meet the needs for 21-cm cosmology it is unlikely we will be able to measure all of the beams from all of the dishes in an instrument with $\sim 10^4$ dishes, and so this beam calibration requirement also forces a specification on uniformity in dish fabrication.

- Gain Considerations – As noted, we require both exquisite control of the gain as well as a high degree of precision in beam mapping. The technology developments currently employed for beam mapping are drone calibration [ref ref ref] and holography [ref]. Depending on the results from the first generation of 21-cm experiments, we may require a steerable dish located near the array to enable holography measurements, and will certainly want to develop beam-mapping techniques with drones that would be suitable for large arrays. We will investigate the possibility of combining drone mapping, holography, and dish baseline uniformity to produce beam maps with the required precision. [PWS – Is this paragraph something of an orphan here?]


## 5. Data flow and processing

[PWS – This sub-section collects any text about R&D projects to help with data flow and any first-stage processing, e.g. building any custom ASIC or FPGA hardware to do correlation products or FFT beam-forming. Note that this is distinct from what's in the later section on Data Analysis, which is about utilizing the primitives for physics.]

- **Scalable Computing.** Computing requirements for a $\sim 10^4$-element interferometer come from both the correlation burden and the storage, transfer, and analysis of the resulting data. We will need to pursue development of back-end computing approaches which can improve the cost scaling both for equipment and power. Examples could be *(i)* generalized GPU programming which will be able to take smoothly take advantage of future hardware, including those in development for next-generation compute clusters at DOE-led HPC resources; *(ii)* using commodity-hosted FPGA's for corollator computing; *(iii)* using/developing dedicated ASIC's, etc.


## 6. Siting and terrestrial RFI mitigation

[PWS – This sub-section collects text on future work to decide on the best site, which should be recognized as an R&D category on its own.]

The frequency range of interest for cosmology is $\sim$ 200-800 MHz, encompassing TV bands ($\sim$200 MHz), cell phones, and various communication and navigation bands. The proliferation of communications over the past few decades has forced new radio telescopes to more remote locations where fewer people mean less radio frequency interference from these sources. The two places remote enough to be able to use most of the 200-800 MHz band, and with the ability to build infrastructure for a large telescope, were selected as the site for the Square Kilometer Array (SKA), in both the Karoo Desert (South Africa) and western Australia. The infrastructure investment from SKA for power and data transmission make these two locations particularly attractive for a site location.


## 7. Physics Algorithm Development

[PWS – This sub-section collects material on R&D work for developing physics algorithms, particularly for dealing with foregrounds; it's not hardware but should be recognized as an R&D area. For now this is distinct from the Data Analysis section, that could be re-visited if too awkward.]

- **Analysis Development.** The technological challenges for 21-cm cosmology include improved analysis and simulations tools, in particular to ensure we can adequately remove foreground emission. First, identifying a reasonable, cost-effective design which will meet all of our goals will require instrument and sky simulations, allowing us to formulate design goals and metrics based on reducing instrument systematics. This analysis must proceed on multiple fronts: initial simulation work for

a fiducial instrument design, adding realistic systematics assessed from current experiments, implementing analysis techniques for mitigating these systematics from those same experiments, systematically combining these techniques across the full redshift range, and identifying the resulting requirements on instrument design. This will allow us to make informed instrument choices to determine cost effectiveness of various options and identify where we require additional effort. In addition to helping specify instrument design requirements, it will potentially allow developments in a variety of ongoing analysis techniques in the field, including redundant baseline calibration algorithms and foreground removal strategies consistent across all frequencies. This analysis effort requires a full end-to-end simulation pipeline based on current work in the 21-cm field and initial work performed for this white paper with a tight connection between the theory, analysis, and instrumentation groups.

[PWS – Nominal end of section 3.2]

## 3. Data Analysis

Delivering science results from 21-cm data sets depends crucially on developing robust data analysis techniques to deal with astrophysical foreground contamination **(and probably other things)**. Even an ideal instrument couples anisotropy in the astrophysical foregrounds into spectral structure with amplitude sometimes in excess of the cosmological signal. There exist in the literature many proposed techniques to separate the cosmological signal from the foregrounds, and a requirement for any 21-cm survey is that these techniques be tested on realistic simulations of data from a proposed instrument configuration.

Foreground mitigation falls broadly into two classes: foreground avoidance and foreground cleaning. Foreground avoidance is the simplest of these two approaches, relying on the fact that contamination produced by a typical interferometer configuration is strongest in certain regions of $k$-space. Producing cosmological results only using the cleanest modes is a simple and effective technique. This technique, however, becomes deeply unsatisfactory at low frequencies, particularly in the dark ages. Here galactic synchrotron and extragalactic point source radiation quickly becomes very bright, typically hundreds of Kelvin at 100 MHz, even at high galactic latitudes. At the same time the window of clean modes dramatically narrows due to the relative scaling of the angular diameter distance and Hubble parameter with redshift [Pober]. Combined this means that at a given threshold for contamination we exclude increasingly large regions of $k$-space at high redshifts, significantly degrading any cosmological result.

Foreground cleaning in conjunction with foreground avoidance then becomes an attractive option. A general feature of foreground cleaning methods is that they rely on detailed knowledge of the instrument response to predict and subtract the actual foreground signal. For instance, given perfect knowledge of the complex beam of each individual antenna, a tomographic map of the sky can be effectively deconvolved to remove the spectral structure induced by the instrument's beam. The residual contamination is set by both the amplitude of the raw contamination and the accuracy with which the beam has been measured. This is similar in spirit to the residual temperature-to-polarization leakage produced by mismatched beams of orthogonal polarizations in CMB $B$-mode searches, which can be accurately predicted and removed given beam measurements despite the fact that the CMB temperature anisotropy "foreground" is orders of magnitude larger than the $B$-mode signal.

The efficacy of any data analysis method depends on a number of factors. There are some which are simply properties of the real sky, such as: the amplitude of the foregrounds relative to the 21-cm signal; and the spatial and spectral structure of the foregrounds. These we cannot change, except by attempting to exclude regions of the sky where they are most problematic. However, there are some factors that we can control through design:

- the optical design of the instrument, particularly the baseline distribution and the primary element, which controls the amount of foreground contamination

- the time stability of the instrument, both the analog signal chain which controls the magnitude of calibration errors, and the optical stability which makes requirements on beam knowledge time dependent

and some that we control through dedicated systems and analysis stages. In particular how we perform:

- real-time instrument calibration, particularly for analog gains

- offline calibration, generally targeting understanding beam properties.

All of these factors, in addition to the more easily understood noise temperature of the front end amplifiers and sky, combine to determine the ultimate errors on cosmological parameters.

In principle, the performance and robustness of any data analysis technique can be tested on a suite of simulations that include the above effects and that bracket a sufficiently wide range of assumptions regarding both the astrophysical foregrounds and the instrument performance. It is possible that different analysis techniques are optimal at different frequencies or for different science goals, but these can and should be tested before committing to a final design. Furthermore, the instrument design should be informed by the requirements of the analysis.
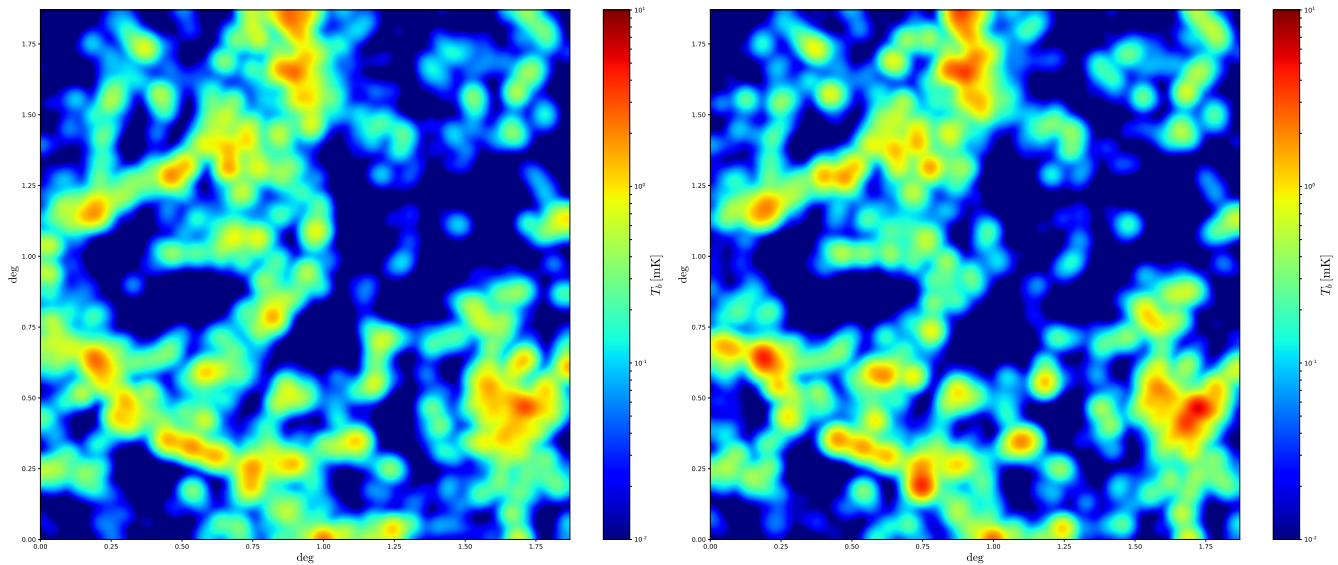
FIG. 19. 21cm maps at a frequency of 710 MHz over a channel width of 1 MHz with an angular resolution of 1.5' over an area of $\simeq 4\,\mathrm{deg}^2$. The left panel has been created from a state-of-the-art hydrodynamic simulation with a computational cost of more than 10 million cpu hours. The 21cm map on the right panel has been made by painting HI on top dark matter halos of an N-body simulation using the a simplification of the ingredients outlined in [197], whose computational cost is several orders of magnitude lower than the full hydro.

## 4. Simulation Needs and Challenges

The challenges facing 21-cm surveys are significant but, at least to $z = 6$, well understood. Producing realistic simulations of data from any instrument configuration and propagating these simulations to final cosmological results is therefore an entirely realistic prospect. The steps are straightforward: (1) produce a suite of full-sky maps of the "true" sky, with one map per frequency and at each frequency bin observed by the instrument**[RS: Is it ever important to account for the exact channel shape which requires generating higher frequency maps and integrating over then channel shape]**; (2) "observe" these maps with a simulation pipeline that contains sufficient realism to capture any and all non-idealities that might produce contamination in the data; (3) feed these mock observations into the data analysis pipeline discussed in the previous section, and the same pipeline that would be used on real data, and produce reduced data and cosmological analyses.

Regarding (1), **[FV: it has been shown that one can take advantage of the fact that neutral hdyrogen in the post-reionization era resides almost entirely inside dark matter halos[197]. Thus, one can calibrate the relation between dark matter halos and HI using hydrodynamic simulations and create 21cm maps via less expensive methods such as N-body or fast numerical simulations like COLA [198].]**

For verification of foreground removal effectiveness gaussian or pseudo-Gaussian 21-cm simulations are largely sufficient [CoLoRec, Alonso; maybe CORA]. However, for targeting sensitivity to specific effects (e.g. non-Gaussian initial conditions), or in cross-correlation with other probes, more accurate simulations constructed from mock-catalogues will be required. This allows us to produce correctly correlated maps for additional tracers (e.g. LSST photometric galaxies), and also for radio point source contribution to the foregrounds. However, the mapping of HI mass into halo mass is still uncertain and will limit the accuracy of such simulations. **[FV: Thus, calibration of those ingredients versus hydrodynamic simulations is desired.]**

As the dominant foreground contribution simulating the galactic synchrotron must be done with care, to ensure that the simulations are not artificially easy to clean. Conceptually a simple approximation can be produced by proceeding from a full sky map at a radio frequency (typically the HASLAM radio survey map at 408 MHz) and scaling this map to different frequencies based on the known spectral index of galactic synchrotron radiation. However this is not sufficient at the dynamic range between the foregrounds and the 21-cm signal and we must be careful to include: spectral variations about a pure power law; small scale angular fluctuations not captured in existing survey; and polarization, including the effects of emission at a wide range of Faraday depths which generates significant spectral structure in the polarized emission.

This last effect means that ideally a 21-cm array should therefore be able to reject polarization with high fidelity lest polarization-to-temperature leakage occur, a reverse of the corresponding temperature-to-polarization leakage problem in CMB. Simulating the effect of mismatched polarization response is therefore crucial, emphasizing the need for accurate simulations of the polarized radio sky to proceed [CORA and CRIME]

In this step, one can change assumptions about the spectral index, the existence of spectral features beyond a power law in the frequency scaling, or spatial variation in the spectral index, to test the robustness of data analysis techniques. A possible model

for how such an analysis would proceed is the CMB Stage-IV $r$ forecasting work, which has similarly explored the range of bias and error on $r$ resulting from incorrect assumptions about the frequency scaling of galactic dust and synchrotron foregrounds.

Regarding (2), a realistic instrument simulation pipeline would take the maps discussed and convolve them with the complex beam for each antenna in the interferometer. This can be done by direct convolution utilising the fact that for a transit telescope it is sufficient to generate a single day of data. However for wide-field transit interferometers this can be more efficiently performed in harmonic space using the $m$-mode formalism ($O(N \log N)$ instead of $O(N^2)$). **[RS: My experience is that the convolution step isn't actually that bad, so I'm not sure if ultimately it will be the most costly step — so I removed that statement]**

For these simulations we need to generate realistic simulations of the telescope beams. Electromagnetic simulation codes such as CST, GRASP and HFSS can be used for this, but achieving the accuracy required is challenging computationally [Tianlai beam paper; HERA beam paper; CHIME beam paper]. An alternate approach is to generate synthetic beams with sufficient complexity to capture the challenges posed by real beam, these are computationally easier to produce, but must be informed by real measurements and electromagnetic simulations to ensure their realism.

Capturing non-idealities in the analog system particularly gain variations in the data, and 1/f noise is mostly straightforward as these can be applied directly to the ideal timestreams. Additionally we need to add in variable sources of emission that may effect our observations such as solar, jovian and lunar emission as well as the effects of RFI at low levels [Harper et al. – satellite RFI for BINGO].

The mock observations are then fed to the data analysis pipeline. In the case of foreground cleaning methods that make use of calibration data, the effect of measurement precision in the calibration data can be tested by perturbing the "known" instrument properties to produce mock calibration data. Ideally, as the noise in the calibration data goes to zero, the contamination in the results also decreases to zero. This procedure can be used to produce benchmarks for gain calibration, beam calibration, etc etc.

MW: As a strategy question, might we not be well served by saying this is a problem where we poor folks could use the help of the Labs and the big-iron simulators, who would then have one more thing to tell DOE they're doing? Isn't DOE wonderful at doing these end-to-end simulations with the science team, instrumentalists and phenomenologists operating together as a single collaboration – unlike those heathen Astronomers?


## 5. Relation to DOE capabilities

This chapter has enumerated analysis challenges for turning the idea of efficiently mapping the universe on large scales using 21-cm radiation into reality. These challenges are not unlike turning the idea of "colliding protons to learn about Higgs" into ATLAS and CMS, two of the biggest and most complex instruments in the history of humanity. If accelerator physics we also turn data from imperfect detectors into useful science output by applicaiton of multi-level calibration schemes realized through careful project management, instrument production and ultimately a complete end-to-end numerical simulation of the measurement process. DOE has unique advantages and history in this field which makes it a particularly useful home for development of this experiment. We divide them in several categories discussed below: technical, management and simulation.

**Technical capabilities.** The first commonality between radio receiver and particle accelerators lies in the RF mode manipulation used to match RF sources to waveguides, and waveguides to accelerator structures. The hardware that performs these mode manipulations is closely related to the matching optics used for radio telescopes. Although the purpose of optics is different, the tricks of the trade remain broadly similar and it is possible to imagine rich cross-pollination of ideas.

DOE also has significant experience with high channel count RF and digitization systems used for the control and diagnostics of large particle accelerators for high energy physics and basic energy science. A large accelerator such as the SLAC LCLSII can include over a thousand channels of RF front ends and high-performance digitizers connected to a distributed data network. In detail accelerator RF systems are optimized differently than radio telescope front ends, with typically higher dynamic range, and lower bandwidth and noise performance, however there remains a lot of commonality between the designs. Once signals are digitized, they need to be moved around using massively multiplexed digital data highways for further real-time processing. The US ATLAS collaboration which currently operates at 25GB/second and near future X-ray detectors are planed to operate at over 1TB/second. Platforms such as FELIX and gfex, that were developed by DOE with accelerators in mind can find very direct applications in real-time 21-cm signal processing.

**Management capabilities.** As we discussed repeatedly in this chapter, part of the calibration strategy is to have elements that are produced to be similar enough that per-element calibration does not need to be complicated. This requires careful management, quality control and metrology. DOE projects include high multiplicity arrays for large scale particle detectors including collaborating on ATLAS and CMS, as well as detectors for X-ray imaging, LSST focal plan detectors and CMB Stage 4 bolometers.

Finally, DOE has experience running large collaborations, traditionally in accelerator particle physics with ATLAS and CMS detectors, but ore recently also in cosmic frontier with the LSST Dark Energy Science Collaboration. The later is at the vanguard of full system simulation with the DESC Data Challenges. Not such effort has been ever been undertaken in traditional astronomy community. As it was argued in this chapter, it will be absolutely essential to perform realistic end-to-end simulations for 21-cm Stage 2 experiment.

**Computing capabilities.** All stages of developing this experiment will require large involvement of computing facilities. The full system simulation as well as actual data processing will require high-throughput computing and efficient storage, handling and processing of massive amounts of data. This can be efficiently addressed through existing and planned infrastructure facilities within the DOE laboratory complex that will also drive new developments in network connectivity between DOE sites. DOE manages NERSC, one of the world's largest high-performance computing systems and has put significant investment into an exascale computing at Argonne National Lab and Oak Ridge National Lab. It also hosts two CERN Tier-1 data centers.

In addition to challenges presented by the data volumes alone, there are massive algorithmic challenges that can be efficiently addressed using existing DOE structures present within Advanced Science Computer Research (ASCR) and SciDAC. On the simulation side these includes running large simulations of the universe. On the data analysis sides, the calibration problems and foreground removal problems can be recast in terms of large-scale linear solvers, error analysis, kernel estimation, machine learning, etc. These problems will benefit from developments in the current exascale initiative and work that has been done on hybrid compute architectures that can be particularly efficient ith large data rates.

At the moment there are small path-finder efforts at various labs not directly funded the by DOE HEP. At BNL a small test-bed experiment BMX has been set-up operating at 1.1-1.5GHz. It has been taking data for 9 months and 100 day cleanest data has been analysed. The results are promising despite the experiment being situated at the lab site which is an extremely poor location in terms of RFI. Early science results include characterization of out-of-band emission from global navigation satellite services that will act as a potential systematic for low-redshift experiments. As the test-bed the system will be used to test various approaches towards beam and gain calibration as well as early digitization prototypes.

At Fermilab, . . .

At SLAC (?), . . .

## 4. FUTURE: SCIENCE WITH DARK AGES

### 1. A new window into the Universe

In the CMB, well-understood linear processes are sufficient to relate observed anisotropies in temperature and polarization to perturbations in the energy density generated during the early universe. This is what makes the CMB such a powerful probe of fundamental physics, limited mainly by diffusion damping [199] that erases anisotropies (and therefore primordial information) on small scales. On the other hand, lower-redshift large-scale structure in principle offers many more accessible modes, but a large portion of these modes are affected by nonlinear processes that are difficult to model. These nonlinearities are less severe at higher redshift: in particular, before the first collapsed objects formed at $z \sim 30$, the limiting scale is the Jeans scale, $k_{\mathrm{J}} \sim 300$ Mpc$^{-1}$ [200]. Since the number of linear modes scales as the cube of the maximum linear wavenumber, observations at this epoch hold great promise for increasing our knowledge of fundamental physics.

The only observable available to us during this epoch is the 21cm hyperfine transition of neutral hydrogen.[5] The theory of the high-redshift 21cm signal is very well understood [202, 203], and for most purposes is well described by linear perturbation theory [200]. From a practical standpoint, the signal, which is in absorption against the CMB back-light, will be very hard to observe for many reasons that are similar to those that hinder the detection of 21cm emission at lower redshifts. In addition, a 21cm photon originating at these very high redshifts will redshift into the low MHz wavebands, which will be hard to observe from the ground due to reflection by the ionosphere. It is estimated that this limitation becomes significant for $z \gtrsim 45$ ($\nu \lesssim$ 30MHz [204]) **[SF: added cite for ionosphere reflection frequency]**, and any signal beyond that would require an experiment outside of the ionosphere, such as in space, or, as has been proposed in Refs. [204**?** , 205] on the far side of the moon. **[AS:Ok, here we need to make sure how hard-core this 45 limit is and put it on the same footing as intro.]**

This certainly implies that any measurement will be very far in the future. For this reason, we will not suggest a specific experiment (which would come with a unique set of limitations), but instead remark upon the general potential of an experiment targeting these observations, that would inevitably build on the progress made with lower-redshift detections. Simply put, the high-redshift 21cm signal will provide a three dimensional window into the linear Universe, providing access to of order $10^{10}$ more modes than the CMB.[6] This tremendous amount of statistical power makes 21cm measurements from the Dark Ages the ultimate probe of the conditions in the early Universe. Exquisite constraints could be expected on many quantities of interest [202], such as the scalar spectral index [206] and primordial non-Gaussianities [101, 102, 207].

Before we present a unique science target, let us briefly highlight two observables discussed earlier, namely features (Sec. 2 7) and non-Gaussianties (Sec. 2 8) that a probe of the Dark Ages could significantly improve.

The detectability of features at high reshifts depends critically on the amplitude, frequency and scale-location of the features, as well as the angular and redshift resolution of the experiment. Forecast show [208] that a cosmic variance limited 21 cm experiment measuring fluctuations in the redshift range $30 \leq z \leq 100$ with a 0.01-MHz bandwidth and sub-arcminute angular resolution could potentially improve bounds by several orders of magnitude for most features compared to current Planck bounds. At the same time, 21 cm tomography also opens up a unique window into features that are located on very small scales ($k \gg 1$ Mpc$^{-1}$).

Besides features in the power spectrum, the same physics generally produces features in all primordial correlation functions. The 21-cm field as a probe of non-Gaussianities and specifically to constrain the bispectrum has been explored in Ref. [106]. Of particular interest is the possible detection of massive particles in the early Universe. Heavy particles with higher order spin can leave distinct features on higher order correlation function [95, 209]. The signal is predicted to be very small but a detection would present the first evidence for a mass hierarchy as predicted by string theory [94]. Because of the smallness of the signal, 21-cm has been suggested [102] to provide the only realistic observable to constrain the presence of these particles. We refer to Ref. [102] for details of the models that could potentially be observed with 21-cm.

Now we will present a single example that is rather unique, concerning the potential signatures of primordial gravitational waves in fluctuations of the observed 21cm intensity. We describe these signatures below, and provide estimates for their constraining power on the amplitude of gravitational wave power left over from the early Universe.

### 2. Gravitational tensor modes

One of the holiest grails in our attempt to understand the physics of the early Universe is the possible detection of primordial gravitational waves. These can be generated by the same early-universe process that generates the seeds for the (scalar) density fluctuations that we observe in the CMB and large-scale structure. Within the paradigm of inflation, the expected level of

---

[5] There is also a hyperfine transition in deuterium nuclei, corresponding to photons with wavelength 92cm. This is in principle observable with the same interferometers designed for 21cm, and would yield a pristine measurement of the primordial deuterium abundance, but will be a much more challenging observation than 21cm [201].

[6] Assuming $10^4$ independent redshift slices in this redshift range, each with for $\ell_{\max} = 10^6 \simeq \ell_{\mathrm{Jeans}}$ [202].

primordial gravitational waves generated during inflation is measured with respect to the production of scalar fluctuations by a relation of the two primordial power spectra:

$$P_\zeta \;=\; A_s k^{-3} \left(\frac{k}{k_*}\right)^{n_s-1}, \tag{8}$$

$$P_h \;=\; r A_s k^{-3} \left(\frac{k}{k_*}\right)^{n_t}. \tag{9}$$

In single-field slow-roll inflation, some of the parameters above are related by $n_s = 1 - 2\eta - 6\epsilon$, $r = 16\epsilon$, and $n_t = -r/8$. Here $\eta$ and $\epsilon$ are two slow-roll parameters, which are proportional to the second and first derivative of the scalar potential respectively and are required to be $\ll 1$ for inflation to last a sufficient time to solve the horizon and flatness problems [210]. In more complicated models, including those with multiple fields, deviations from slow-roll, and non-canonical kinetics, these relations will be altered, pick up additional degrees of freedom, or break altogether. The relation between the scale dependence and the amplitude of primordial waves is particularly interesting. A deviation from a red spectrum would indicate a violation of the null energy condition, and suggest the spectrum was not generated from the vacuum (see e.g. [211, 212]), or could rule out inflation as the source of gravitational waves [213].

Current attempts using the B-mode polarization signal in the CMB aim to detect $r$ as low as $10^{-3}$ [98], providing an interesting science target in terms of the field excursion during inflation [214]. Unfortunately, it is quite possible given the nature of $r$, which effectively describes the energy scale of inflation, that the actual level of primordial gravitational waves is orders of magnitude below $10^{-3}$. Measurements beyond this level will be difficult using CMB B-modes, mostly due to B-modes generated through lensing of E-modes, which obscure primordial B-modes at the level of $10^2$ for ground-based observations. Delensing methods can mitigate a large fraction, but this becomes increasingly hard for smaller values of $r$ Ok, I have to check this statement more carefully. At the very least we know there wont be any lensed scalar contribution in 21cm since there is no intrinsic 21cm polarization at high redshift Many other probes of primordial gravitational waves face significant challenges. For example, direct detection using interferometers (e.g. LIGO and (E)LISA) is unlikely given the relatively small scales probed by such experiments [215], and methods utilizing the polarized Sunyaev-Zel'dovich effect require very low noise levels in the CMB and an exquisite measurement of free electrons in the Universe [**?** ].

Measurements of large-scale structure during the Dark Ages will be affected by a gravitational wave background in several ways, and observations over a large enough volume have the potential to see these effects at high significance. We will highlight two such effects here:

1. **Tidal fossils**: After a large-scale tensor mode enters the horizon, it will induce a specific kind of inhomogeneity into the statistics of the density field, similar to what happens with the tidal field generated by scalar perturbations at second order. While the original tensor mode will decay with time, its imprint on large-scale structure will not, leaving behind a "fossil" that can be detected at later times using an appropriate estimator [125, 216, 217]. The power spectrum of this estimator is directly connected to the primordial tensor power spectrum, and therefore to the tensor-to-scalar ratio, with constraining power scaling with the inverse of the number of observed modes. Ref. [216] has argued that a Dark Ages survey could use this effect to constrain $r$ to the $10^{-6}$ level.

2. **Curl lensing**: Like density fluctuations, gravitational waves can affect the paths of photons as they travel through the universe. Unlike density fluctuations, however, gravitational waves generate a curl component of a reconstructed deflection field. The potential of these curl modes as a probe of gravitational waves has been studied e.g. in Refs. [218–222]. The constraining power of this method also scales with the inverse of the number of modes, and in Ref. [220] it was shown that in principle a measurement of curl lensing from the Dark Ages could provide a constraint as low as $r = 10^{-9}$.

A full treatment of all effects induced due to the presence of large-scale tensor perturbations, including the two effects above, was performed in Refs. [125, 223]. Observationally, it is not evident that all of these effects can be easily separated. In our forecast below, we will assume that tidal fossils and curl lensing can be distinguished. We hope to report in the near future to what extent these effects can indeed be separated (for example, through bias-hardened estimators, as recently explored in Ref. [121] for the case of scalar lensing).

We consider a Dark Ages 21cm survey over $30 < z < 150$, corresponding to a comoving volume of roughly $900\,(h^{-1}\mathrm{Gpc})^3$. The number of modes is set by the maximum observable wavenumbers along and perpendicular to the line of sight, $k_{\parallel\mathrm{max}}$ and $k_{\perp\mathrm{max}}$. We assume sufficient frequency resolution to access the Jeans scale in the line-of-sight direction, $k_{\parallel\mathrm{max}} \sim 300\mathrm{Mpc}^{-1}$. In the transverse direction, we map $k_{\perp\mathrm{max}}$ into the corresponding baseline $b$ that can observe that wavenumber. This mapping is redshift-dependent; for the tidal fossil forecast, we evaluate it at $z = 30$ since this is where the signal to noise peaks. For the curl lensing forecast, we split the survey into four equal redshift bins, evaluate the mapping (and any other relevant redshift-dependent quantities) at the midpoint of each bin, and combine the separate forecasts from the different bins. Note that $b$ is not necessarily the longest baseline present in the instrument, but rather the maximum baseline at which all shorter modes are signal-dominated.
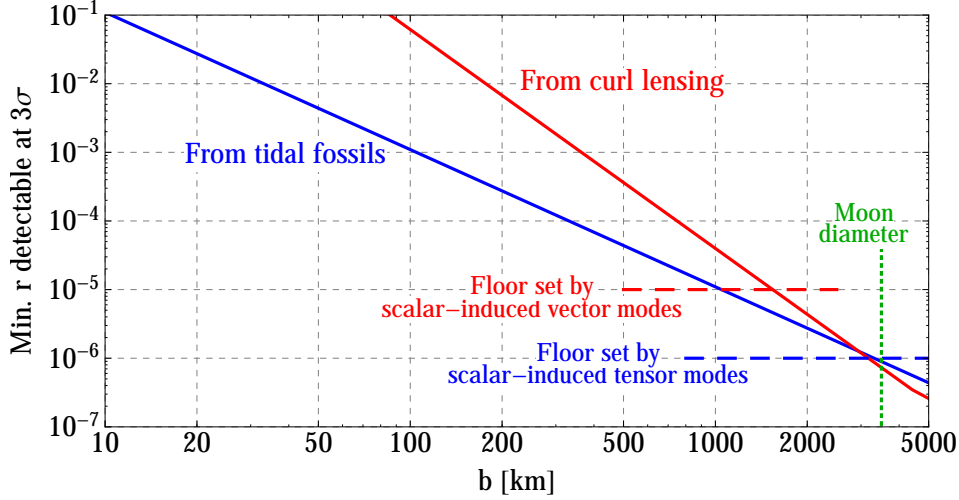
43

FIG. 20. The minimum value of the tensor-to-scalar ratio $r$ detectable with a Dark Ages 21cm survey, as a function of the maximum baseline $b$ for which 21cm observations are signal-dominated. Blue and red curves correspond to the tidal fossil and curl lensing methods discussed in the main text. The corresponding dashed lines indicate floors at which the primordial GW signal becomes dominated by the next-strongest signal in each method. We find that for $b \gtrsim \mathcal{O}(100\text{km})$, $r$ can be detected at a lower level than with CMB-S4 ($\sim 10^{-3}$), while an interferometer covering a large portion of the moon can detect $r$ as low as $10^{-6}$. Achieving even a fraction of this precision would be impossible for any other known probe of primordial GWs. **[SF: Make sure this last statement is true!]**

For tidal fossils, we adopt the quadratic estimator from Ref. [217], using their expression for the estimator noise with the survey properties given above. For curl lensing, we use a modification of the formalism from Ref. [121], which simply amounts to a change in filters applied to the observed 21cm fluctuations. We ignore nonlinearities in the 21cm field, which will slightly degrade the signal to noise at the longest baselines we consider. The ability to detect lensing is affected by shearing of coordinates at the source redshift by gravitational waves present at that redshift; we incorporate this "metric shear" in our forecasts, following Ref. [218].[7] The curl lensing power spectrum is computed using a modified version of CAMB [224], and we compute the 21cm brightness temperature power spectrum following Ref. [207].

In Fig. 20, we plot the minimum value of $r$ detectable at $3\sigma$ by either method, assuming that primordial gravitational waves are the dominant signal in each case. We have also indicated the levels at which other effects begin to dominate the primordial signal. For curl lensing, vector perturbations generated at second order by primordial scalar perturbations produce the dominant signal if $r \lesssim 10^{-5}$ [225, 226]. Contaminants in the tidal fossil estimator have not been extensively investigated, but tensor perturbations generated by second-order scalar couplings have been found to enter other observables at the level of $r \sim 10^{-6}$ (e.g. [227]), so we take this to be the relevant floor.[8]

We find that an interferometer with baselines of at least a few hundred kilometers would be able to constrain $r$ to the level of $10^{-3}$, equivalent to the target for CMB-S4, with even larger arrays being able to beat this target. Such arrays are clearly a highly ambitious notion, but currently represent the only feasible way to detect primordial gravitational waves at a lower level than CMB-S4. At the extreme limit of feasibility, an array covering a large fraction of the Moon's surface (corresponding to a maximal baseline of 3500 km, the Moon's diameter), could in principle detect $r$ as low as $10^{-6}$. Achieving even a fraction of this goal would result in a large scientific payoff, which motivates further research and development in this direction.

---

[7] Important differences between our forecast and that of Ref. [220] include the incorporation of metric shear, which degrades the signal to noise, and the use of a fully 3-dimensional formalism that accounts for correlations caused by long modes along the line of sight.

[8] These second-order contributions can be exactly computed once the amplitude of scalar perturbations is known, and could in principle then be subtracted from a measurement of tidal fossils or curl lensing to access values of $r$ smaller than the floors we have quoted. However, cosmic variance will prevent us from obtaining sufficiently precise measurements for this procedure to work. Our forecasts do not include cosmic variance, and therefore indicate the values of $r$ that can be detected by a rejection of the null hypothesis that either effect is absent. **[SF: This could probably be explained better...]**

## 5. CONCLUSIONS

In this white paper, we have provided an overview of 21-cm cosmology, and argued that there is a unique opportunity for the US cosmology community to take a leading role in this field by beginning to plan for a second-generation experiment. We reiterate three main reasons for doing so:

- **The experiment will address pressing science questions.** There have not been major discoveries implying new physics in the past two decades. The collider experiments, while achieving important milestones such as direct detection of the Higgs boson, have not detected supersymmetry or any other hint of beyond the standard model physics. In cosmology, the minimal $w = -1$ $\Lambda$CDM model has avoided any definitive observational challenge. We are proposing a Stage 2 21-cm experiment that could advance three possible avenues for finding new physics: deviations from the standard expansion history at high redshift, features in the primordial power spectrum, and measurements of primordial non-Gaussianity. The first item has potential to directly address some pressing dark energy questions, such as the timing of dark energy domination, while the second and third items are theoretically well-motivated searches that a large 21-cm array is particularly suited to address. In addition to these cornerstone measurements, the experiment will open up a trove of new capabilities, such as providing new sources for gravitational lensing, measuring cosmic expansion in real time, and identifying or characterizing exotic transient phenomena in the radio. Finally, a Stage 2 experiment would represent a crucial proving ground towards the ultimate goal of opening up the cosmic Dark Ages for direct observations.

- **Now is time to do it.** After the current generation flagship dark energy experiments LSST and DESI, there is not an obvious path to continue following in optical dark energy studies. To get an order of magnitude improvement will in all likelihood require a new telescope and large investments. Pivoting to 21-cm would allow US to become a leader in a fundamentally new and different cosmological observable. Moore's law improvements in the corresponding technology will continue to make this possibility attractive and cost-effective in the foreseeable future.

- **The US national lab complex has the right expertise.** A Stage 2 21-cm experiment will be a large experiment requiring significant R&D and a large analysis collaboration, and will have significant infrastructural and production components. Traditionally, such experiments were done under auspices of the DOE, as the main mission-driven high energy physics agency. In particular, the DOE brings know-how in RF technology from accelerator and light-source facilities, as well as considerable expertise in high-performance computing (which is crucial, given the potentially enormous data volumes of a Stage 2 experiment). Additionally, the experience of building and managing large production programs and scientific communities in large HEP-style collaborations make the DOE a natural home for an experiment like this. As argued, the science case naturally extends beyond dark energy and here other agencies will probably join the effort in a mode similar to how LSST is being built and operated.

In the core of this white paper, Chapters 2 and 3, we have made a case for a concrete experimental design that is an order of magnitude larger than the current generation of 21-cm experiments. We have made forecasts and listed the numerous technical challenges. These first steps elucidate the works that lies ahead. The work should progress on three main fronts:

- **Strengthen the science case.** More work needs to be done to strenghten the science case. All science forecasts should be done with the same forecasting code that will use concrete observing strategy and baseline distributions rather than idealized approximations. Special emphasis must be paid to the modelling of instrumental *systematics* to push beyond forecasts that assume all measurements are thermal noise limited beyond some simple (though conservative) data cuts to deal with foregrounds. These detailed forecasts should be used to optimize the design and understand the pros and cons of different choices for array parameters. The full scientific implications of specific measurements, such as lensing and tidal reconstruction, as well as synergies with other probes and planned surveys, should be better understood.

- **Research and develop hardware and calibration systems.** In Chapter 3, we have outlined a number of developments that must occur before a Stage 2 experiment. Some of them will improve the systematics, and some of them simply control the cost and reliability of such a large experiment. Some of these developments can be designed and tested in laboratory environments, but some will have to employ either 21-cm test-beds such as the BMX experiment at BNL or actual Stage 1 experiments. These development need to start as soon as possible in order to to be able to converge on an actual design in time.

- **Fully understand implications of Stage 1 experiments.** Stage 1 experiments will provide invaluable experience that should be absorbed. Have they achieved not just the primary scientific goals, but also the expected noise performance and systematics control? What were the dominant issues? On this front, one should take advantage of the considerable US presence in 21-cm experiments targeting Cosmic Dawn and reionization. While the scientific output of these experiments lies beyond the DOE purview, the resulting lessons in hardware and data analysis are directly transferable to our proposed Stage 2 experiment.

Finally, there are programmatic issues with proposing such an experiment. The writing of this white paper helped to generate a kernel collaboration and identify core issues. The next steps are submission to the Astronomy and Astrophysics Decadal Survey and later to the Snowmass and P5 processes, as the beginning of a path towards harnessing the considerable power of 21-cm cosmology.

## ACKNOWLEDGMENTS

## Appendix A: Forecasting assumptions

The Stage 2 experiment was assumed to be a compact array of 6-m fully illuminated dishes in a square grid with $256 \times 256$ configuration. We assumed integration time of 5 years (at 100% efficiency) over half the sky ($f_{\rm sky} = 0.5$) with a system noise temperature of $T_{\rm sys} = 50$K.

At these frequencies is eclipsed by the sky temperature which we take to be

$$T_{\rm sky}(f) = \left( \frac{f}{400 \text{MHz}} \right)^{-2.75} 25\text{K} + 2.7\text{K}. \tag{A1}$$

This approximation is consistent with assumptions made in the SKA forecasting exercise **[AS:cite]** and also with effective temperature derived by averaging $T^{-2}$ over the Haslam 408MHz galaxy map **[AS:cite]** (i.e. approximately taking into account the inverse variance weighting one might do in practice)

The brightness temperature is assumed to be

$$T_{\rm b} = 180\text{mK}(1+z)^2 \left( H(z)/H_0(z) \right)^{-1} \times \left( 4 \times 10^{-4}(1+z)^{0.6} \right), \tag{A2}$$

where the expression in the last bracket approximates the cosmic evolution of $\Omega_{\rm HI}$. This is consistent with [65] and other recent literature. For derivation of brightness temperature, see e.g. [228]. We have in addition assumed evolution of cosmic $\Omega_{\rm HI}$ from [229].

The total power-spectrum signal observed by the radio interferometer is given by

$$P(\mathbf{k}) = (b + f\mu^2)^2 P(k) + P_{\rm SN} + P_{\rm N}, \tag{A3}$$

where the first term is the large-scale power spectrum modeled using linear biasing and redshift-space distortions, $P_{\rm SN}$ is the shot-noise contribution from halos making up the neutral hydrogen signal (and usually irrelevant) and $P_{\rm N}$ is the noise coming from the finite system temperature of the instrument.

At high redshifts considered here, the linear biasing assumption should be an excellent approximation, down the relatively agresive scales of $k_{\rm max} = 0.4h$/Mpc (see e.g. Figure 7). For neutral hydrogen large-scale bias and shot-noise, we used results from [44]. While the shot-noise term is highly uncertain, it is also very sub-dominant and does not significantly affects results. We assume a Planck 2015 best-fit cosmology, an assumption that should not affect the results in any significant way.

For the system noise, we assumed the limit of uniform coverage in the $u - v$ plane, namely

$$P_N = T_{\rm sys}^2 r^2 \left( \frac{\lambda(1+z)}{H(z)} \right) \left( \frac{\lambda^2}{A_e} \right)^2 \left( \frac{\pi u_{\rm max}^2}{N_r^2 t} \right) \left( \frac{S_{\rm Area}}{\text{FOV}} \right), \tag{A4}$$

where $r$ is the comoving distance to the observed slice, $\lambda_0 \sim 21$cm is the transition rest-frame frequency, $\lambda = \lambda_0(1+z)$ is the observing wavelength, $u_{\rm max}$ is the maximum baseline, $N_r$ si the number of receivers, $S_{\rm area}$ is the total survey area and FOV is the field of view of each receiver. Quantity $A_e = 3/4\pi D^2 \eta$ is the area per feed where we for simplicity assume unit efficiency $\eta = 1$.

The $N_w = 3\times$ primary-beam wedge assumption was realised by only considering modes that satisfy

$$k_\parallel > k_\perp \frac{rH(z)}{c(1+z)} \sin(\theta_w), \tag{A5}$$

where $\theta_w$ is the maximum angle at which fringes from a monochromatic point source can enter the measurement and be confused with a non-monochromatic source at phase center. Given that beam shape is idealised in our experiment, we take $\theta_w = N_w 1.22\lambda/2D$[9], although other choices can be found in the literature, e.g. $\theta_w = N_w 1.06\lambda/2D$ [230].

[EJA:\jcap command not working properly in bib]

---

[9] We note that the factor of 2 in the denominator here is ad-hoc, for an airy disk, the first null as measured from the center is at $1.22\lambda/D$ and we then take this distance to represent an effective full width

[1] S. Dodelson, K. Heitmann, C. Hirata, K. Honscheid, A. Roodman, U. Seljak, A. Slosar, and M. Trodden, ArXiv e-prints (2016), arXiv:1604.07821 [astro-ph.IM].

[2] K. Dawson, J. Frieman, K. Heitmann, B. Jain, S. Kahn, R. Mandelbaum, S. Perlmutter, and A. Slosar, ArXiv e-prints (2018), arXiv:1802.07216.

[3] W. Percival, Physics Today 70, 32 (2017).

[4] HI4PI Collaboration, N. Ben Bekhti, L. Flöer, R. Keller, J. Kerp, D. Lenz, B. Winkel, J. Bailin, M. R. Calabretta, L. Dedes, H. A. Ford, B. K. Gibson, U. Haud, S. Janowiecki, P. M. W. Kalberla, F. J. Lockman, N. M. McClure-Griffiths, T. Murphy, H. Nakanishi, D. J. Pisano, and L. Staveley-Smith, A&A 594, A116 (2016), arXiv:1610.06175.

[5] T.-C. Chang, U.-L. Pen, K. Bandura, and J. B. Peterson, Nature 466, 463 (2010).

[6] M. Davis, J. A. Newman, S. M. Faber, and A. C. Phillips, in *Deep Fields*, edited by S. Cristiani, A. Renzini, and R. E. Williams (2001) p. 241, astro-ph/0012189.

[7] A. L. Coil, M. Davis, D. S. Madgwick, J. A. Newman, C. J. Conselice, M. Cooper, R. S. Ellis, S. M. Faber, D. P. Finkbeiner, P. Guhathakurta, N. Kaiser, D. C. Koo, A. C. Phillips, C. C. Steidel, B. J. Weiner, C. N. A. Willmer, and R. Yan, ApJ 609, 525 (2004), astro-ph/0305586.

[8] K. W. Masui, E. R. Switzer, N. Banavar, K. Bandura, C. Blake, L.-M. Calin, T.-C. Chang, X. Chen, Y.-C. Li, Y.-W. Liao, A. Natarajan, U.-L. Pen, J. B. Peterson, J. R. Shaw, and T. C. Voytek, ApJ 763, L20 (2013), arXiv:1208.0331 [astro-ph.CO].

[9] M. J. Drinkwater, R. J. Jurek, C. Blake, D. Woods, K. A. Pimbblet, K. Glazebrook, R. Sharp, M. B. Pracy, S. Brough, M. Colless, W. J. Couch, S. M. Croom, T. M. Davis, D. Forbes, K. Forster, D. G. Gilbank, M. Gladders, B. Jelliffe, N. Jones, I.-H. Li, B. Madore, D. C. Martin, G. B. Poole, T. Small, E. Wisnioski, T. Wyder, and H. K. C. Yee, MNRAS 401, 1429 (2010), arXiv:0911.4246.

[10] E. R. Switzer, K. W. Masui, K. Bandura, L.-M. Calin, T.-C. Chang, X.-L. Chen, Y.-C. Li, Y.-W. Liao, A. Natarajan, U.-L. Pen, J. B. Peterson, J. R. Shaw, and T. C. Voytek, MNRAS 434, L46 (2013), arXiv:1304.3712 [astro-ph.CO].

[11] D. R. DeBoer, A. R. Parsons, J. E. Aguirre, P. Alexander, Z. S. Ali, A. P. Beardsley, G. Bernardi, J. D. Bowman, R. F. Bradley, C. L. Carilli, C. Cheng, E. de Lera Acedo, J. S. Dillon, A. Ewall-Wice, G. Fadana, N. Fagnoni, R. Fritz, S. R. Furlanetto, B. Glendenning, B. Greig, J. Grobbelaar, B. J. Hazelton, J. N. Hewitt, J. Hickish, D. C. Jacobs, A. Julius, M. Kariseb, S. A. Kohn, T. Lekalake, A. Liu, A. Loots, D. MacMahon, L. Malan, C. Malgas, M. Maree, Z. Martinot, N. Mathison, E. Matsetela, A. Mesinger, M. F. Morales, A. R. Neben, N. Patra, S. Pieterse, J. C. Pober, N. Razavi-Ghods, J. Ringuette, J. Robnett, K. Rosie, R. Sell, C. Smith, A. Syce, M. Tegmark, N. Thyagarajan, P. K. G. Williams, and H. Zheng, Publications of the Astronomical Society of the Pacific 129, 045001 (2017).

[12] A. R. Parsons, D. C. Backer, G. S. Foster, M. C. H. Wright, R. F. Bradley, N. E. Gugliucci, C. R. Parashare, E. E. Benoit, J. E. Aguirre, D. C. Jacobs, C. L. Carilli, D. Herne, M. J. Lynch, J. R. Manley, and D. J. Werthimer, AJ 139, 1468 (2010).

[13] M. P. van Haarlem, M. W. Wise, A. W. Gunst, G. Heald, J. P. McKean, J. W. T. Hessels, A. G. de Bruyn, R. Nijboer, J. Swinbank, R. Fallows, M. Brentjens, A. Nelles, R. Beck, H. Falcke, R. Fender, J. Hörandel, L. V. E. Koopmans, G. Mann, G. Miley, H. Röttgering, B. W. Stappers, R. A. M. J. Wijers, S. Zaroubi, M. van den Akker, A. Alexov, J. Anderson, K. Anderson, A. van Ardenne, M. Arts, A. Asgekar, I. M. Avruch, F. Batejat, L. Bähren, M. E. Bell, M. R. Bell, I. van Bemmel, P. Bennema, M. J. Bentum, G. Bernardi, P. Best, L. Bîrzan, A. Bonafede, A.-J. Boonstra, R. Braun, J. Bregman, F. Breitling, R. H. van de Brink, J. Broderick, P. C. Broekema, W. N. Brouw, M. Brüggen, H. R. Butcher, W. van Cappellen, B. Ciardi, T. Coenen, J. Conway, A. Coolen, A. Corstanje, S. Damstra, O. Davies, A. T. Deller, R.-J. Dettmar, G. van Diepen, K. Dijkstra, P. Donker, A. Doorduin, J. Dromer, M. Drost, A. van Duin, J. Eislöffel, J. van Enst, C. Ferrari, W. Frieswijk, H. Gankema, M. A. Garrett, F. de Gasperin, M. Gerbers, E. de Geus, J.-M. Grießmeier, T. Grit, P. Gruppen, J. P. Hamaker, T. Hassall, M. Hoeft, H. A. Holties, A. Horneffer, A. van der Horst, A. van Houwelingen, A. Huijgen, M. Iacobelli, H. Intema, N. Jackson, V. Jelic, A. de Jong, E. Juette, D. Kant, A. Karastergiou, A. Koers, H. Kollen, V. I. Kondratiev, E. Kooistra, Y. Koopman, A. Koster, M. Kuniyoshi, M. Kramer, G. Kuper, P. Lambropoulos, C. Law, J. van Leeuwen, J. Lemaitre, M. Loose, P. Maat, G. Macario, S. Markoff, J. Masters, R. A. McFadden, D. McKay-Bukowski, H. Meijering, H. Meulman, M. Mevius, E. Middelberg, R. Millenaar, J. C. A. Miller-Jones, R. N. Mohan, J. D. Mol, J. Morawietz, R. Morganti, D. D. Mulcahy, E. Mulder, H. Munk, L. Nieuwenhuis, R. van Nieuwpoort, J. E. Noordam, M. Norden, A. Noutsos, A. R. Offringa, H. Olofsson, A. Omar, E. Orrú, R. Overeem, H. Paas, M. Pandey-Pommier, V. N. Pandey, R. Pizzo, A. Polatidis, D. Rafferty, S. Rawlings, W. Reich, J.-P. de Reijer, J. Reitsma, G. A. Renting, P. Riemers, E. Rol, J. W. Romein, J. Roosjen, M. Ruiter, A. Scaife, K. van der Schaaf, B. Scheers, P. Schellart, A. Schoenmakers, G. Schoonderbeek, M. Serylak, A. Shulevski, J. Sluman, O. Smirnov, C. Sobey, H. Spreeuw, M. Steinmetz, C. G. M. Sterks, H.-J. Stiepel, K. Stuurwold, M. Tagger, Y. Tang, C. Tasse, I. Thomas, S. Thoudam, M. C. Toribio, B. van der Tol, O. Usov, M. van Veelen, A.-J. van der Veen, S. ter Veen, J. P. W. Verbiest, R. Vermeulen, N. Vermaas, C. Vocks, C. Vogt, M. de Vos, E. van der Wal, R. van Weeren, H. Weggemans, P. Weltevrede, S. White, S. J. Wijnholds, T. Wilhelmsson, O. Wucknitz, S. Yatawatta, P. Zarka, A. Zensus, and J. van Zwieten, A&A 556, A2 (2013), arXiv:1305.3550 [astro-ph.IM].

[14] S. J. Tingay, R. Goeke, J. D. Bowman, D. Emrich, S. M. Ord, D. A. Mitchell, M. F. Morales, T. Booler, B. Crosse, R. B. Wayth, C. J. Lonsdale, S. Tremblay, D. Pallot, T. Colegate, A. Wicenec, N. Kudryavtseva, W. Arcus, D. Barnes, G. Bernardi, F. Briggs, S. Burns, J. D. Bunton, R. J. Cappallo, B. E. Corey, A. Deshpande, L. Desouza, B. M. Gaensler, L. J. Greenhill, P. J. Hall, B. J. Hazelton, D. Herne, J. N. Hewitt, M. Johnston-Hollitt, D. L. Kaplan, J. C. Kasper, B. B. Kincaid, R. Koenig, E. Kratzenberg, M. J. Lynch, B. Mckinley, S. R. Mcwhirter, E. Morgan, D. Oberoi, J. Pathikulangara, T. Prabu, R. A. Remillard, A. E. E. Rogers, A. Roshi, J. E. Salah, R. J. Sault, N. Udaya-Shankar, F. Schlagenhaufer, K. S. Srivani, J. Stevens, R. Subrahmanyan, M. Waterson, R. L. Webster, A. R. Whitney, A. Williams, C. L. Williams, and J. S. B. Wyithe, PASA 30, e007 (2013), arXiv:1206.6945 [astro-ph.IM].

[15] G. Paciga, J. G. Albert, K. Bandura, T.-C. Chang, Y. Gupta, C. Hirata, J. Odegova, U.-L. Pen, J. B. Peterson, J. Roy, J. R. Shaw, K. Sigurdson, and T. Voytek, MNRAS 433, 639 (2013).

[16] J. D. Bowman, A. E. E. Rogers, R. A. Monsalve, T. J. Mozdzen, and N. Mahesh, Nature 555, 67 (2018).

[17] C. Feng and G. Holder, ArXiv e-prints (2018), arXiv:1802.07432.

[18] R. Hills, G. Kulkarni, P. D. Meerburg, and E. Puchwein, (2018), arXiv:1805.01421 [astro-ph.CO].

[19] S. Fraser, A. Hektor, G. Hütsi, K. Kannike, C. Marzo, L. Marzola, C. Spethmann, A. Racioppi, M. Raidal, V. Vaskonen, and H. Veermäe, ArXiv e-prints (2018), arXiv:1803.03245 [hep-ph].

[20] R. Barkana, N. J. Outmezguine, D. Redigolo, and T. Volansky, ArXiv e-prints (2018), arXiv:1803.03091 [hep-ph].

[21] A. Berlin, D. Hooper, G. Krnjaic, and S. D. McDermott, ArXiv e-prints (2018), arXiv:1803.02804 [hep-ph].

[22] R. Barkana, Nature 555, 71 (2018), arXiv:1803.06698.

[23] T. R. Slatyer and C.-L. Wu, ArXiv e-prints (2018), arXiv:1803.09734.

[24] S. Hirano and V. Bromm, ArXiv e-prints (2018), arXiv:1803.10671.

[25] D. A. Neufeld, G. R. Farrar, and C. F. McKee, ArXiv e-prints (2018), arXiv:1805.08794.

[26] S. Yoshiura, K. Takahashi, and T. Takahashi, ArXiv e-prints (2018), arXiv:1805.11806.

[27] M. Chianese, P. Di Bari, K. Farrag, and R. Samanta, ArXiv e-prints (2018), arXiv:1805.11717 [hep-ph].

[28] A. A. Costa, R. C. G. Landim, B. Wang, and E. Abdalla, ArXiv e-prints (2018), arXiv:1803.06944.

[29] J. C. Hill and E. J. Baxter, ArXiv e-prints (2018), arXiv:1803.07555.

[30] T. Moroi, K. Nakayama, and Y. Tang, ArXiv e-prints (2018), arXiv:1804.10378 [hep-ph].

[31] N. Houston, C. Li, T. Li, Q. Yang, and X. Zhang, ArXiv e-prints (2018), arXiv:1805.04426 [hep-ph].

[32] P. Sikivie, ArXiv e-prints (2018), arXiv:1805.05577.

[33] Y. Wang and G.-B. Zhao, ArXiv e-prints (2018), arXiv:1805.11210.

[34] G. D'Amico, P. Panci, and A. Strumia, ArXiv e-prints (2018), arXiv:1803.03629.

[35] Y. Yang, ArXiv e-prints (2018), arXiv:1803.05803.

[36] K. Cheung, J.-L. Kuo, K.-W. Ng, and Y.-L. Sming Tsai, ArXiv e-prints (2018), arXiv:1803.09398.

[37] S. Clark, B. Dutta, Y. Gao, Y.-Z. Ma, and L. E. Strigari, ArXiv e-prints (2018), arXiv:1803.09390 [astro-ph.HE].

[38] A. Hektor, G. Hütsi, L. Marzola, M. Raidal, V. Vaskonen, and H. Veermäe, ArXiv e-prints (2018), arXiv:1803.09697.

[39] A. Lidz and L. Hui, ArXiv e-prints (2018), arXiv:1805.01253.

[40] M. Safarzadeh, E. Scannapieco, and A. Babul, ArXiv e-prints (2018), arXiv:1803.08039.

[41] A. Schneider, ArXiv e-prints (2018), arXiv:1805.00021.

[42] A. Liu, J. R. Pritchard, M. Tegmark, and A. Loeb, Phys. Rev. D 87, 043002 (2013), arXiv:1211.3743 [astro-ph.CO].

[43] A. Ghosh, F. Mertens, and L. V. E. Koopmans, Mon. Not. Roy. Astron. Soc. 474, 4552 (2018), arXiv:1709.06752 [astro-ph.CO].

[44] E. Castorina and F. Villaescusa-Navarro, MNRAS 471, 1788 (2017), arXiv:1609.05157.

[45] J. C. Pober, MNRAS 447, 1705 (2015), arXiv:1411.2050.

[46] G. Gubitosi, F. Piazza, and F. Vernizzi, ??jnlJ. Cosmology Astropart. Phys. 2, 032 (2013), arXiv:1210.0201 [hep-th].

[47] J. Bloomfield, É. É. Flanagan, M. Park, and S. Watson, ??jnlJ. Cosmology Astropart. Phys. 8, 010 (2013), arXiv:1211.7054 [astro-ph.CO].

[48] E. Bellini and I. Sawicki, ??jnlJ. Cosmology Astropart. Phys. 7, 050 (2014), arXiv:1404.3713.

[49] B. P. Abbott, R. Abbott, T. D. Abbott, F. Acernese, K. Ackley, C. Adams, T. Adams, P. Addesso, R. X. Adhikari, V. B. Adya, and et al., ApJ 848, L13 (2017), arXiv:1710.05834 [astro-ph.HE].

[50] L. Lombriser and A. Taylor, ??jnlJ. Cosmology Astropart. Phys. 3, 031 (2016), arXiv:1509.08458.

[51] P. Creminelli and F. Vernizzi, Physical Review Letters 119, 251302 (2017), arXiv:1710.05877.

[52] J. Sakstein and B. Jain, Physical Review Letters 119, 251303 (2017), arXiv:1710.05893.

[53] J. M. Ezquiaga and M. Zumalacárregui, Physical Review Letters 119, 251304 (2017), arXiv:1710.05901.

[54] T. Baker, E. Bellini, P. G. Ferreira, M. Lagos, J. Noller, and I. Sawicki, Physical Review Letters 119, 251301 (2017), arXiv:1710.06394.

[55] L. Amendola, M. Kunz, I. D. Saltas, and I. Sawicki, Physical Review Letters 120, 131101 (2018), arXiv:1711.04825.

[56] M. Raveri, P. Bull, A. Silvestri, and L. Pogosian, Phys. Rev. D 96, 083509 (2017), arXiv:1703.05297.

[57] S. Alam, M. Ata, S. Bailey, F. Beutler, D. Bizyaev, J. A. Blazek, A. S. Bolton, J. R. Brownstein, A. Burden, C.-H. Chuang, J. Comparat, A. J. Cuesta, K. S. Dawson, D. J. Eisenstein, S. Escoffier, H. Gil-Marín, J. N. Grieb, N. Hand, S. Ho, K. Kinemuchi, D. Kirkby, F. Kitaura, E. Malanushenko, V. Malanushenko, C. Maraston, C. K. McBride, R. C. Nichol, M. D. Olmstead, D. Oravetz, N. Padmanabhan, N. Palanque-Delabrouille, K. Pan, M. Pellejero-Ibanez, W. J. Percival, P. Petitjean, F. Prada, A. M. Price-Whelan, B. A. Reid, S. A. Rodríguez-Torres, N. A. Roe, A. J. Ross, N. P. Ross, G. Rossi, J. A. Rubiño-Martín, S. Saito, S. Salazar-Albornoz, L. Samushia, A. G. Sánchez, S. Satpathy, D. J. Schlegel, D. P. Schneider, C. G. Scóccola, H.-J. Seo, E. S. Sheldon, A. Simmons, A. Slosar, M. A. Strauss, M. E. C. Swanson, D. Thomas, J. L. Tinker, R. Tojeiro, M. V. Magaña, J. A. Vazquez, L. Verde, D. A. Wake, Y. Wang, D. H. Weinberg, M. White, W. M. Wood-Vasey, C. Yèche, I. Zehavi, Z. Zhai, and G.-B. Zhao, MNRAS 470, 2617 (2017), arXiv:1607.03155.

[58] H. du Mas des Bourboux, J.-M. Le Goff, M. Blomqvist, N. G. Busca, J. Guy, J. Rich, C. Yèche, J. E. Bautista, É. Burtin, K. S. Dawson, D. J. Eisenstein, A. Font-Ribera, D. Kirkby, J. Miralda-Escudé, P. Noterdaeme, N. Palanque-Delabrouille, I. Pâris, P. Petitjean, I. Pérez-Ràfols, M. M. Pieri, N. P. Ross, D. J. Schlegel, D. P. Schneider, A. Slosar, D. H. Weinberg, and P. Zarrouk, A&A 608, A130 (2017), arXiv:1708.02225.

[59] A. Slosar, V. Iršič, D. Kirkby, S. Bailey, N. G. Busca, T. Delubac, J. Rich, É. Aubourg, J. E. Bautista, V. Bhardwaj, M. Blomqvist, A. S. Bolton, J. Bovy, J. Brownstein, B. Carithers, R. A. C. Croft, K. S. Dawson, A. Font-Ribera, J.-M. Le Goff, S. Ho, K. Honscheid, K.-G. Lee, D. Margala, P. McDonald, B. Medolin, J. Miralda-Escudé, A. D. Myers, R. C. Nichol, P. Noterdaeme, N. Palanque-Delabrouille, I. Pâris, P. Petitjean, M. M. Pieri, Y. Piškur, N. A. Roe, N. P. Ross, G. Rossi, D. J. Schlegel, D. P. Schneider, N. Suzuki, E. S. Sheldon, U. Seljak, M. Viel, D. H. Weinberg, and C. Yèche, ??jnlJ. Cosmology Astropart. Phys. 4, 026 (2013), arXiv:1301.3459.

[60] M. Ata, F. Baumgarten, J. Bautista, F. Beutler, D. Bizyaev, M. R. Blanton, J. A. Blazek, A. S. Bolton, J. Brinkmann, J. R. Brownstein, E. Burtin, C.-H. Chuang, J. Comparat, K. S. Dawson, A. de la Macorra, W. Du, H. du Mas des Bourboux, D. J. Eisenstein, H. Gil-Marín, K. Grabowski, J. Guy, N. Hand, S. Ho, T. A. Hutchinson, M. M. Ivanov, F.-S. Kitaura, J.-P. Kneib, P. Laurent, J.-M. Le Goff, J. E. McEwen, E.-M. Mueller, A. D. Myers, J. A. Newman, N. Palanque-Delabrouille, K. Pan, I. Pâris, M. Pellejero-Ibanez, W. J. Percival, P. Petitjean, F. Prada, A. Prakash, S. A. Rodríguez-Torres, A. J. Ross, G. Rossi, R. Ruggeri, A. G. Sánchez, S. Satpathy,

D. J. Schlegel, D. P. Schneider, H.-J. Seo, A. Slosar, A. Streblyanska, J. L. Tinker, R. Tojeiro, M. Vargas Magaña, M. Vivek, Y. Wang, C. Yèche, L. Yu, P. Zarrouk, C. Zhao, G.-B. Zhao, and F. Zhu, MNRAS **473**, 4773 (2018), arXiv:1705.06373.

[61] E. A. Kazin, J. Koda, C. Blake, N. Padmanabhan, S. Brough, M. Colless, C. Contreras, W. Couch, S. Croom, D. J. Croton, T. M. Davis, M. J. Drinkwater, K. Forster, D. Gilbank, M. Gladders, K. Glazebrook, B. Jelliffe, R. J. Jurek, I.-h. Li, B. Madore, D. C. Martin, K. Pimbblet, G. B. Poole, M. Pracy, R. Sharp, E. Wisnioski, D. Woods, T. K. Wyder, and H. K. C. Yee, MNRAS **441**, 3524 (2014), arXiv:1401.0358.

[62] DESI Collaboration, A. Aghamousa, J. Aguilar, S. Ahlen, S. Alam, L. E. Allen, C. Allende Prieto, J. Annis, S. Bailey, C. Balland, and et al., ArXiv e-prints (2016), arXiv:1611.00036 [astro-ph.IM].

[63] R. Laureijs, J. Amiaux, S. Arduini, J. . Auguères, J. Brinchmann, R. Cole, M. Cropper, C. Dabin, L. Duvet, A. Ealet, and et al., ArXiv e-prints (2011), arXiv:1110.3193 [astro-ph.CO].

[64] A. Font-Ribera, P. McDonald, N. Mostek, B. A. Reid, H.-J. Seo, and A. Slosar, **??**jnlJ. Cosmology Astropart. Phys. **5**, 023 (2014), arXiv:1308.4164.

[65] A. Obuljen, E. Castorina, F. Villaescusa-Navarro, and M. Viel, ArXiv e-prints (2017), arXiv:1709.07893.

[66] É. Aubourg, S. Bailey, J. E. Bautista, F. Beutler, V. Bhardwaj, D. Bizyaev, M. Blanton, M. Blomqvist, A. S. Bolton, J. Bovy, H. Brewington, J. Brinkmann, J. R. Brownstein, A. Burden, N. G. Busca, W. Carithers, C.-H. Chuang, J. Comparat, R. A. C. Croft, A. J. Cuesta, K. S. Dawson, T. Delubac, D. J. Eisenstein, A. Font-Ribera, J. Ge, J.-M. Le Goff, S. G. A. Gontcho, J. R. Gott, J. E. Gunn, H. Guo, J. Guy, J.-C. Hamilton, S. Ho, K. Honscheid, C. Howlett, D. Kirkby, F. S. Kitaura, J.-P. Kneib, K.-G. Lee, D. Long, R. H. Lupton, M. V. Magaña, V. Malanushenko, E. Malanushenko, M. Manera, C. Maraston, D. Margala, C. K. McBride, J. Miralda-Escudé, A. D. Myers, R. C. Nichol, P. Noterdaeme, S. E. Nuza, M. D. Olmstead, D. Oravetz, I. Pâris, N. Padmanabhan, N. Palanque-Delabrouille, K. Pan, M. Pellejero-Ibanez, W. J. Percival, P. Petitjean, M. M. Pieri, F. Prada, B. Reid, J. Rich, N. A. Roe, A. J. Ross, N. P. Ross, G. Rossi, J. A. Rubiño-Martín, A. G. Sánchez, L. Samushia, R. T. Génova-Santos, C. G. Scóccola, D. J. Schlegel, D. P. Schneider, H.-J. Seo, E. Sheldon, A. Simmons, R. A. Skibba, A. Slosar, M. A. Strauss, D. Thomas, J. L. Tinker, R. Tojeiro, J. A. Vazquez, M. Viel, D. A. Wake, B. A. Weaver, D. H. Weinberg, W. M. Wood-Vasey, C. Yèche, I. Zehavi, G.-B. Zhao, and BOSS Collaboration, Phys. Rev. D **92**, 123516 (2015), arXiv:1411.1074.

[67] C. Blake, S. Brough, M. Colless, C. Contreras, W. Couch, S. Croom, D. Croton, T. M. Davis, M. J. Drinkwater, K. Forster, D. Gilbank, M. Gladders, K. Glazebrook, B. Jelliffe, R. J. Jurek, I.-h. Li, B. Madore, D. C. Martin, K. Pimbblet, G. B. Poole, M. Pracy, R. Sharp, E. Wisnioski, D. Woods, T. K. Wyder, and H. K. C. Yee, MNRAS **425**, 405 (2012), arXiv:1204.3674.

[68] F. Beutler, C. Blake, M. Colless, D. H. Jones, L. Staveley-Smith, G. B. Poole, L. Campbell, Q. Parker, W. Saunders, and F. Watson, MNRAS **423**, 3430 (2012), arXiv:1204.4725.

[69] T. Okumura, C. Hikage, T. Totani, M. Tonegawa, H. Okada, K. Glazebrook, C. Blake, P. G. Ferreira, S. More, A. Taruya, S. Tsujikawa, M. Akiyama, G. Dalton, T. Goto, T. Ishikawa, F. Iwamuro, T. Matsubara, T. Nishimichi, K. Ohta, I. Shimizu, R. Takahashi, N. Takato, N. Tamura, K. Yabe, and N. Yoshida, PASJ **68**, 38 (2016), arXiv:1511.08083.

[70] F. Beutler, H.-J. Seo, S. Saito, C.-H. Chuang, A. J. Cuesta, D. J. Eisenstein, H. Gil-Marín, J. N. Grieb, N. Hand, F.-S. Kitaura, C. Modi, R. C. Nichol, M. D. Olmstead, W. J. Percival, F. Prada, A. G. Sánchez, S. Rodriguez-Torres, A. J. Ross, N. P. Ross, D. P. Schneider, J. Tinker, R. Tojeiro, and M. Vargas-Magaña, MNRAS **466**, 2242 (2017), arXiv:1607.03150.

[71] S. de la Torre, E. Jullo, C. Giocoli, A. Pezzotta, J. Bel, B. R. Granett, L. Guzzo, B. Garilli, M. Scodeggio, M. Bolzonella, U. Abbas, C. Adami, D. Bottini, A. Cappi, O. Cucciati, I. Davidzon, P. Franzetti, A. Fritz, A. Iovino, J. Krywult, V. Le Brun, O. Le Fèvre, D. Maccagni, K. Małek, F. Marulli, M. Polletta, A. Pollo, L. A. M. Tasca, R. Tojeiro, D. Vergani, A. Zanichelli, S. Arnouts, E. Branchini, J. Coupon, G. De Lucia, O. Ilbert, T. Moutard, L. Moscardini, J. A. Peacock, R. B. Metcalf, F. Prada, and G. Yepes, A&A **608**, A44 (2017), arXiv:1612.05647.

[72] G.-B. Zhao, Y. Wang, S. Saito, H. Gil-Marín, W. J. Percival, D. Wang, C.-H. Chuang, R. Ruggeri, E.-M. Mueller, F. Zhu, A. J. Ross, R. Tojeiro, I. Pâris, A. D. Myers, J. L. Tinker, E. Burtin, P. Zarrouk, F. Beutler, F. Baumgarten, J. E. Bautista, J. R. Brownstein, K. S. Dawson, J. Hou, A. de la Macorra, G. Rossi, J. A. Peacock, A. G. Sánchez, A. Shafieloo, D. P. Schneider, and C. Zhao, ArXiv e-prints (2018), arXiv:1801.03043.

[73] M. Zumalacárregui, E. Bellini, I. Sawicki, J. Lesgourgues, and P. G. Ferreira, **??**jnlJ. Cosmology Astropart. Phys. **8**, 019 (2017), arXiv:1605.06102.

[74] D. Blas, J. Lesgourgues, and T. Tram, **??**jnlJ. Cosmology Astropart. Phys. **7**, 034 (2011), arXiv:1104.2933.

[75] J. Chluba, J. Hamann, and S. P. Patil, Int. J. Mod. Phys. **D24**, 1530023 (2015), arXiv:1505.01834 [astro-ph.CO].

[76] F.-Y. Cyr-Racine, R. de Putter, A. Raccanelli, and K. Sigurdson, Phys. Rev. **D89**, 063517 (2014), arXiv:1310.3278 [astro-ph.CO].

[77] P. D. Meerburg, R. A. M. J. Wijers, and J. P. van der Schaar, MNRAS **421**, 369 (2012), arXiv:1109.5264 [astro-ph.CO].

[78] H. Peiris, R. Easther, and R. Flauger, JCAP **1309**, 018 (2013), arXiv:1303.2616 [astro-ph.CO].

[79] P. D. Meerburg and D. N. Spergel, Phys. Rev. **D89**, 063537 (2014), arXiv:1308.3705 [astro-ph.CO].

[80] R. Easther and R. Flauger, JCAP **1402**, 037 (2014), arXiv:1308.3736 [astro-ph.CO].

[81] P. A. R. Ade *et al.* (Planck), Astron. Astrophys. **594**, A20 (2016), arXiv:1502.02114 [astro-ph.CO].

[82] R. Flauger, L. McAllister, E. Silverstein, and A. Westphal, (2014), arXiv:1412.1814 [hep-th].

[83] A. Achúcarro, V. Atal, P. Ortiz, and J. Torrado, Phys. Rev. **D89**, 103006 (2014), arXiv:1311.2552 [astro-ph.CO].

[84] X. Chen and M. H. Namjoo, Phys. Lett. **B739**, 285 (2014), arXiv:1404.1536 [astro-ph.CO].

[85] X. Chen, M. H. Namjoo, and Y. Wang, JCAP **1502**, 027 (2015), arXiv:1411.2349 [astro-ph.CO].

[86] M. Alvarez, T. Baldauf, J. R. Bond, N. Dalal, R. de Putter, O. Doré, D. Green, C. Hirata, Z. Huang, D. Huterer, D. Jeong, M. C. Johnson, E. Krause, M. Loverde, J. Meyers, P. D. Meerburg, L. Senatore, S. Shandera, E. Silverstein, A. Slosar, K. Smith, M. Zaldarriaga, V. Assassi, J. Braden, A. Hajian, T. Kobayashi, G. Stein, and A. van Engelen, ArXiv e-prints (2014), arXiv:1412.4671.

[87] X. Chen, Advances in Astronomy **2010**, 638979 (2010), arXiv:1002.1416 [astro-ph.CO].

[88] J. M. Maldacena, JHEP **05**, 013 (2003), arXiv:astro-ph/0210603 [astro-ph].

[89] P. Creminelli and M. Zaldarriaga, JCAP **0410**, 006 (2004), arXiv:astro-ph/0407059 [astro-ph].

[90] E. Komatsu, N. Afshordi, N. Bartolo, D. Baumann, J. R. Bond, E. I. Buchbinder, C. T. Byrnes, X. Chen, D. J. H. Chung, A. Cooray, P. Creminelli, N. Dalal, O. Dore, R. Easther, A. V. Frolov, J. Khoury, W. H. Kinney, L. Kofman, K. Koyama, L. Leblond, J.-L. Lehners, J. E. Lidsey, M. Liguori, E. A. Lim, A. Linde, D. H. Lyth, J. Maldacena, S. Matarrese, L. McAllister, P. McDonald, S. Mukohyama, B. Ovrut, H. V. Peiris, A. Riotto, Y. Rodrigues, M. Sasaki, R. Scoccimarro, D. Seery, A. Sefusatti, K. M. Smith, A. A. Starobinsky, P. J. Steinhardt, F. Takahashi, M. Tegmark, A. J. Tolley, L. Verde, B. D. Wandelt, D. Wands, S. Weinberg, M. Wyman, A. P. S. Yadav, and M. Zaldarriaga, in *astro2010: The Astronomy and Astrophysics Decadal Survey*, Astronomy, Vol. 2010 (2009) arXiv:0902.4759 [astro-ph.CO].

[91] X. Chen and Y. Wang, JCAP **1004**, 027 (2010), arXiv:0911.3380 [hep-th].

[92] D. Baumann and D. Green, Phys. Rev. **D85**, 103520 (2012), arXiv:1109.0292 [hep-th].

[93] T. Noumi, M. Yamaguchi, and D. Yokoyama, JHEP **06**, 051 (2013), arXiv:1211.1624 [hep-th].

[94] N. Arkani-Hamed and J. Maldacena, (2015), arXiv:1503.08043 [hep-th].

[95] H. Lee, D. Baumann, and G. L. Pimentel, JHEP **12**, 040 (2016), arXiv:1607.03735 [hep-th].

[96] Planck Collaboration, P. A. R. Ade, N. Aghanim, C. Armitage-Caplan, M. Arnaud, M. Ashdown, F. Atrio-Barandela, J. Aumont, C. Baccigalupi, A. J. Banday, and et al., A&A **571**, A24 (2014), arXiv:1303.5084.

[97] Planck Collaboration, P. A. R. Ade, N. Aghanim, M. Arnaud, F. Arroja, M. Ashdown, J. Aumont, C. Baccigalupi, M. Ballardini, A. J. Banday, and et al., A&A **594**, A17 (2016), arXiv:1502.01592.

[98] K. N. Abazajian, P. Adshead, Z. Ahmed, S. W. Allen, D. Alonso, K. S. Arnold, C. Baccigalupi, J. G. Bartlett, N. Battaglia, B. A. Benson, C. A. Bischoff, J. Borrill, V. Buza, E. Calabrese, R. Caldwell, J. E. Carlstrom, C. L. Chang, T. M. Crawford, F.-Y. Cyr-Racine, F. De Bernardis, T. de Haan, S. di Serego Alighieri, J. Dunkley, C. Dvorkin, J. Errard, G. Fabbian, S. Feeney, S. Ferraro, J. P. Filippini, R. Flauger, G. M. Fuller, V. Gluscevic, D. Green, D. Grin, E. Grohs, J. W. Henning, J. C. Hill, R. Hlozek, G. Holder, W. Holzapfel, W. Hu, K. M. Huffenberger, R. Keskitalo, L. Knox, A. Kosowsky, J. Kovac, E. D. Kovetz, C.-L. Kuo, A. Kusaka, M. Le Jeune, A. T. Lee, M. Lilley, M. Loverde, M. S. Madhavacheril, A. Mantz, D. J. E. Marsh, J. McMahon, P. D. Meerburg, J. Meyers, A. D. Miller, J. B. Munoz, H. N. Nguyen, M. D. Niemack, M. Peloso, J. Peloton, L. Pogosian, C. Pryke, M. Raveri, C. L. Reichardt, G. Rocha, A. Rotti, E. Schaan, M. M. Schmittfull, D. Scott, N. Sehgal, S. Shandera, B. D. Sherwin, T. L. Smith, L. Sorbo, G. D. Starkman, K. T. Story, A. van Engelen, J. D. Vieira, S. Watson, N. Whitehorn, and W. L. Kimmy Wu, ArXiv e-prints (2016), arXiv:1610.02743.

[99] P. D. Meerburg, J. Meyers, A. van Engelen, and Y. Ali-Haïmoud, Phys. Rev. D **93**, 123511 (2016), arXiv:1603.02243.

[100] A. Cooray, Physical Review Letters **97**, 261301 (2006), astro-ph/0610257.

[101] A. Pillepich, C. Porciani, and S. Matarrese, ApJ **662**, 1 (2007), astro-ph/0611126.

[102] P. D. Meerburg, M. Münchmeyer, J. B. Muñoz, and X. Chen, **??**jnlJ. Cosmology Astropart. Phys. **3**, 050 (2017), arXiv:1610.06559.

[103] A. Lidz, E. J. Baxter, P. Adshead, and S. Dodelson, Phys. Rev. D **88**, 023534 (2013), arXiv:1304.8049 [astro-ph.CO].

[104] Y. Mao, A. D'Aloisio, J. Zhang, and P. R. Shapiro, Phys. Rev. D **88**, 081303 (2013), arXiv:1305.0313.

[105] D. Crociani, L. Moscardini, M. Viel, and S. Matarrese, MNRAS **394**, 133 (2009), arXiv:0809.3909.

[106] Y. Xu, J. Hamann, and X. Chen, Phys. Rev. D **94**, 123518 (2016), arXiv:1607.00817.

[107] H. Tashiro and S. Ho, MNRAS **431**, 2017 (2013), arXiv:1205.0563.

[108] A. D'Aloisio, J. Zhang, P. R. Shapiro, and Y. Mao, MNRAS **433**, 2900 (2013), arXiv:1304.6411.

[109] S. Camera, M. G. Santos, and R. Maartens, MNRAS **448**, 1035 (2015), arXiv:1409.8286.

[110] Y.-C. Li and Y.-Z. Ma, Phys. Rev. D **96**, 063525 (2017), arXiv:1701.00221.

[111] D. Karagiannis, A. Lazanu, M. Liguori, A. Raccanelli, N. Bartolo, and L. Verde, ArXiv e-prints (2018), arXiv:1801.09280.

[112] P. A. R. Ade *et al.* (Planck), Astron. Astrophys. **594**, A15 (2016), arXiv:1502.01591 [astro-ph.CO].

[113] M. A. Troxel *et al.* (DES), (2017), arXiv:1708.01538 [astro-ph.CO].

[114] R. Mandelbaum, (2017), arXiv:1710.03235 [astro-ph.CO].

[115] A. R. Cooray, New Astron. **9**, 173 (2004), arXiv:astro-ph/0309301 [astro-ph].

[116] U.-L. Pen, New Astron. **9**, 417 (2004), arXiv:astro-ph/0305387 [astro-ph].

[117] O. Zahn and M. Zaldarriaga, Astrophys. J. **653**, 922 (2006), arXiv:astro-ph/0511547 [astro-ph].

[118] R. B. Metcalf and S. D. M. White, Mon. Not. Roy. Astron. Soc. (2006), 10.1111/j.1365-2966.2007.12212.x, [Mon. Not. Roy. Astron. Soc.381,447(2007)], arXiv:astro-ph/0611862 [astro-ph].

[119] A. Pourtsidou and R. B. Metcalf, Mon. Not. Roy. Astron. Soc. **439**, L36 (2014), arXiv:1311.4484 [astro-ph.CO].

[120] A. Romeo, R. B. Metcalf, and A. Pourtsidou, (2017), 10.1093/mnras/stx2733, arXiv:1708.01235 [astro-ph.CO].

[121] S. Foreman, P. D. Meerburg, A. van Engelen, and J. Meyers, (2018), arXiv:1803.04975 [astro-ph.CO].

[122] T. Lu and U.-L. Pen, Mon. Not. Roy. Astron. Soc. **388**, 1819 (2008), arXiv:0710.1108 [astro-ph].

[123] T. Lu, U.-L. Pen, and O. Dore, Phys. Rev. **D81**, 123015 (2010), arXiv:0905.0499 [astro-ph.CO].

[124] U.-L. Pen, R. Sheth, J. Harnois-Deraps, X. Chen, and Z. Li, (2012), arXiv:1202.5804 [astro-ph.CO].

[125] F. Schmidt, E. Pajer, and M. Zaldarriaga, Phys. Rev. **D89**, 083507 (2014), arXiv:1312.5616 [astro-ph.CO].

[126] H.-M. Zhu, U.-L. Pen, Y. Yu, X. Er, and X. Chen, Phys. Rev. **D93**, 103504 (2016), arXiv:1511.04680 [astro-ph.CO].

[127] H.-M. Zhu, U.-L. Pen, Y. Yu, and X. Chen, (2016), arXiv:1610.07062 [astro-ph.CO].

[128] C. Alcock and B. Paczynski, Nature **281**, 358 (1979).

[129] K. N. Abazajian *et al.* (CMB-S4), (2016), arXiv:1610.02743 [astro-ph.CO].

[130] D. Baumann, D. Green, and B. Wallisch, Phys. Rev. Lett. **117**, 171301 (2016), arXiv:1604.08614 [astro-ph.CO].

[131] D. Baumann, D. Green, and B. Wallisch, (2017), arXiv:1712.08067 [astro-ph.CO].

[132] G. Aslanyan and R. Easther, Phys. Rev. **D91**, 123523 (2015), arXiv:1504.03682 [astro-ph.CO].

[133] C. D. Leonard, P. Bull, and R. Allison, Phys. Rev. D **94**, 023502 (2016), arXiv:1604.01410.

[134] A. Witzemann, P. Bull, C. Clarkson, M. G. Santos, M. Spinelli, and A. Weltman, MNRAS (2018), 10.1093/mnrasl/sly062, arXiv:1711.02179.

[135] I. P. Carucci, F. Villaescusa-Navarro, and M. Viel, **??**jnlJ. Cosmology Astropart. Phys. **4**, 001 (2017), arXiv:1611.07527.

[136] G. J. Hill, K. Gebhardt, E. Komatsu, N. Drory, P. J. MacQueen, J. Adams, G. A. Blanc, R. Koehler, M. Rafal, M. M. Roth, A. Kelz, C. Gronwall, R. Ciardullo,  and D. P. Schneider, in *Panoramic Views of Galaxy Formation and Evolution*, Astronomical Society of the Pacific Conference Series, Vol. 399, edited by T. Kodama, T. Yamada,  and K. Aoki (2008) p. 115, arXiv:0806.0183.

[137] J. D. Cohn, M. White, T.-C. Chang, G. Holder, N. Padmanabhan,  and O. Doré, MNRAS 457, 2068 (2016), arXiv:1511.07377.

[138] A. G. Kim, E. V. Linder, J. Edelstein,  and D. Erskine, Astroparticle Physics 62, 195 (2015), arXiv:1402.6614.

[139] H.-R. Yu, T.-J. Zhang,  and U.-L. Pen, Physical Review Letters 113, 041303 (2014), arXiv:1311.2363.

[140] L. B. Newburgh, K. Bandura, M. A. Bucher, T.-C. Chang, H. C. Chiang, J. F. Cliche, R. Davé, M. Dobbs, C. Clarkson, K. M. Ganga, T. Gogo, A. Gumba, N. Gupta, M. Hilton, B. Johnstone, A. Karastergiou, M. Kunz, D. Lokhorst, R. Maartens, S. Macpherson, M. Mdlalose, K. Moodley, L. Ngwenya, J. M. Parra, J. Peterson, O. Recnik, B. Saliwanchik, M. G. Santos, J. L. Sievers, O. Smirnov, P. Stronkhorst, R. Taylor, K. Vanderlinde, G. Van Vuuren, A. Weltman,  and A. Witzemann, in *Ground-based and Airborne Telescopes VI*, Proc. SPIE, Vol. 9906 (2016) p. 99065X, arXiv:1607.02059 [astro-ph.IM].

[141] M. Bailes, A. Jameson, C. Flynn, T. Bateman, E. D. Barr, S. Bhandari, J. D. Bunton, M. Caleb, D. Campbell-Wilson, W. Farah, B. Gaensler, A. J. Green, R. W. Hunstead, F. Jankowski, E. F. Keane, V. V. Krishnan, T. Murphy, M. O'Neill, S. Osłowski, A. Parthasarathy, V. Ravi, P. Rosado,  and D. Temby, PASA 34, e045 (2017), arXiv:1708.09619 [astro-ph.IM].

[142] M. Amiri, K. Bandura, P. Berger, M. Bhardwaj, M. M. Boyce, P. J. Boyle, C. Brar, M. Burhanpurkar, P. Chawla, J. Chowdhury, J. F. Cliche, M. D. Cranmer, D. Cubranic, M. Deng, N. Denman, M. Dobbs, M. Fandino, E. Fonseca, B. M. Gaensler, U. Giri, A. J. Gilbert, D. C. Good, S. Guliani, M. Halpern, G. Hinshaw, C. Hofer, A. Josephy, V. M. Kaspi, T. L. Landecker, D. Lang, H. Liao, K. W. Masui, J. Mena-Parra, A. Naidu, L. B. Newburgh, C. Ng, C. Patel, U.-L. Pen, T. Pinsonneault-Marotte, Z. Pleunis, M. Rafiei Ravandi, S. M. Ransom, A. Renard, P. Scholz, K. Sigurdson, S. R. Siegel, K. M. Smith, I. H. Stairs, S. P. Tendulkar, K. Vanderlinde,  and D. V. Wiebe, ArXiv e-prints  (2018), arXiv:1803.11235 [astro-ph.IM].

[143] D. R. Lorimer, M. Bailes, M. A. McLaughlin, D. J. Narkevic,  and F. Crawford, Science 318, 777 (2007), arXiv:0709.4301.

[144] D. Thornton, B. Stappers, M. Bailes, B. Barsdell, S. Bates, N. D. R. Bhat, M. Burgay, S. Burke-Spolaor, D. J. Champion, P. Coster, N. D'Amico, A. Jameson, S. Johnston, M. Keith, M. Kramer, L. Levin, S. Milia, C. Ng, A. Possenti,  and W. van Straten, Science 341, 53 (2013), arXiv:1307.1628 [astro-ph.HE].

[145] K. Masui, H.-H. Lin, J. Sievers, C. J. Anderson, T.-C. Chang, X. Chen, A. Ganguly, M. Jarvis, C.-Y. Kuo, Y.-C. Li, Y.-W. Liao, M. McLaughlin, U.-L. Pen, J. B. Peterson, A. Roman, P. T. Timbie, T. Voytek,  and J. K. Yadav, Nature 528, 523 (2015), arXiv:1512.00529 [astro-ph.HE].

[146] S. Chatterjee, C. J. Law, R. S. Wharton, S. Burke-Spolaor, J. W. T. Hessels, G. C. Bower, J. M. Cordes, S. P. Tendulkar, C. G. Bassa, P. Demorest, B. J. Butler, A. Seymour, P. Scholz, M. W. Abruzzo, S. Bogdanov, V. M. Kaspi, A. Keimpema, T. J. W. Lazio, B. Marcote, M. A. McLaughlin, Z. Paragi, S. M. Ransom, M. Rupen, L. G. Spitler,  and H. J. van Langevelde, Nature 541, 58 (2017), arXiv:1701.01098 [astro-ph.HE].

[147] S. P. Tendulkar, C. G. Bassa, J. M. Cordes, G. C. Bower, C. J. Law, S. Chatterjee, E. A. K. Adams, S. Bogdanov, S. Burke-Spolaor, B. J. Butler, P. Demorest, J. W. T. Hessels, V. M. Kaspi, T. J. W. Lazio, N. Maddox, B. Marcote, M. A. McLaughlin, Z. Paragi, S. M. Ransom, P. Scholz, A. Seymour, L. G. Spitler, H. J. van Langevelde,  and R. S. Wharton, ApJ 834, L7 (2017), arXiv:1701.01100 [astro-ph.HE].

[148] H. Tanimura, G. Hinshaw, I. G. McCarthy, L. Van Waerbeke, Y.-Z. Ma, A. Mead, A. Hojjati,  and T. Tröster, ArXiv e-prints  (2017), arXiv:1709.05024.

[149] A. de Graaff, Y.-C. Cai, C. Heymans,  and J. A. Peacock, ArXiv e-prints  (2017), arXiv:1709.10378.

[150] M. McQuinn, ApJ 780, L33 (2014), arXiv:1309.4451.

[151] K. W. Masui and K. Sigurdson, Physical Review Letters 115, 121301 (2015), arXiv:1506.01704.

[152] P. Chawla, V. M. Kaspi, A. Josephy, K. M. Rajwade, D. R. Lorimer, A. M. Archibald, M. E. DeCesar, J. W. T. Hessels, D. L. Kaplan, C. Karako-Argaman, V. I. Kondratiev, L. Levin, R. S. Lynch, M. A. McLaughlin, S. M. Ransom, M. S. E. Roberts, I. H. Stairs, K. Stovall, J. K. Swiggum,  and J. van Leeuwen, ApJ 844, 140 (2017), arXiv:1701.07457 [astro-ph.HE].

[153] Z. Arzoumanian, A. Brazier, S. Burke-Spolaor, S. Chamberlin, S. Chatterjee, B. Christy, J. M. Cordes, N. J. Cornish, F. Crawford, H. Thankful Cromartie, K. Crowter, M. E. DeCesar, P. B. Demorest, T. Dolch, J. A. Ellis, R. D. Ferdman, E. C. Ferrara, E. Fonseca, N. Garver-Daniels, P. A. Gentile, D. Halmrast, E. A. Huerta, F. A. Jenet, C. Jessup, G. Jones, M. L. Jones, D. L. Kaplan, M. T. Lam, T. J. W. Lazio, L. Levin, A. Lommen, D. R. Lorimer, J. Luo, R. S. Lynch, D. Madison, A. M. Matthews, M. A. McLaughlin, S. T. McWilliams, C. Mingarelli, C. Ng, D. J. Nice, T. T. Pennucci, S. M. Ransom, P. S. Ray, X. Siemens, J. Simon, R. Spiewak, I. H. Stairs, D. R. Stinebring, K. Stovall, J. K. Swiggum, S. R. Taylor, M. Vallisneri, R. van Haasteren, S. J. Vigeland, W. Zhu,  and The NANOGrav Collaboration, ApJS 235, 37 (2018), arXiv:1801.01837 [astro-ph.HE].

[154] S. R. Taylor, C. M. F. Mingarelli, J. R. Gair, A. Sesana, G. Theureau, S. Babak, C. G. Bassa, P. Brem, M. Burgay, R. N. Caballero, D. J. Champion, I. Cognard, G. Desvignes, L. Guillemot, J. W. T. Hessels, G. H. Janssen, R. Karuppusamy, M. Kramer, A. Lassus, P. Lazarus, L. Lentati, K. Liu, S. Osłowski, D. Perrodin, A. Petiteau, A. Possenti, M. B. Purver, P. A. Rosado, S. A. Sanidas, R. Smits, B. Stappers, C. Tiburzi, R. van Haasteren, A. Vecchio, J. P. W. Verbiest,  and EPTA Collaboration, Physical Review Letters 115, 041101 (2015), arXiv:1506.08817 [astro-ph.HE].

[155] R. M. Shannon, V. Ravi, W. A. Coles, G. Hobbs, M. J. Keith, R. N. Manchester, J. S. B. Wyithe, M. Bailes, N. D. R. Bhat, S. Burke-Spolaor, J. Khoo, Y. Levin, S. Oslowski, J. M. Sarkissian, W. van Straten, J. P. W. Verbiest,  and J.-B. Wang, Science 342, 334 (2013), arXiv:1310.4569.

[156] J. H. Taylor and J. M. Weisberg, ApJ 345, 434 (1989).

[157] M. Kramer, I. H. Stairs, R. N. Manchester, M. A. McLaughlin, A. G. Lyne, R. D. Ferdman, M. Burgay, D. R. Lorimer, A. Possenti, N. D'Amico, J. M. Sarkissian, G. B. Hobbs, J. E. Reynolds, P. C. C. Freire,  and F. Camilo, Science 314, 97 (2006), astro-ph/0609417.

[158] K. Stovall, R. S. Lynch, S. M. Ransom, A. M. Archibald, S. Banaszak, C. M. Biwer, J. Boyles, L. P. Dartez, D. Day, A. J. Ford, J. Flanigan, A. Garcia, J. W. T. Hessels, J. Hinojosa, F. A. Jenet, D. L. Kaplan, C. Karako-Argaman, V. M. Kaspi, V. I. Kondratiev, S. Leake, D. R. Lorimer, G. Lunsford, J. G. Martinez, A. Mata, M. A. McLaughlin, M. S. E. Roberts, M. D. Rohr, X. Siemens, I. H. Stairs, J. van Leeuwen, A. N. Walker,  and B. L. Wells, ApJ 791, 67 (2014), arXiv:1406.5214 [astro-ph.HE].

[159] K. M. Smith, ArXiv e-prints (2016), arXiv:1610.06831 [astro-ph.HE].

[160] J. B. Peterson, K. Bandura, and U. L. Pen, ArXiv Astrophysics e-prints (2006), arXiv:astro-ph/0606104.

[161] J. D. Bowman, I. Cairns, D. L. Kaplan, T. Murphy, D. Oberoi, L. Staveley-Smith, W. Arcus, D. G. Barnes, G. Bernardi, F. H. Briggs, S. Brown, J. D. Bunton, A. J. Burgasser, R. J. Cappallo, S. Chatterjee, B. E. Corey, A. Coster, A. Deshpande, L. deSouza, D. Emrich, P. Erickson, R. F. Goeke, B. M. Gaensler, L. J. Greenhill, L. Harvey-Smith, B. J. Hazelton, D. Herne, J. N. Hewitt, M. Johnston-Hollitt, J. C. Kasper, B. B. Kincaid, R. Koenig, E. Kratzenberg, C. J. Lonsdale, M. J. Lynch, L. D. Matthews, S. R. McWhirter, D. A. Mitchell, M. F. Morales, E. H. Morgan, S. M. Ord, J. Pathikulangara, T. Prabu, R. A. Remillard, T. Robishaw, A. E. E. Rogers, A. A. Roshi, J. E. Salah, R. J. Sault, N. U. Shankar, K. S. Srivani, J. B. Stevens, R. Subrahmanyan, S. J. Tingay, R. B. Wayth, M. Waterson, R. L. Webster, A. R. Whitney, A. J. Williams, C. L. Williams, and J. S. B. Wyithe, PASA **30**, e031 (2013), arXiv:1212.5151 [astro-ph.IM].

[162] G. Bernardi, L. J. Greenhill, D. A. Mitchell, S. M. Ord, B. J. Hazelton, B. M. Gaensler, A. de Oliveira-Costa, M. F. Morales, N. Udaya Shankar, R. Subrahmanyan, R. B. Wayth, E. Lenc, C. L. Williams, W. Arcus, B. S. Arora, D. G. Barnes, J. D. Bowman, F. H. Briggs, J. D. Bunton, R. J. Cappallo, B. E. Corey, A. Deshpande, L. deSouza, D. Emrich, R. Goeke, D. Herne, J. N. Hewitt, M. Johnston-Hollitt, D. Kaplan, J. C. Kasper, B. B. Kincaid, R. Koenig, E. Kratzenberg, C. J. Lonsdale, M. J. Lynch, S. R. McWhirter, E. Morgan, D. Oberoi, J. Pathikulangara, T. Prabu, R. A. Remillard, A. E. E. Rogers, A. Roshi, J. E. Salah, R. J. Sault, K. S. Srivani, J. Stevens, S. J. Tingay, M. Waterson, R. L. Webster, A. R. Whitney, A. Williams, and J. S. B. Wyithe, ApJ **771**, 105 (2013), arXiv:1305.6047.

[163] S. Tingay, R. Goeke, J. N. Hewitt, E. Morgan, R. A. Remillard, C. L. Williams, J. D. Bowman, E. Emrich, S. M. Ord, T. Booler, B. Crosse, D. Pallot, W. Arcus, T. Colegate, P. J. Hall, D. Herne, M. J. Lynch, F. Schlagenhaufer, S. Tremblay, R. B. Wayth, M. Waterson, D. A. Mitchell, R. J. Sault, R. L. Webster, J. S. B. Wyithe, M. F. Morales, B. J. Hazelton, A. Wicenec, A. Williams, D. Barnes, G. Bernardi, L. J. Greenhill, J. C. Kasper, F. Briggs, B. McKinley, J. D. Bunton, L. deSouza, R. Koenig, J. Pathikulangara, J. Stevens, R. J. Cappallo, B. E. Corey, B. B. Kincaid, E. Kratzenberg, C. J. Lonsdale, S. R. McWhirter, A. E. E. Rogers, J. E. Salah, A. R. Whitney, A. Deshpande, T. Prabu, A. Roshi, N. Udaya-Shankar, K. S. Srivani, R. Subrahmanyan, B. M. Gaensler, M. Johnston-Hollitt, D. L. Kaplan, and D. Oberoi, in *Resolving The Sky - Radio Interferometry: Past, Present and Future* (2012) p. 36, arXiv:1212.1327 [astro-ph.IM].

[164] Z. S. Ali, A. R. Parsons, H. Zheng, J. C. Pober, A. Liu, J. E. Aguirre, R. F. Bradley, G. Bernardi, C. L. Carilli, C. Cheng, D. R. DeBoer, M. R. Dexter, J. Grobbelaar, J. Horrell, D. C. Jacobs, P. Klima, D. H. E. MacMahon, M. Maree, D. F. Moore, N. Razavi, I. I. Stefan, W. P. Walbrugh, and A. Walker, ApJ **809**, 61 (2015), arXiv:1502.06016.

[165] J. C. Pober, Z. S. Ali, A. R. Parsons, M. McQuinn, J. E. Aguirre, G. Bernardi, R. F. Bradley, C. L. Carilli, C. Cheng, D. R. De-Boer, M. R. Dexter, S. R. Furlanetto, J. Grobbelaar, J. Horrell, D. C. Jacobs, P. J. Klima, S. A. Kohn, A. Liu, D. H. E. MacMahon, M. Maree, A. Mesinger, D. F. Moore, N. Razavi-Ghods, I. I. Stefan, W. P. Walbrugh, A. Walker, and H. Zheng, ApJ **809**, 62 (2015), arXiv:1503.00045.

[166] A. Ewall-Wice, J. Hewitt, A. Mesinger, J. S. Dillon, A. Liu, and J. Pober, MNRAS **458**, 2710 (2016), arXiv:1511.04101.

[167] A. R. Parsons, A. Liu, J. E. Aguirre, Z. S. Ali, R. F. Bradley, C. L. Carilli, D. R. DeBoer, M. R. Dexter, N. E. Gugliucci, D. C. Jacobs, P. Klima, D. H. E. MacMahon, J. R. Manley, D. F. Moore, J. C. Pober, I. I. Stefan, and W. P. Walbrugh, ApJ **788**, 106 (2014), arXiv:1304.4991.

[168] K. Bandura, G. E. Addison, M. Amiri, J. R. Bond, D. Campbell-Wilson, L. Connor, J.-F. Cliche, G. Davis, M. Deng, N. Denman, M. Dobbs, M. Fandino, K. Gibbs, A. Gilbert, M. Halpern, D. Hanna, A. D. Hincks, G. Hinshaw, C. Höfer, P. Klages, T. L. Landecker, K. Masui, J. Mena Parra, L. B. Newburgh, U.-l. Pen, J. B. Peterson, A. Recnik, J. R. Shaw, K. Sigurdson, M. Sitwell, G. Smecher, R. Smegal, K. Vanderlinde, and D. Wiebe, in *Society of Photo-Optical Instrumentation Engineers (SPIE) Conference Series*, Society of Photo-Optical Instrumentation Engineers (SPIE) Conference Series, Vol. 9145 (2014) p. 22, arXiv:1406.2288 [astro-ph.IM].

[169] K. Bandura, J. F. Cliche, M. A. Dobbs, A. J. Gilbert, D. Ittah, J. Mena Parra, and G. Smecher, Journal of Astronomical Instrumentation **5**, 1641004 (2016).

[170] P. Berger, L. B. Newburgh, M. Amiri, K. Bandura, J.-F. Cliche, L. Connor, M. Deng, N. Denman, M. Dobbs, M. Fandino, A. J. Gilbert, D. Good, M. Halpern, D. Hanna, A. D. Hincks, G. Hinshaw, C. Hofer, A. M. Johnson, T. L. Landecker, K. W. Masui, J. M. Parra, N. Oppermann, U.-L. Pen, J. B. Peterson, A. Recnik, T. Robishaw, J. R. Shaw, S. Siegel, K. Sigurdson, K. Smith, E. Storer, I. Tretyakov, K. Van Gassen, K. Vanderlinde, and D. Wiebe, arXiv.org (2016), 1607.01473v1.

[171] L. B. Newburgh, G. E. Addison, M. Amiri, K. Bandura, J. R. Bond, L. Connor, J.-F. Cliche, G. Davis, M. Deng, N. Denman, M. Dobbs, M. Fandino, H. Fong, K. Gibbs, A. Gilbert, E. Griffin, M. Halpern, D. Hanna, A. D. Hincks, G. Hinshaw, C. Höfer, P. Klages, T. Landecker, K. Masui, J. M. Parra, U.-L. Pen, J. Peterson, A. Recnik, J. R. Shaw, K. Sigurdson, M. Sitwell, G. Smecher, R. Smegal, K. Vanderlinde, and D. Wiebe, in *Society of Photo-Optical Instrumentation Engineers (SPIE) Conference Series*, Society of Photo-Optical Instrumentation Engineers (SPIE) Conference Series, Vol. 9145 (2014) p. 4, arXiv:1406.2267 [astro-ph.IM].

[172] J. R. Shaw, K. Sigurdson, U.-L. Pen, A. Stebbins, and M. Sitwell, arXiv.org (2013), 1302.0327v1.

[173] J. R. Shaw, K. Sigurdson, M. Sitwell, A. Stebbins, and U.-L. Pen, arXiv.org (2014a), 1401.2095v1.

[174] A. R. Offringa, R. B. Wayth, N. Hurley-Walker, D. L. Kaplan, N. Barry, A. P. Beardsley, M. E. Bell, G. Bernardi, J. D. Bowman, F. Briggs, J. R. Callingham, R. J. Cappallo, P. Carroll, A. A. Deshpande, J. S. Dillon, K. S. Dwarakanath, A. Ewall-Wice, L. Feng, B.-Q. For, B. M. Gaensler, L. J. Greenhill, P. Hancock, B. J. Hazelton, J. N. Hewitt, L. Hindson, D. C. Jacobs, M. Johnston-Hollitt, A. D. Kapińska, H.-S. Kim, P. Kittiwisit, E. Lenc, J. Line, A. Loeb, C. J. Lonsdale, B. McKinley, S. R. McWhirter, D. A. Mitchell, M. F. Morales, E. Morgan, J. Morgan, A. R. Neben, D. Oberoi, S. M. Ord, S. Paul, B. Pindor, J. C. Pober, T. Prabu, P. Procopio, J. Riding, N. Udaya Shankar, S. Sethi, K. S. Srivani, L. Staveley-Smith, R. Subrahmanyan, I. S. Sullivan, M. Tegmark, N. Thyagarajan, S. J. Tingay, C. M. Trott, R. L. Webster, A. Williams, C. L. Williams, C. Wu, J. S. Wyithe, and Q. Zheng, PASA **32**, e008 (2015), arXiv:1501.03946 [astro-ph.IM].

[175] B. S. Arora, J. Morgan, S. M. Ord, S. J. Tingay, N. Hurley-Walker, M. Bell, G. Bernardi, N. D. R. Bhat, F. Briggs, J. R. Callingham, A. A. Deshpande, K. S. Dwarakanath, A. Ewall-Wice, L. Feng, B.-Q. For, P. Hancock, B. J. Hazelton, L. Hindson, D. Jacobs, M. Johnston-Hollitt, A. D. Kapińska, N. Kudryavtseva, E. Lenc, B. McKinley, D. Mitchell, D. Oberoi, A. R. Offringa, B. Pindor, P. Procopio, J. Riding, L. Staveley-Smith, R. B. Wayth, C. Wu, Q. Zheng, J. D. Bowman, R. J. Cappallo, B. E. Corey, D. Emrich, R. Goeke, L. J.

Greenhill, D. L. Kaplan, J. C. Kasper, E. Kratzenberg, C. J. Lonsdale, M. J. Lynch, S. R. McWhirter, M. F. Morales, E. Morgan, T. Prabu, A. E. E. Rogers, A. Roshi, N. U. Shankar, K. S. Srivani, R. Subrahmanyan, M. Waterson, R. L. Webster, A. R. Whitney, A. Williams, and C. L. Williams, PASA **32**, e029 (2015), arXiv:1507.01184 [astro-ph.IM].

[176] P. Procopio, R. B. Wayth, J. Line, C. M. Trott, H. T. Intema, D. A. Mitchell, B. Pindor, J. Riding, S. J. Tingay, M. E. Bell, J. R. Callingham, K. S. Dwarakanath, B.-Q. For, B. M. Gaensler, P. J. Hancock, L. Hindson, N. Hurley-Walker, M. Johnston-Hollitt, A. D. Kapińska, E. Lenc, B. McKinley, J. Morgan, A. Offringa, L. Staveley-Smith, C. Wu, and Q. Zheng, PASA **34**, e033 (2017), arXiv:1707.02288 [astro-ph.IM].

[177] J. C. Pober, A. R. Parsons, J. E. Aguirre, Z. Ali, R. F. Bradley, C. L. Carilli, D. DeBoer, M. Dexter, N. E. Gugliucci, D. C. Jacobs, P. J. Klima, D. MacMahon, J. Manley, D. F. Moore, I. I. Stefan, and W. P. Walbrugh, ApJ **768**, L36 (2013), arXiv:1301.7099.

[178] H.-J. Seo and C. M. Hirata, MNRAS **456**, 3142 (2016), arXiv:1508.06503.

[179] A. Liu and M. Tegmark, MNRAS **419**, 3491 (2012), arXiv:1106.0007 [astro-ph.CO].

[180] M. Tegmark and M. Zaldarriaga, Phys. Rev. D **79**, 083530 (2009), arXiv:0805.4414.

[181] A. Liu, M. Tegmark, S. Morrison, A. Lutomirski, and M. Zaldarriaga, MNRAS **408**, 1029 (2010), arXiv:1001.5268 [astro-ph.IM].

[182] C. L. Carilli, B. Nikolic, N. Thyagarajan, K. Gale-Sides, Z. Abdurashidova, J. E. Aguirre, P. Alexander, Z. S. Ali, Y. Balfour, A. P. Beardsley, G. Bernardi, J. D. Bowman, R. F. Bradley, J. Burba, C. Cheng, D. R. DeBoer, M. Dexter, E. de~Lera~Acedo, J. S. Dillon, A. Ewall-Wice, G. Fadana, N. Fagnoni, R. Fritz, S. R. Furlanetto, A. Ghosh, B. Glendenning, B. Greig, J. Grobbelaar, Z. Halday, B. J. Hazelton, J. N. Hewitt, J. Hickish, D. C. Jacobs, A. Julius, M. Kariseb, S. A. Kohn, M. Kolopanis, T. Lekalake, A. Liu, A. Loots, D. MacMahon, L. Malan, C. Malgas, M. Maree, Z. Martinot, E. Matsetela, A. Mesinger, M. Molewa, M. F. Morales, A. R. Neben, A. R. Parsons, N. Patra, S. Pieterse, P. La Plante, J. C. Pober, N. Razavi-Ghods, J. Ringuette, J. Robnett, K. Rosie, R. Sell, P. Sims, C. Smith, A. Syce, P. K. ~G. Williams, and H. Zheng, ArXiv e-prints (2018), arXiv:1805.00953 [astro-ph.IM].

[183] J. S. Dillon, S. A. Kohn, A. R. Parsons, J. E. Aguirre, Z. S. Ali, G. Bernardi, N. S. Kern, W. Li, A. Liu, C. D. Nunhokee, and J. C. Pober, MNRAS **477**, 5670 (2018), arXiv:1712.07212 [astro-ph.IM].

[184] V. Ram Marthi and J. Chengalur, in *Astronomical Society of India Conference Series*, Astronomical Society of India Conference Series, Vol. 13 (2014) pp. 393–394, arXiv:1310.1449 [astro-ph.IM].

[185] J. S. Dillon and A. R. Parsons, ApJ **826**, 181 (2016), arXiv:1602.06259 [astro-ph.IM].

[186] J. L. Sievers, ArXiv e-prints (2017), arXiv:1701.01860 [astro-ph.IM].

[187] X. Chen, in *International Journal of Modern Physics Conference Series*, International Journal of Modern Physics Conference Series, Vol. 12 (2012) pp. 256–263, arXiv:1212.6278 [astro-ph.IM].

[188] U.-L. Pen, New A **9**, 417 (2004), astro-ph/0305387.

[189] M. Tegmark and M. Zaldarriaga, Phys. Rev. D **79**, 083530 (2009), arXiv:0805.4414.

[190] M. Tegmark and M. Zaldarriaga, Phys. Rev. D **82**, 103501 (2010), arXiv:0909.0001 [astro-ph.CO].

[191] K. W. Masui, J. R. Shaw, C. Ng, K. M. Smith, K. Vanderlinde, and A. Paradise, ArXiv e-prints (2017), arXiv:1710.08591 [astro-ph.IM].

[192] M. Sokolowski, T. Colegate, A. T. Sutinjo, D. Ung, R. Wayth, N. Hurley-Walker, E. Lenc, B. Pindor, J. Morgan, D. L. Kaplan, M. E. Bell, J. R. Callingham, K. S. Dwarakanath, B.-Q. For, B. M. Gaensler, P. J. Hancock, L. Hindson, M. Johnston-Hollitt, A. D. Kapińska, B. McKinley, A. R. Offringa, P. Procopio, L. Staveley-Smith, C. Wu, and Q. Zheng, PASA **34**, e062 (2017), arXiv:1710.07478 [astro-ph.IM].

[193] D. C. Jacobs, J. Burba, J. Bowman, A. R. Neben, B. Stinnett, and L. Turner, ArXiv e-prints (2016), arXiv:1610.02607 [astro-ph.IM].

[194] G. Virone, A. M. Lingua, M. Piras, A. Cina, F. Perini, J. Monari, F. Paonessa, O. A. Peverini, G. Addamo, and R. Tascone, IEEE Antennas and Wireless Propagation Letters **13**, 169 (2014).

[195] G. Pupillo, G. Naldi, G. Bianchi, A. Mattana, J. Monari, F. Perini, M. Poloni, M. Schiaffino, P. Bolli, A. Lingua, I. Aicardi, H. Bendea, P. Maschio, M. Piras, G. Virone, F. Paonessa, Z. Farooqui, A. Tibaldi, G. Addamo, O. A. Peverini, R. Tascone, and S. J. Wijnholds, Experimental Astronomy **39**, 405 (2015).

[196] C. Chang, C. Monstein, A. Refregier, A. Amara, A. Glauser, and S. Casura, PASP **127**, 1131 (2015), arXiv:1505.05885 [astro-ph.IM].

[197] F. Villaescusa-Navarro and e. al., in prep. (2018).

[198] S. Tassev, M. Zaldarriaga, and D. J. Eisenstein, **??**jnlJ. Cosmology Astropart. Phys. **6**, 036 (2013), arXiv:1301.0322 [astro-ph.CO].

[199] J. Silk, ApJ **151**, 459 (1968).

[200] Y. Ali-Haimoud, P. D. Meerburg, and S. Yuan, Phys. Rev. **D89**, 083506 (2014), arXiv:1312.4948 [astro-ph.CO].

[201] K. Sigurdson and S. R. Furlanetto, Phys. Rev. Lett. **97**, 091301 (2006), arXiv:astro-ph/0505173 [astro-ph].

[202] A. Loeb and M. Zaldarriaga, Phys. Rev. Lett. **92**, 211301 (2004), arXiv:astro-ph/0312134 [astro-ph].

[203] A. Lewis and A. Challinor, Phys. Rev. **D76**, 083005 (2007), arXiv:astro-ph/0702600 [ASTRO-PH].

[204] S. Jester and H. Falcke, New A Rev. **53**, 1 (2009), arXiv:0902.0493 [astro-ph.CO].

[205] J. O. Burns, R. Bradley, K. Tauscher, S. Furlanetto, J. Mirocha, R. Monsalve, D. Rapetti, W. Purcell, D. Newell, D. Draper, R. Mac-Dowall, J. Bowman, B. Nhan, E. J. Wollack, A. Fialkov, D. Jones, J. C. Kasper, A. Loeb, A. Datta, J. Pritchard, E. Switzer, and M. Bicay, ApJ **844**, 33 (2017), arXiv:1704.02651 [astro-ph.IM].

[206] P. Adshead, R. Easther, J. Pritchard, and A. Loeb, JCAP **1102**, 021 (2011), arXiv:1007.3748 [astro-ph.CO].

[207] J. B. Muñoz, Y. Ali-Haïmoud, and M. Kamionkowski, Phys. Rev. D **92**, 083508 (2015), arXiv:1506.04152.

[208] X. Chen, P. D. Meerburg, and M. M??nchmeyer, JCAP **1609**, 023 (2016), arXiv:1605.09364 [astro-ph.CO].

[209] D. Baumann, G. Goon, H. Lee, and G. L. Pimentel, (2017), arXiv:1712.06624 [hep-th].

[210] A. H. Guth, Phys. Rev. D **23**, 347 (1981).

[211] J. L. Cook and L. Sorbo, Phys. Rev. **D85**, 023534 (2012), [Erratum: Phys. Rev.D86,069901(2012)], arXiv:1109.0022 [astro-ph.CO].

[212] R. Namba, M. Peloso, M. Shiraishi, L. Sorbo, and C. Unal, JCAP **1601**, 041 (2016), arXiv:1509.07521 [astro-ph.CO].

[213] J. Khoury, B. A. Ovrut, P. J. Steinhardt, and N. Turok, Phys. Rev. **D64**, 123522 (2001), arXiv:hep-th/0103239 [hep-th].

[214] D. H. Lyth, Phys. Rev. Lett. **78**, 1861 (1997), arXiv:hep-ph/9606387 [hep-ph].

[215] P. D. Meerburg, R. Hlo??ek, B. Hadzhiyska, and J. Meyers, Phys. Rev. **D91**, 103505 (2015), arXiv:1502.00302 [astro-ph.CO].

[216] K. W. Masui and U.-L. Pen, Physical Review Letters **105**, 161302 (2010), arXiv:1006.4181 [astro-ph.CO].

[217] K. W. Masui, U.-L. Pen, and N. Turok, Phys. Rev. Lett. **118**, 221301 (2017), arXiv:1702.06552 [astro-ph.CO].

[218] S. Dodelson, E. Rozo, and A. Stebbins, Phys. Rev. Lett. **91**, 021301 (2003), arXiv:astro-ph/0301177 [astro-ph].

[219] C. Li and A. Cooray, Phys. Rev. **D74**, 023521 (2006), arXiv:astro-ph/0604179 [astro-ph].

[220] L. Book, M. Kamionkowski, and F. Schmidt, Phys. Rev. Lett. **108**, 211301 (2012), arXiv:1112.0567 [astro-ph.CO].

[221] N. E. Chisari, C. Dvorkin, and F. Schmidt, Phys. Rev. **D90**, 043527 (2014), arXiv:1406.4871 [astro-ph.CO].

[222] C. Sheere, A. van Engelen, P. D. Meerburg, and J. Meyers, Phys. Rev. **D96**, 063508 (2017), arXiv:1610.09365 [astro-ph.CO].

[223] F. Schmidt and D. Jeong, Phys. Rev. **D86**, 083513 (2012), arXiv:1205.1514 [astro-ph.CO].

[224] A. Lewis, A. Challinor, and A. Lasenby, Astrophys. J. **538**, 473 (2000), arXiv:astro-ph/9911177 [astro-ph].

[225] S. Saga, D. Yamauchi, and K. Ichiki, Phys. Rev. **D92**, 063533 (2015), arXiv:1505.02774 [astro-ph.CO].

[226] S. Saga, Phys. Rev. **D94**, 063523 (2016), arXiv:1607.03973 [astro-ph.CO].

[227] D. Baumann, P. J. Steinhardt, K. Takahashi, and K. Ichiki, Phys. Rev. **D76**, 084019 (2007), arXiv:hep-th/0703290 [hep-th].

[228] R. A. Battye, I. W. A. Browne, C. Dickinson, G. Heron, B. Maffei, and A. Pourtsidou, MNRAS **434**, 1239 (2013), arXiv:1209.0343 [astro-ph.CO].

[229] N. H. M. Crighton, M. T. Murphy, J. X. Prochaska, G. Worseck, M. Rafelski, G. D. Becker, S. L. Ellison, M. Fumagalli, S. Lopez, A. Meiksin, and J. M. O'Meara, MNRAS **452**, 217 (2015), arXiv:1506.02037.

[230] J. C. Pober, A. Liu, J. S. Dillon, J. E. Aguirre, J. D. Bowman, R. F. Bradley, C. L. Carilli, D. R. DeBoer, J. N. Hewitt, D. C. Jacobs, M. McQuinn, M. F. Morales, A. R. Parsons, M. Tegmark, and D. J. Werthimer, ApJ **782**, 66 (2014), arXiv:1310.7031.